CONSTRUCTION OF TRANSFECTION VECTORS TO TARGET *Plasmodium berghei* APICAL MEMBRANE ANTIGEN 1 (AMA1) AND AUTOPHAGY RELATED 18 (ATG18) GENES, AND CHARACTERIZATION OF RECOMBINANT PARASITES

M.Sc. Thesis

2017

Submitted to

CENTRAL DEPARTMENT OF BIOTECHNOLOGY

Tribhuvan University

Kirtipur, Kathmandu, Nepal

Navin Adhikari

CONSTRUCTION OF TRANSFECTION VECTORS TO TARGET *Plasmodium berghei* APICAL MEMBRANE ANTIGEN 1 (AMA1) AND AUTOPHAGY RELATED 18 (ATG18) GENES, AND CHARACTERIZATION OF RECOMBINANT PARASITES

M.Sc. Thesis

2017

Submitted to

Central Department of Biotechnology

Tribhuvan University

Kirtipur, Kathmandu, Nepal

By

Navin Adhikari

Supervisors

Prof. Dr. Tilak R. Shrestha (CDBT)

Dr. Puran Singh Sijwali (CCMB)

TU Registration No: 5-3-28-106-2014

Declaration by the Candidate

I, hereby, declare that the thesis report entitled **"Construction of transfection vectors to target *Plasmodium berghei* Apical Membrane Antigen 1 (AMA1*)* and Autophagy related 18 (ATG18*)* genes, and characterization of recombinant parasites"** submitted by me, Navin Adhikari (Reg. No. 5-3-28-106-2014), to Tribhuvan University, Kirtipur, Nepal with supervision of Prof. Dr. Tilak R. Shrestha for partial fulfilment of requirement for the degree of M.Sc. in Biotechnology is a record of bonafide research work carried out by me. This work was carried out under the guidance of Dr. Puran Singh Sijwali at Centre for Cellular and Molecular Biology, Hyderabad, India during February-September 2017. I further declare that the work reported in this thesis has not been submitted elsewhere, either in part or in full, for the award of any other degree or diploma.

Date: ……. Signature of the candidate

Dedicated to my PARENTS and Science

ACKNOWLEDGEMENTS

I am very delighted to use this space to express my gratitude towards the individuals and organizations to make my short research experience in Center for Cellular and Molecular Biology (CCMB) a very memorable journey.

I express my heartfelt gratitude to **Prof. Dr. Tilak R. Shrestha**, my supervisor at Central Department of Biotechnology, Tribhuvan University, for his valuable guidance, critical review and meaningful interpretation of data. Scientific writing and presentation skills are essence of research, and science mingles with art in doing so. I would like to thank Dr. Tilak for suggesting valuable arts in my thesis to make it simpler and more understandable. Without his efforts, this project would not have been a part of the department.

As science has no borders, I was excited to go from Nepal and join CCMB for MSc thesis. I feel fortunate to get the opportunity to work with **Dr. Puran Singh Sijwali, Principal Scientist,** in his esteemed laboratory. I remember my first meeting with Dr. Puran when he stated, 'we do not wait here man' and I sensed him as a person with great zeal for research, which would contribute to public health. His keen interest and active discussions regarding my project made me understand and design my work plan, and work harder to achieve research goals. His critical thinking allowed me to trace new ways for clearing any hurdles that appeared. I was overwhelmed to have his confidence on me, which allowed me to work alone, as well as in a team. In his mentorship, I got an opportunity to plunge myself into practical research and learn new molecular and cell biology techniques. Again, I would like to thank Dr. Puran for training me and enhancing my overall skills, which would surely be as asset for my Doctoral studies.

I am grateful to **Dr. Rakesh Kumar Mishra**, Director of CCMB, for providing me an official approval to work in great CCMB environment and to manage my lodging at CCMB Staff Quarters.

I would like to thank **Dr. Krishna Das Manandhar**, Head of the Central Department of Biotechnology at my university, for official processing to carry out this research work at CCMB. I am also grateful to **Prof. Rajani Malla**, former head of department, for her care and encouragements. I am thankful to all the faculties of CDBT for making this MSc journey fruitful.

I am grateful to **Dr. Thanumalayan**, Senior Technical Officer at CCMB, who was always beside me for scientific and non-scientific discussions. He was always polite and insisted to learn from mistakes. He helped me with the molecular biology tools for cloning and preparing *Plasmodium berghei* transfection constructs. I would always appreciate his

view on applied research for industrial level. I want to thank him for being a great mentor, colleague, a friend and guardian.

I feel glad to have worked with **Ms. Renu S** who trained me in animal handling, BioSafety Level II labwork, blotting and imaging techniques. Despite her busy schedule and time-point experiments, she helped me a lot whenever needed. I hope some findings of this report would be valuable to her PhD journey and wish her best of luck.

I thank all my Malaria Research lab mates **Amit**, **Divya**, **Zeba**, **Deepak**, **Manish**, **Nandita** and **Dr. Dinesh** for assisting me in all possible ways directly or indirectly. I am thankful to all my R & D lab mates for maintaining a great working environment and filling up with humor to make it lively.

In this endeavor, I want to thank some special friend **Amit**, brother **Manish** for adding so much to my life. I cannot forget big brothers **Sampath** and **Soumik** in my flat at CCMB Staff Quarters who made my living more valuable. In the same group were Madhuri, Arun, Pooja, Sroddha, and Sukanya whom I want to remember and wish good luck for research career.

I cannot miss my classmate from CDBT Ms. **Rashmi** in giving vote of thanks for sharing times in CCMB regarding work and other discussions. All of my MSc friends were badly missed, actually I was missing the fun that all of them were having in CDBT.

AT LAST, what I am today is my mother and father's continuous efforts and GOD'S grace upon me. I have no words to thank my mother, father and brother who always supported me and encouraged me with their best wishes throughout my educational career.

Thank you all who extended their helping hands as well as who encouraged me to excel more.

ABBREVIATIONS AND SYMBOLS

Bp	basepair(s)
Hrs	hours
Kb	kilobase
kDa	kilo Dalton
mA	milliampere(s)
mg	milligram(s)
min	minute(s)
ml	milliliter(s)
mM	millimolar(s)
mV	millivolt(s)
nm	nanometer(s)
nM	nanomolar(s)
ºC	degree Celsius
rpm	revolutions per minute
sec	second(s)
V	Volt(s)
µg	microgram(s)
µl	microlitre(s)
µM	micromolar(s)
AMA	Apical Membrane Antigen
ATG18/A18	Autophagy related 18
BLAST	Basic Local Alignment Search Tool
BME/β-ME	beta-mercaptoethanol
BSA	Bovine Serum Albumin
CDART	Conserved Domain Architecture Retrieval Tool
cDD	*E. coli* Destabilizing Domain
CDS	Coding sequence
COPII	coat protein complex II
DAPI	4,6-diamidino-2-phenylIndole
DMSO	Dimethyl sulfoxide
DNA	Deoxyribo nucleic acid
DTT	Dithiothreitol
EDTA	Ethylenediamine tetraacetic acid
FBS	Fetal Bovine Serum
FRRG	phenylalanine–arginine–arginine–glycine
FV	Food vacuole
gDNA	genomic DNA

GFP	(enhanced) Green Fluorescent Protein
hDHFR	human DiHydro Folate Reductase
HRP	Horsh Radish Peroxidase
HRP	Histidine Rich Protein
IFA	Immunofluorescence assay
KD	KnockDown
KI	KnockIn
KO	KnockOut
MR4	Malaria Research and Reference Reagent Resource Center
MSP	Merozoite Surface Protein
NCBI	National Centre for Biotechnology Information
OD	Optical density
PAGE	Poly-acrylamide gel electrophoresis
PAS	phagophore assembly site/ preautophagosomal structure
PbANKA	*Plasmodium berghei* ANKA strain
PBS	Phosphate buffered saline
pDNA	Plasmid DNA
PE	phosphatidylethanolamine
Pf	*Plasmodium falciparum*
Pfam	Protein family database
PI3P	phosphatidylinositol-3-phosphate
PIPES	piperazine-N,N'-bis(2-ethanesulfonic acidà
PtdIns3P	refer PI3P
PvAC	*Plasmodium* vivax Actin
PyαTb	*Plasmodium yoelii* alpha tubulin
RBC	Red Blood Cell / Erythrocyte
RNA	Ribonucleic acid
rpm	revolutions per minute
RPMI	Rosewell Park Memorial Institute
RT	Room temperature
SGD	Saccharomyces Genome Database
SDS	Sodium dodecyl sulfate
TORC1	target of rapamycin complex 1
TRAPPIII	transport protein particle III
UTR	untranslated region
WD40	tryptophan (W) –aspartate (D) 40 domain
WHO	World Health Organization
WT	wild type

LIST OF TABLES

LIST OF FIGURES

TABLE OF CONTENTS

ABSTRACT

Apical membrane antigen 1 (AMA1) protein of *Plasmodium* is involved in host-pathogen interactions leading to invasion of erythrocytes by merozoites. It is conserved in all Apicomplexan parasites, and is an essential protein for *Plasmodium* development. AMA1 is also considered a potential vaccine candidate. Towards understanding the effect of AMA1 knockdown on parasite development and induction of immune responses, attempts were made to generate AMA1 knockdown *Plasmodium berghei* parasites, which would have the potential as a whole parasite vaccine in mice. Similarly, Autophagy related 18 (ATG18) protein has key roles in the formation of autophagosomes and vesicle biogenesis in yeast model. It was investigated for its localization and functional characterization in *Plasmodium*. Transfection plasmids were constructed for homology-based double crossover integration (homologous recombination) at the AMA1 and ATG18 genes loci of *P. berghei* ANKA strain. After successful recombination in AMA1 gene locus, AMA1 would be followed by a reporter gene Green Fluorescent Protein (GFP) only in knockin parasites (AMA1 KI) and another Destabilizing Domain (cDD) addition to GFP in knockdown parasites (AMA1 KD). As AMA1 is an essential protein, parasites with these AMA1-GFP or AMA1-GFP-cDD fusion proteins could not invade host cell and undergo schizogony. Thus, modification in AMA1 did not result in enough parasitemia of recombinant parasites in Balb/c mice suggesting highly conserved structure of AMA1 protein and lack of function upon modification. However, alternate strategies are required to generate AMA1 knockdown parasites. Similarly, in ATG18 locus, ATG18 would be replaced by GFP in knockout parasites (ATG18 KO) while ATG18 would be followed by GFP and cDD in knockdown parasites (ATG18 KD). ATG18 KO parasites could not maintain cellular homeostatis and develop further, thus enough parasitemia was not achieved in mice while generation of ATG18 KD parasites with ATG18-GFP-cDD fusion protein was successful, suggesting that ATG18 is essential for parasite development. The genomic (Polymerase Chain Reaction- PCR), cellular (fluorescent microscopy) and proteomic (western blotting) analyses of knockdown parasites confirmed the presence of ATG18-GFP-cDD in ATG18 locus of recombinant parasite genome and also the fusion protein expression. Food vacuolar localization of GFP fluorescence in ATG18 KD parasites suggests a role of ATG18 in the biogenesis of food vacuole and/or food vacuole-associated activities. These ATG18 KD parasites will be invaluable for identification of the specific functions of *Plasmodium* ATG18 during parasite development, which need to be explored.

Keywords:

AMA1, ATG18, autophagy, host-pathogen interaction, apicomplexan, fusion protein, homologous recombination, knock in, knockdown, knockout

CHAPTER 1
INTRODUCTION

1.1 Background of the study

Malaria is one of the most severe parasite-caused public health problems worldwide. It is a leading cause of death and morbidity in many developing countries, mostly affecting young children and pregnant women. According to the WHO (*World Malaria Report*, 2017), 216 million cases and 445,000 deaths were estimated to have occurred in 2016. The occurrence and distribution of malaria is found to depend on various climatic factors such as temperature, humidity and rainfall. The high incidence of malaria cases and deaths in tropical and sub-tropical regions are due to the most favorable environment for the life cycle of malaria transmission vector (CDC - Malaria, 2017).

1.1.1 A short history on Malaria

The term malaria was derived from Italian word mal'aria meaning bad air. Malaria has evolved along with the humans for thousands of years as the references to the periodic malarial fever has been found to be documented as early as 2700 BC in China. The major breakthroughs in the history of malaria research was the discovery of parasite in the blood of malaria patient by Charles Louis Alphonse Laveran, a French army surgeon, in 1880 and the discovery that mosquitoes are the vectors for transmission of the avian malarial parasites by Sir Ronald Ross in 1897. As malaria was one of the highly devastating infectious diseases throughout the world, these discoveries were enough to ignite the malarial research. Soon in 1899, human malaria parasite *Plasmodium* was identified and since then, its complex life cycle and preventive and curative drugs have been studied (CDC - Malaria - About Malaria - History, 2017).

1.1.2 Life cycle of *Plasmodium*

Plasmodium is a protozoan parasite, which goes through complex multi-stage life cycle in two hosts: the mosquito and the vertebrates (birds and mammals). While more than 150 *Plasmodium* species have been identified to infect vertebrates, four species are the parasites of humans, utilizing them as natural intermediate host namely *P. falciparum, P. vivax, P. malariae* and *P. ovale*. *Plasmodium* species are obligate parasites that switch between the vertebrate host and Anopheles mosquito (Cox, 2010) .

The life cycle of *Plasmodium* (Figure 1.1) consists mainly of four phases, which are liver stage, blood stage, gametocytic stage and sporogony. During the blood meal, mosquito injects saliva to prevent blood clotting, and allow sucking the blood continuously. If the mosquito vector is infected with *Plasmodium*, its sporozoite stage is injected along with

saliva. In the host, the circulatory system carries the sporozoites until they reach and invade liver cells. The intracellular parasite undergoes multiple asexual replication inside a single liver cell producing thousands of merozoites known as exoerythrocytic schizogony; schizogony referring to the multiple karyokinesis without cytokinesis in parasite. The merozoites then undergo liver cell egress and are released in the blood stream.

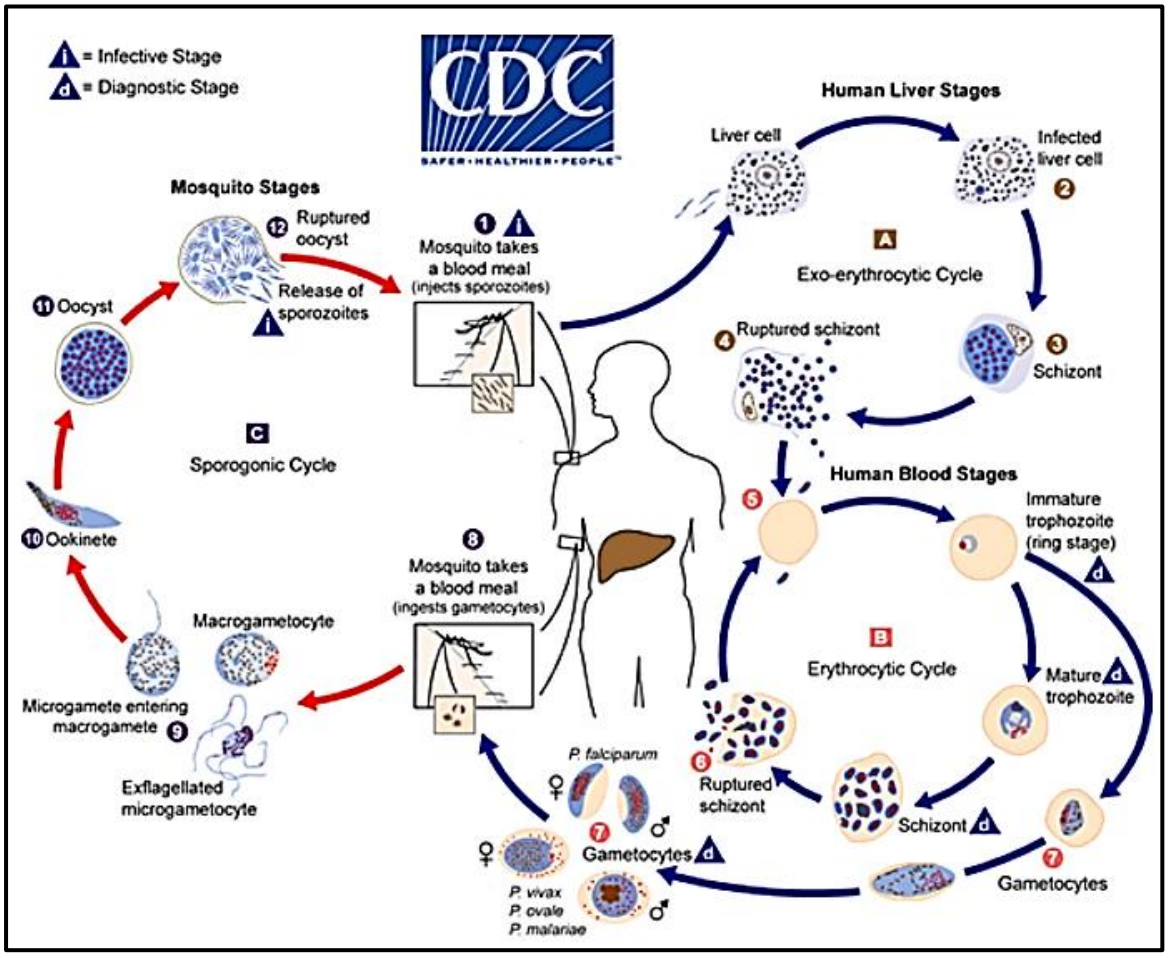

Figure 1. 1 Life cycle of *Plasmodium falciparum*. A) Pre-erythrocytic schizogony in liver of host, B) Erythrocytic schizogony in erythrocytes of host and C) Sporogony cycle in mosquito vector. (Source CDC-Centers for Disease Control and Prevention)

Some *Plasmodium* species like *P. vivax* and *P. ovale* have tendency to halt their life cycle before exoerythrocytic schizogony. This dormant stage, termed as 'hypnozoite', will invade liver cells but does not multiply within it for several weeks to months. The hypnozoites undergo reactivation later and undergo schizogony causing a relapse of infection. The situation termed 'recrudescence' comes to play during relapse which literally means the revival of material which was previously stabilized; parasitemia in case of malaria (CDC - Malaria).

The mature merozoites experience surface molecular changes and express certain proteins, which make them capable of invading the host erythrocytes. The erythrocytic

schizogony is the blood stage replicative cycle, which starts form the early trophozoite stage, morphologically ring shaped. The trophozoites feed on the host RBC cytoplasm and enlarge to occupy most of the RBC. The hemoglobin is degraded to heme and globin peptides by enzymes present in the food vacuole, the amino acids from globin are used by the parasite. The free haem, being toxic to parasites, is polymerized to form haemozoin, which appears like a pigment in the infected cell. Schizogony occurs as in the liver stage and the merozoites are released upon rupture of infected RBCs. These merozoites restart erythrocytic schizogony by infecting fresh RBCs. Each event of erythrocyte rupture is often associated with the intermittent fever in the host. The infected erythrocytes of specifically *P. falciparum* parasite in trophozoite and schizont stage can adhere to endothelial lining of blood capillaries in vital organs such as brain, heart and lungs. This prevents clearance of parasites from host and is associated with a complex condition termed cerebral malaria.

Some of the schizonts get commited to form gametocytes; the merozoites released from these schizonts will ultimately differentiate to form macro or microgametocytes. These gametocytes require the environment inside the body of mosquito to differentiate; else, they undergo death and disappear from circulation. The gametocytes, if taken up by mosquito during blood meal, reach midgut to form mature macro/micro gametes (gametogenesis). The microgamete undergoes flagellation and becomes highly motile, allowing it to migrate and fuse with the macrogamete, forming the zygote, which develops into a motile, invasive stage termed ookinete that invades the midgut epithelium and settles in the basal lamina.

The ookinete develops into oocyst, which undergoes asexual reproduction to form thousands of sporozoites (sporogony). Upon maturation, the oocyst bursts to release motile sporozoites, which penetrate the basal lamina of midgut and reach the body cavity (haemocoel). These sporozoites have the recognition molecule, which help them adhere to salivary gland. They invade the salivary gland and stay in its lumen, which passes into the vertebrate host during the new blood meal, thus starting a new cycle.

1.1.3 Host parasite interaction

Plasmodium, being an intracellular parasite, has continuous interactions with the host and makes modifications in the host as well as in itself, to complete its multi-stage lifecycle. The host-parasite interactions involve the parasite entering the host cell and then modifying the host cell, i.e.

A) Host erythrocyte invasion
B) Host erythrocyte modification

Plasmodium, being an apicomplexan parasite, has apical organelles (micronemes, rhoptries and dense granules) for host erythrocyte invasion. Among the motile and invasive forms of *Plasmodium*, sporozoite, merozoite and ookinete have similar mechanisms of invasion. Invasion of erythrocytes by merozoites is a rapid (only about 20 seconds) and specific process during which several molecular processes occur consecutively (Figure 1.2). Merozoite has different surface proteins, which mediate its attachment to the host erythrocytes; the most characterized one is the Merozoite Surface Protein-1 (MSP1). The reorientation of parasite occurs such that the apical end, containing apical organelles, attaches to the host cell. Simultaneously, the erythrocyte membrane invaginates itself allowing the entry of parasite. The secretory proteins from apical organelles come into play during this stage among which Apical Membrane Antigen-1 (AMA1) and Rhoptry neck (RON) proteins are most studied. These adhesin like secretory proteins are involved in ligand-receptor interactions and form tight junctions. The erythrocyte cytoskeleton degenerates and parasitophorous vacuolar membrane (PVM) starts to appear. The junction has a glidosome protein complex which confers the gliding motility to merozoites and ultimately entry into the host erythrocyte by closure of PVM and erythrocyte membrane (Gratzer & Dluzewski, 1993).

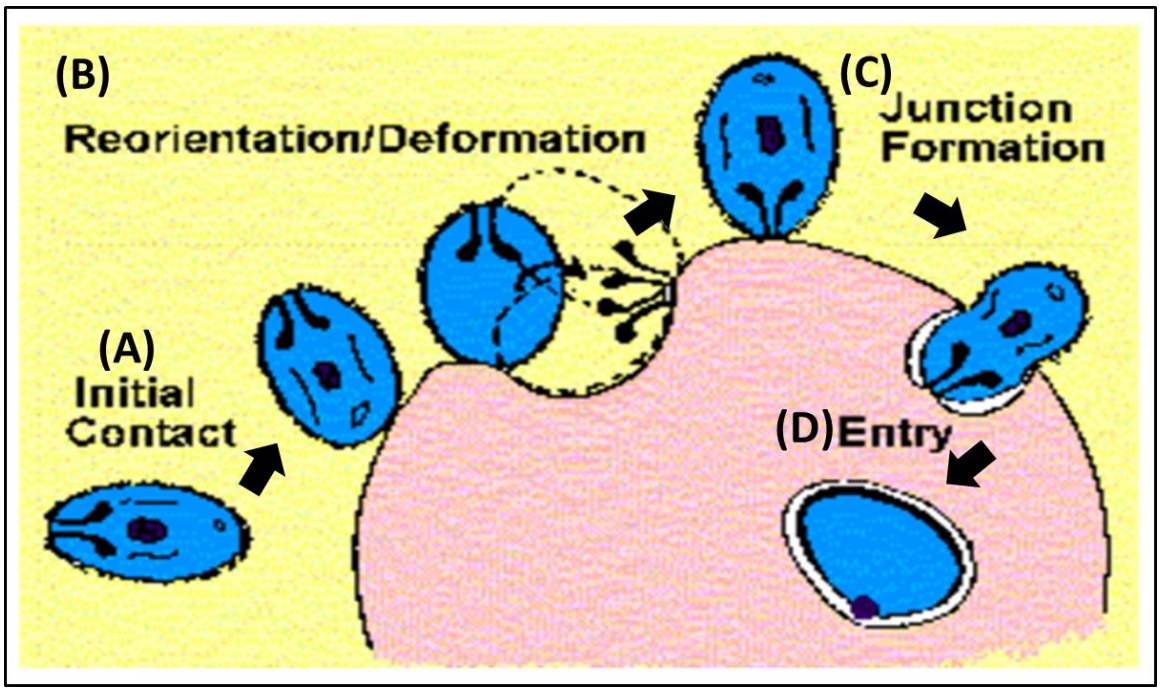

Figure 1. 2 Invasion of erythrocyte by merozoites. The merozoites come in contact (A) to the host cell by surface proteins and later reorients (B) to attach by apical end. The junction is formed (C) and parasite enters host cell (D) by gliding motility (Gratzer and Dluzewski, 1993).

1.1.4 Challenges to control and eradicate malaria

Various preventive and curative measures have been adopted till date against the deadliest parasitic disease, malaria. Use of drugs against the parasite or the mosquito

vector have had encouraging success but did not eliminate the disease. However, the emergence of drug-resistance in parasites against the commonly used drugs like chloroquine, mefloquine, sulphadoxine, pyrimethamine is a real threat. At present, the treatment of *Plasmodium* infection relies on the artemisinins-based drug combinations. New hope has come with the RTS,S, a recombinant circumsporozoite protein based malaria vaccine, approved by European Medicines Agency (EMA) to be implemented from 2018 in Africa. For the long term and effective protection, search for a potential vaccine candidate is ongoing but limited success is achieved due to the complex life cycle of *Plasmodium* and the lack of thorough understanding of parasite biology and immunological responses to the parasite.

1.1.5 AMA1 as a potential vaccine candidate

AMA1 is a conserved integral membrane protein secreted by micronemes of apicomplexan parasites. During invasion, AMA1 is exposed on the merozoite membrane while RON protein complex is injected into the host cell. The RON protein component exposes itself and acts as a receptor for AMA1 binding (Figure 1.3). AMA1-RON forms a tight junction, which might form the glidosome later. (Reviewed in Devine et al., 2017).

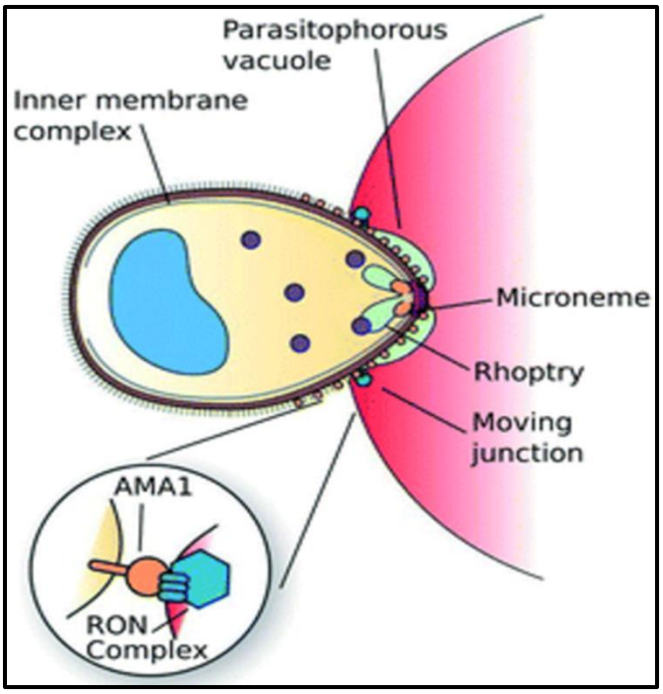

Figure 1. 3 Role of AMA1 in host cell invasion. AMA1 binds to the RON (Roptry Neck ptotein) complex on host cell membrane injected by itself which later forms gliding junction.

Failure to generate AMA1 knockout parasite suggested essentiality of AMA1 (Triglia et al., 2000). However, contradictory result have also been reported (Bargieri et al., 2013), which indicate that AMA1 has no role in erythrocyte invasion and AMA1-RON complex is not essential but might be important. However, one cannot deny the fact that anti-

AMA1 antibodies have inhibited invasion and parasite growth in-vitro (Richard et al., 2010). Several AMA1 inhibitory drug discovery approaches are also undergoing but is challenging due to lack of molecular structure of small molecule complexes (Devine et al., 2017).

1.1.6 Autophagy

The term 'autophagy' is derived from the Greek word meaning 'eating of self' and was first coined by Christian de Duve in 1963 when he observed degradation of mitochondria and other intra-cellular structures within lysosomes of rat liver perfused with the pancreatic hormone glucagon (Glick et al., 2010). Autophagy involves the degradation of intracellular macro molecular components in lysosomes (or vacuole in yeast and plants). Autophagy is a self-degradative process in a cell in response to nutrient stress. In other prospects, autophagy is a salvage pathway for amino acid synthesis and energy balance. Autophagy is a multifunctional pathway involved in regulating cellular homeostasis, cell metabolism, growth, development and the balance between cell survival and cell death. Autophagy is induced by starvation and stresses (Hain & Bosch, 2013).

1.1.7 Types of autophagy

Yeast (*Saccharomyces cerevisiae*) is the most studied eukaryotic model organism for autophagy. Depending upon the size of cargo engulfed by autophagic body, the principle types are macroautophagy, microautophagy and micronucleophagy (Figure 1.4). Macroautophagy is the engulfment of bulk cytoplasm or the larger organelles into autophagosome. After engulfing, the autophagosome fuses with the vacuole forming an autophagic body. During microautophagy, the organelles to be degraded, like peroxisomes and plastids, come along the vacuolar membrane and are engulfed by the invaginating membrane. Micronucleophagy is also a similar process of engulfing the nuclear envelope and content. In all types of autophagy, the cargo is degraded by hydrolases inside the vacuole. The salvage pathway results in new metabolites, i.e., amino acids, sugars, and nucleotides that are transported into the cytoplasm later and used either as a source of energy or as building blocks for the synthesis of new macromolecules (Reggiori & Klionsky, 2013). In other prospects, autophagy can be selective or non-selective process. The non-selective microautophagy involves the vacuolar invagination and formation of intravacuolar vesicles followed by degradation while the selective cargo like mitochondria, nucleus, and peroxisomes is directly taken up by vacuole and subsequently hydrolyzed.

1.1.8 Molecular insights on autophagy

The autophagy machinery is regulated by about 35 autophagy related genes written as ATG and the components that interplay can be divided into five systems:

1. ATG1-ATG13 kinase complex- forms the inner core, activated by starvation
2. ATG9 vesicle proteins- recruits transmembrane ATG9 protein
3. PI3K complex (ATG6/14/38, Vps15/34)- forms PI3P required for following complex
4. ATG2-ATG18 complex – activates, bind to ATG9 on PAS
5. Ubl conjugation system (ATG8-phosphatidylethanolamine (PE) and ATG5-12/16)
    a. attaches to membrane, lipid PE binds to outer surface

The autophagy pathway is studied in yeast model in detail (Figure 1.5). One of the most important inducing factor of autophagy is nutrient starvation, as the first signaling condition for autophagy; ATG13 is inactive during nutrient enriched condition due to hyperphosphorylation by the target of rapamycin complex 1 (TORC1) kinase. Therefore, the starvation or rapamycin treatment inhibits TORC1, thus hypophosphorylating ATG13 activates and recruits other core components like ATG1 and ATG17 at the phagophore assembly site (PAS). After the core assembly, the only transmembrane component of autophagy machinery, ATG9, along with other proteins like transport protein particle III (TRAPPIII) and coat protein complex II (COPII) nucleates the core machinery. The phosphoinositide-3-kinase (PI3K) complex-I generates the phosphatidylinositol-3-phosphate (PtdIns3P) that is required to recruit other factors involved in phagophore elongation, such as the ATG2–ATG18 complex and the ATG8–phosphatidylethanolamine (ATG8–PE). Because of this membrane expansion, cargo destined for autophagy is surrounded by membrane and engulfed into a double-membrane vesicle called the autophagosome. Autophagosomes then transport to vacuoles in yeast (lysosomes in higher animals). Docking and fusion of the outer membrane initiates the formation of a double-membrane phagophore that is degraded by hydrolases (Farré & Subramani, 2016).

1.1.9 ATG18 in Saccharomyces cerevisiae

ATG18 is a peripheral membrane protein, which has 7 WD40 (tryptophan-aspartate) repeats forming a 7 bladed β-propeller (Figure 2.6). Through a conserved phenylalanine–arginine–arginine–glycine (FRRG) motif in β-propeller, ATG18 binds to both PtdIns3P and PtdIns(3,5)P2, and this binding is essential for its localization to the preautophagosomal structure (PAS) (Nair et al., 2010). ATG18 localizes to both the PAS and to punctate structures at the vacuolar membrane, and also suggested to be involved in cytoplasm to vacuolar targeting (cvt) pathway (SGD Saccharomyces Genome Database, 2017). ATG18 in yeast is found to be a non- essential gene as the knockout of ATG18 was found to have slow autophagy but did not completely bypass or inhibit the growth and development.

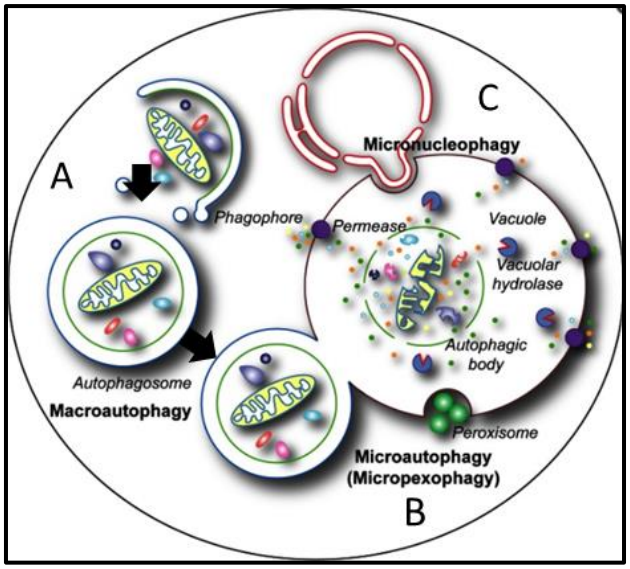

Figure 1. 4 Major autophagy types in yeast, A- macroautophagy (phagophore develops around cargo to form autophagosome and fuses to vacuole), B- microautophagy (engulfment of organelles by vacuole; here micropexophagy to engulf peroxisome is shown) and C- micronucleophagy (engulfs nuclear envelope and then its content) (Reggiori & Klionsky, 2013)

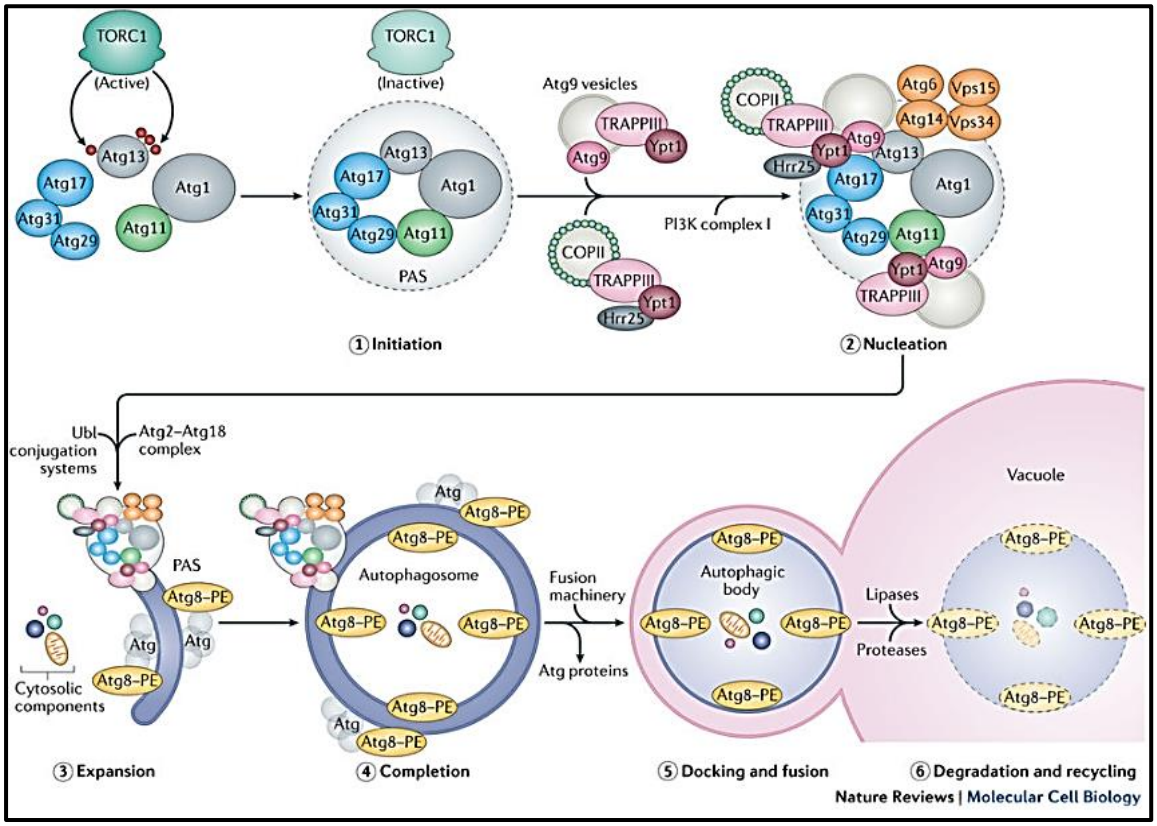

Figure 1. 5 Autophagy pathway in yeast. (1) Initiation: As autophagy signal induces by starvation, the initiation molecules involving ATG1-ATG13 kinase complex accumulate (2) Nucleation: Initiating molecules form core which is nucleated by transmembrane ATG9 vesicle proteins (3) Expansion: The membrane recruits PI3K complex and ATG2-ATG18 complex to further expand (4) Completion: Ubl conjugation system i.e. ATG8-phosphatidylethanolamine also involves to complete the membrane and engulf cargo forming autophagosome (5) Docking and fusion with vacuole and (6) Degradation and Recycling of cargo starts by vacuolar hydrolases. (Farré & Subramani, 2016)

1.1.10 Autophagy in *Plasmodium*

The homology search of yeast ATG proteins as queries against *Plasmodium* database (PlasmoDB : The *Plasmodium* Genomics Resource, 2017) gave many hits, predicting the presence of autophagy repertoire. The proteins involved in induction, core formation (nucleation), phagophore assembly, autophagosome formation have already been predicted in *Plasmodium* (Navale et al, 2014). Moreover, the presence of autophagy in multiple stages of parasite development is predicted based on the presence of transcripts and peptide fragments. Therefore, studying the effect of autophagy related proteins on the parasite growth and development becomes crucial. The identification of therapeutic drugs targeting the proteins of autophagy machinery holds a great future prospect. *Plasmodium* ATG18, if found to be essential, it would serve the purpose of study.

1.1.11 Introduction to genome editing

The method of predicting gene function by manipulating the genome is called as reverse genetics. Among various gene manipulation techniques, the ones used in this study are introduced below.

Gene knockout can simply be referred to as deletion or complete removal of a gene from the target organism. This refers to the removal of both allele of a gene in case of a diploid organism. Thus, the effect of knocking out a gene would help to determine its original function by studying the appearance of change in any phenotype of the organism. Gene knockout is an important technique to study the roles of genes which has been sequenced but their function is still unknown. Gene knockout is a method of creation of transgenic animal and knockout mice has been used for various researches so far. The gene knockout is done in the single cell stage to make knockout mice.

Gene knockin can simply be referred to as insertion of a foreign gene to desired organism. Gene knockin is done such that the TARGET gene sequence is not altered, and the foreign gene is inserted before or after the coding region of TARGET. In a particular region, the targeted gene is knocked in to know the function as well as interaction among them. Generally, Green Fluorescent Protein (GFP) coding gene is inserted to a TARGET gene such that TARGET-GFP fusion protein is formed. This helps to study the protein interaction (effect of fusing GFP to TARGET) and predicts the expression, localization and function of TARGET protein at different stages of life cycle.

Gene knockdown is also like gene knockin, however in knockdown the inserted gene contains a regulatory gene which allows to control the expression of TARGET. The TARGET gene sequence is not altered or deleted but only its expression is controlled.

These all gene manipulation techniques are done by homologous recombination and the construct has a selectable marker gene, which allows distinguishing recombinants from non-recombinants.

1.2 Rationale of the study

The essentiality of AMA1 has been established mostly in *P. falciparum*, so knockout of AMA1 was not done in *P. berghei*. In this study, we attempted to generate *Plasmodium berghei* AMA1 knockdown (KD) parasite by regulating the protein levels using a *E. coli* destabilizing domain (cDD) fused to the C-terminal of AMA1-eGFP. The rationale was that AMA1 KD *P. berghei* merozoites would not be able to invade erythrocytes in the absence of the drug trimethoprim, however it would induce strong immune response as all the other antigens would be expressed. The future prospect of this study would be to challenge the AMA1 KD parasite infected mice by the wild type parasite and analyze the potency of AMA1 KD parasites as whole organism vaccine.

Since ATG18 in yeast is important for expansion of phagophore membrane, we wanted to study its role in autophagy machinery of *Plasmodium*. In this study, ATG18 gene knockout and knockdown in *Plasmodium berghei* was attempted to find out the essentiality of ATG18, and to check the localization of ATG18 in different stages during parasite development.

1.3 Objectives

1.3.1 General Objectives

1. To generate AMA1 knockin and AMA1 knockdown *Plasmodium berghei* parasites
2. To generate ATG18 knockout and ATG18 knockdown *P. berghei* parasites
3. To confirm (characterize) the generated recombinant parasites

1.3.2 Specific Objectives

1. To study the presence of AMA1 and ATG18 protein family in *P. berghei* by bioinformatics analysis
2. To design *P. berghei* transfection construct targeting AMA1 knockin and AMA1 knockdown
3. To design *P. berghei* transfection construct targeting ATG18 knockout and ATG18 knockdown
4. To generate recombinant parasites by transfection in *P. berghei*
5. To confirm the AMA1 knockin, AMA1 knockdown, ATG18 knockout and ATG18 knockout recombinant parasites if generated

1.4 Research hypothesis

1.4.1 Null hypothesis

The AMA1 recombinants (AMA1 KI and AMA1 KD) and ATG18 recombinants (ATG18 KO and ATG18 KD) parasites cannot be generated by homologous recombination at AMA1 and ATG18 locus.

1.4.2 Alternative hypothesis

The AMA1 recombinants (AMA1 KI and AMA1 KD) and ATG18 recombinants (ATG18 KO and ATG18 KD) parasites can be generated by homologous recombination at AMA1 and ATG18 locus.

CHAPTER 2
LITERATURE REVIEW

2.1 Use of antimalarial drugs

The history of plant extracts for treatment of malaria dates back to the evolving of the disease itself. Many drugs were available until 1950s, but any single drug available was not effective against all developmental stages of *Plasmodium*. Considering the fact, in 1949, Malaria Subcommittee of Colonial Medical Research Committee published a recommendation on use of these drugs ("USE OF ANTIMALARIAL DRUGS," 1954)). Drugs, according to their use, were classified for destruction of pre-erythrocytic phase (pyrimethamine, biguanil), erythrocytic phase (chloroquine, mepacrine), and late exoerythrocytic phase and gametocytes (8-aminoquinolines). But in the following decades, the parasites developed resistance to many of these drugs as a result of spontaneous mutations in them which either modified the drug target or their accessibility to drug (PETERS, 1970). The overuse of drugs exposed the parasite to inadequate levels of drug and selection of resistant mutants' occurred causing evolution of drug resistance in *Plasmodium* (Watkins & Mosobo, 1993). Soon in 1998, WHO reported artemisinin and its derivatives as the most rapidly acting antimalarial drugs that are effective even against multidrug resistant *falciparum* infection replacing previously mentioned first line and second line drugs (Htoo et al., 2000; McIntosh & Olliaro, 1998; White & Olliaro, 1998). Since then, artemisinin based combination therapy came into application with high efficacy thus reduced parasite burden. However, parasites have developed resistance even against artemisinin by present date and hopes have landed to a potent vaccine to prevent morbidity and mortality.

2.2 Whole parasite vaccine approach

After the discovery of malaria parasite and its life cycle, an effective malaria vaccine has been the goal of international research. With the development of in-vitro culture of microbes, whole organism vaccine was attempted for diseases like tuberculosis, polio, measles, mumps, etc (Reviewed in Zepp, 2010). Research on whole organism blood stage malaria vaccine started on animal model in 1940s. Killed and adjuvanted *P. lophurae* and *P. knowlesi* infected RBCs were able to show protective immunity in ducks and monkeys (Sommer et al., 1947; Sommer et al., 1948). Later, protection against the human malarial parasite *P. falciparum* was also achieved in the *Aotus* monkeys (Siddiqui et al., 1979). After the need of adjuvant to enhance the immunogenicity of parasite was found, this strategy was shadowed due to lack of compatible adjuvant for human (reviewed in McCarthy & Good, 2010). After the cloning and recombinant expression of

Plasmodium sporozoite and merozoites started (Ellis et al., 1983; Kemp et al., 1983), subunit vaccine approach was booming. However, due to the further challenges in subunit vaccine, again the whole parasite vaccine approach has regained the value with new parasite attenuation methods.

2.3 Radiation-attenuated parasites

Early studies establishing the potential of radiation attenuated parasites to induce protective immunity dates back to 1960s. Radiation attenuated *P. berghei* sporozoites (RAS) isolated from gamma irradiated malaria infected mosquitoes were able to show immunity against mice (Nussenzweig et al., 1967) as well as against *Rhesus* and *Aotus* monkey later (Gwadz et al., 1979; Wellde et al., 1979). The in-vitro studies showed that RAS were able to invade liver cells but unable to undergo liver stage schizogony (Sigler et al., 1984). Soon, the *P. falciparum* RAS developed by similar strategy was taken to human trials (Clyde et al., 1973; Rieckmann et al., 1979). The protection efficiency was very low, only 5 in 1000, and the protection lasted only for about 9 weeks, so this RAS approach was discouraged considering impracticable (Hoffman et al., 2002). Recently, the radiation attenuated blood stage *P. berghei* was studied with protective immunity but later, reversion occurred to virulent phenotype causing infection (Gerald et al., 2011).

2.4 Development of gene attenuation strategies

Although the modification of *Plasmodium* genome started only after its sequencing was complete in 2002(Gardner et al., 2002), the first successful transfection was reported in 1993 on gamete and zygote stage of *P. gallinaceum* with transient luciferase gene expression (Goonewardene et al., 1993). In 1995, two groups first reported transfection of red blood cell stages of *P. berghei* (van Dijk et al., 1995) and *P. falciparum* (Wu et al., 1995). The second group reported the homologous recombination of exogenous DNA into the *Plasmodium* genome in 1996 in which pyrimethamine-resistant form of DHFR-TS was used for the selection of recombinants (Wu et al., 1996). Rather than episomal transfection, integrative transfection has been the versatile method for gene targeting. Homology of less than 300bp is enough for crossover to occur (Nunes et al., 1999) and double crossover can make deletions of large DNA fragments (Pace et al., 2000). Targeting a gene by homologous recombination may undergo single crossover (SCO) or double crossover (DCO) (Figure 2.1) (Carvalho & Ménard, 2005)

After that, the attempt to edit *Plasmodium* genome was with the flippase (Flp)/Flp recognition target (FRT) system in which excision of MSP1 gene arrested the parasite in late liver stage (Combe et al., 2009). Similar to FRT system, Cre/loxP system was used to make gene deletions in the blood stage using the Cre recombinase (Collins et al., 2013).

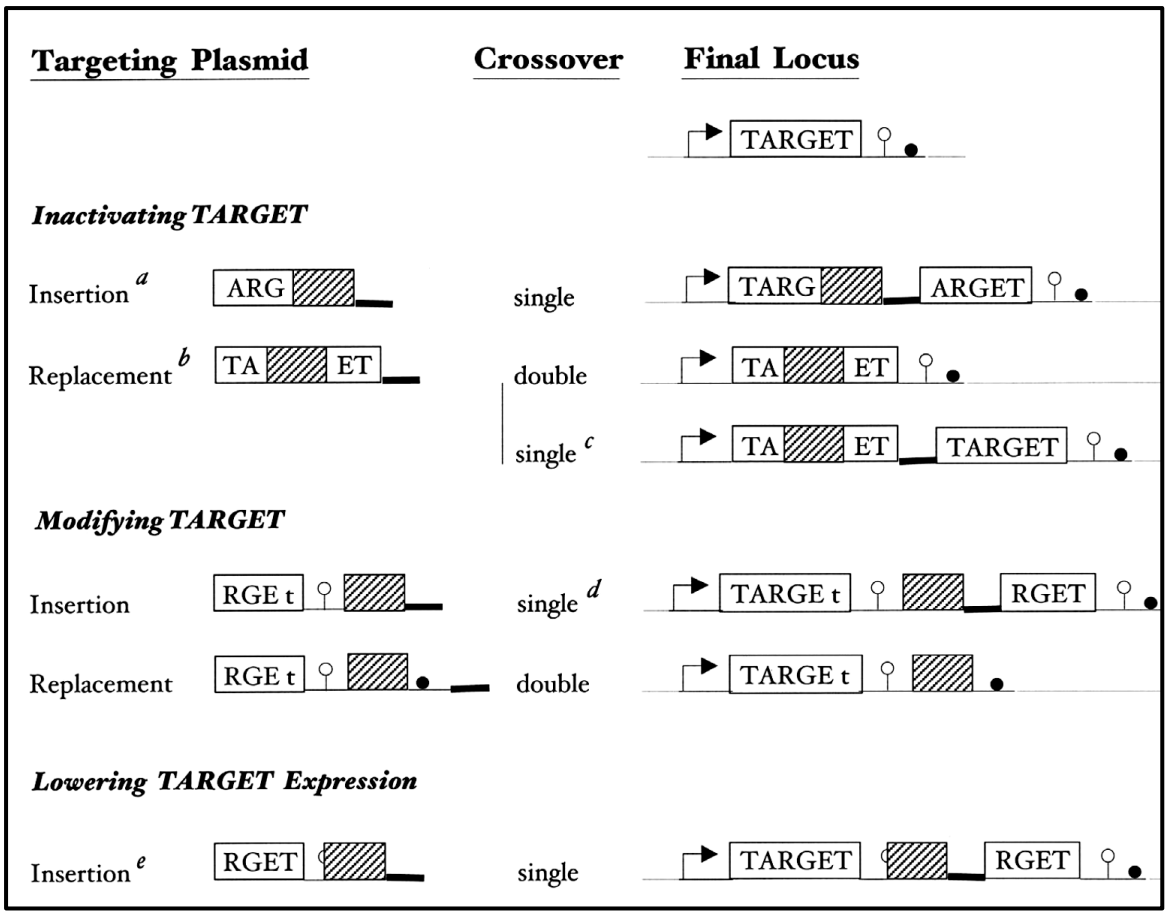

Figure 2. 1 Gene targeting in *Plasmodium* by homologous recombination. The targeted gene is named TARGET and targeting construct is in left. The selectable marker is symbolized by a grey box, the bacterial plasmid by thick lines, 5' UTR by an arrow, and the 3' UTR by an open circle. a The insertion plasmid must contain an internal fragment of the gene. b The replacement plasmid should be designed to delete part or all of the TARGET. c The single cross over (SCO) shown involves the 5' regions of homology (TA) to create a full-length target gene copy. d For the gene modification (t) to be recovered in the first, expressed and full-length duplicate, the SCO must occur upstream from the modification. e The 3' sequence necessary for gene expression is truncated. (Carvalho & Ménard, 2005)

With the application of the CRISPR/Cas9 system for *Plasmodium*, genome editing has been more straightforward by making double strand breaks (DSB) (Ghorbal et al., 2014; Wagner et al., 2014). Recently, zinc-finger nuclease (ZFN)-induced DSB of DNA was found to result in the generation of attenuated parasite with liver stage arrest (Singer et al., 2015).

2.5 Genetically attenuated parasites

New molecular and genetic approaches to make attenuated parasite came into being only after the group of scientist led by Dr. Gardner published the genome sequence of *P. falciparum* in 2002 (Gardner, et al., 2002). Since then, the gene annotation has started and extended which is essential for understanding *Plasmodium* biology. Immunization with genetically attenuated parasites has been first reported effective in 2008 in which

P. yoelii parasite with disrupted purine nucleoside phosphorylase (PNP) gene was generated (Ting et al., 2008). Since then, many other genes like nucleoside transporter 1 (NT1) involved in purine transport (Aly et al., 2010), plasmepsin-4 involved in hemoglobin digestion (Spaccapelo et al., 2010), and other virulence genes like PfEMP1, MSP, AMA have been modified to study the immunogenicity of attenuated parasites (Stanisic & Good, 2015). However, the search for more potent virulent gene for attenuation is still a big research question.

2.6 *Plasmodium berghei* as a model organism

The taxonomic classification of *P. berghei* is as follows: Domain: Eukaryota, Phylum: Apicomplexa, Class: Aconoidasida, Order: Chromatorida, Family: Plasmodiidae, Genus: *Plasmodium*, Species: *P. berghei*. (Source: Taxonomy - NCBI)

P. berghei is the first rodent malaria parasite identified by Vincke & Lips in 1948. Since then three other species, *P. yoelii, P. vinckei* and *P. chabaudi* have been identified and being studied. The rodent malaria parasites are used for the study of mammalian malaria due to their similarity in structure, physiology and life cycle. The most significant reason for the study on rodent malaria parasite like *P. berghei* would be that they do not infect humans and rodents also being mammals, the basic infection biology is the same. With the development of in-vitro culture of parasite blood stages, direct study would be more relevant however; strict supervision and control methods need to be adopted for preventing infection. Thus, the rodent parasites are established as a valuable parasite model to study life cycle of parasite, host-parasite interaction and drug and vaccine development. As the life cycle, genome organization and metabolic pathways of all mammalian malaria parasites is conserved, its use as a model organism seems to be equally convenient with lesser risk of infection and reduced cost of culture in biosafety lab (Ager, 1984).

The rodent malaria parasites are slightly different in morphology, development cycle, size and iso-enzymes. To study different aspects of human malaria, immunopathology, experimental cerebral malaria are studied in *P. berghei* as it causes severe pathology; drug testing is done in *P. chabaudi* as it causes chronic but non-lethal infection while liver stage infection and immunity is studied in *P. yoelii* (Leiden Malaria Research | LUMC, 2017.).(Leiden Malaria Research | LUMC, 2017.).

2.7 Review of AMA1

To target some of the plasmodia antigens, synthesis and test of antibodies started in 1980s. In 1982, a merozoite surface antigen of *P. knowlesi* was found to react efficiently with the produced monoclonal antibody, thus inhibiting in-vitro growth of the parasite

(Deans et al., 1982; Deans et al., 1984). Biosynthesis of PfAMA1 was known to occur in the micronemes in the late schizont stage undergoing few processing to express in the merozoites surface (Bannister et al., 2003; Peterson et al., 1989). After discovering its presence in all apicomplexans and undergoes cleavage while trafficking to merozoites membrane, it got its name apical membrane antigen (Narum & Thomas, 1994). Discovering the involvement of *Toxoplasma gondi* homologue of AMA1 in host cell invasion (Hehl et al., 2000) led to the more robust research on structural and functional aspect of AMA1. The study of AMA1 structure were already started (M. Nair et al., 2002) and was completed when the crystal structure of PvAMA1 was reported (Pizarro et al., 2005). Then more attempts have been made to study AMA1 has therapeutics target as well as vaccine candidate. In the molecular mechanisms of invasion, it is predicted that AMA1 is exposed on the merozoite membrane while RON protein complex is injected into the host cell. The RON protein component exposes itself and acts as a receptor for AMA1 binding (Srinivasan et al., 2011).

2.8 Sequence and structure of PbAMA1

PbAMA1 gene is 1671 bps long and has no intron (Figure 2.2). The UTR sequences of the AMA1 gene has not been annotated in the PlasmoDB, so their exact size is not clear.

Figure 2. 2 Diagrammatic representation of *P. berghei* AMA1 gene locus, showing 5' UTR, full length exon without introns (1671bp) and 3' UTR region. The size of UTRs of AMA1 gene has not still been annotated in PlasmoDB.

The transmembrane protein AMA1 is one of the most studied protein in Apicomplexa phylum. It is believed to be unique to apicomplexan and is a structurally conserved protein of length 560 in most *Plasmodium* species (except 622 aa in *P. falciparum*) (Hodder et al., 1996). AMA1 is an integral membrane protein with short C-terminal of protein (50 aa length) lying inside the cytosol and has conserved Tyr residues. The N-terminal ectodomain of protein contains conserved 30 cysteine residues which folds by disulfide bond between cysteine residues to form prosequence and three domains; DI, DII and DIII (Remarque et al., 2008). Structural polymorphisms are found but they lie on the surface towards one side (Chesne-Seck et al., 2005). AMA1 is shown to be essential for host cell invasion by several groups and is a long standing malaria vaccine candidate (Triglia et al., 2000).

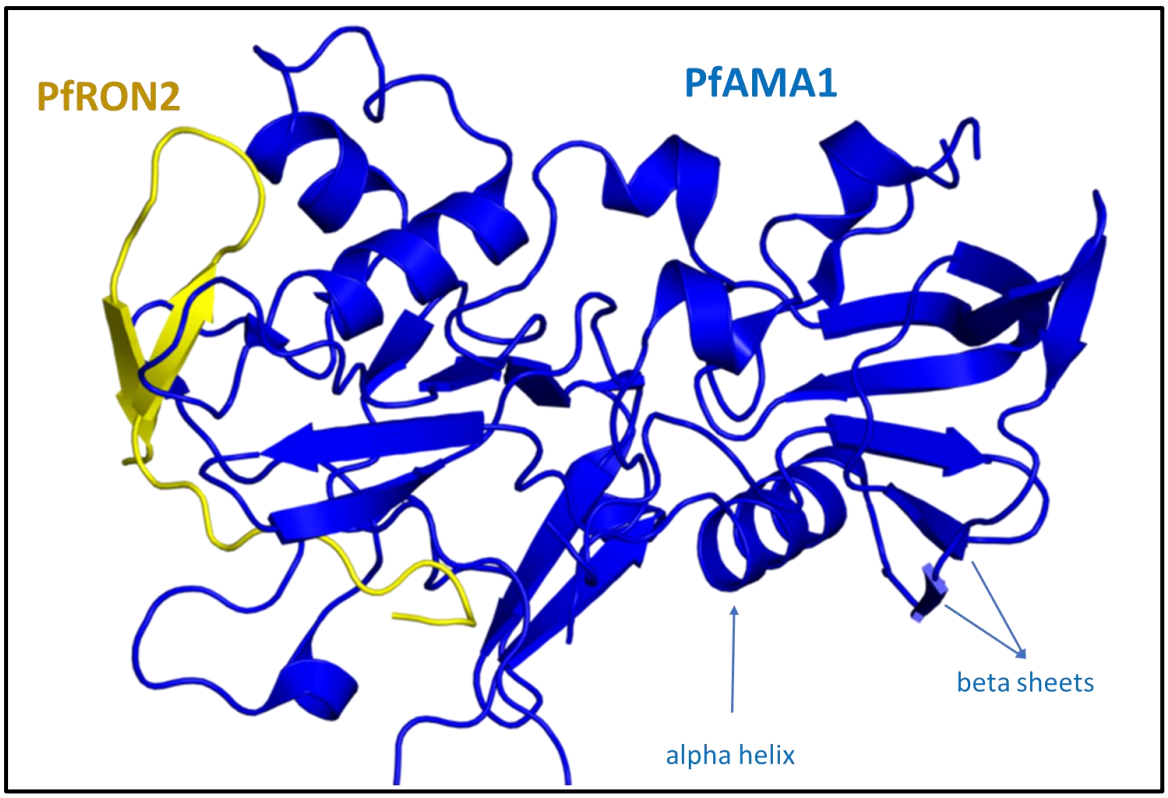

Figure 2. 3 Crystal structure of *Plasmodium falciparum* AMA1 (blue) in complex with 29aa *PfRON2* peptide (yellow) [PDB entry 3SRI]. The figure is 1.6 A^{o} resolution X-ray crystallography image. AMA1 is heterodimeric with secondary structures alpha helices, beta sheets and turns while RON2 is with beta sheets and turns. (Source RCSB PDB ID 3SRI)

The structure of *Plasmodium falciparum* AMA1 is reported in part (Source- Uniprot database). Among the full-length 622 amino acids (aa), first 24 aa is signal peptide while extracellular (25- 546), transmembrane (547- 567) and cytoplasmic (568-622) domains are reported among which extracellular segment forms domains I, II and III. 3D structure of protein is available for segment 97-442 (Source- Protein DataBank PDB ID 3SRI- Figure 2.3) which reports the preferred assembly of AMA1 as heterodimer.

2.9 Autophagy in *Plasmodium*

Autophagy was reported in *P. falciparum* and *P. vivax* infected human liver tissues for the first time by Brito et al.(1969) where pigment clumping was observed in different sized food vacuoles. Autophagic cell death induced by chloroquine and artemisinin treatment was postulated in 2000s (Chen et al., 2000; Totino et al., 2008). Although autophagy has been established as a multifunctional pathway in eukaryotes, its selective advantage is not clear in *Plasmodium*. However, bioinformatics analysis have found the orthologues of autophagy proteins like ATG1, ATG3, ATG7, ATG8, ATG18 and others in *Plasmodium falciparum* (Reviewed in Hain & Bosch, 2013). Functions of many of the plasmodial ATG genes are still a topic of research while ATG8 has been established as the autophagy marker protein playing role in autophagosome-lysosome fusion

(Kitamura et al., 2012; Navale et al., 2014). There has not been much study on essentiality of *Plasmodium* ATG18 after which it can be targeted for therapeutics to prevent parasite growth.

2.10 Review of ATG18

Unlike AMA1, ATG18 is not involved in the pathogenesis; autophagy is rather a housekeeping mechanism developed by eukaryotes to regulate cellular homeostasis and maintain balance between cell life and death. Therefore, it is obvious that ATG18 homologue might be present in all eukaryotes with similar function. A partial autophagy machinery in *Plasmodium falciparum* was reported based upon the identified homologs of autophagy repertoire. Similar to ScATG18, PfATG18 also has phosphatidylinositol 3-phosphate (PtdIns3P) binding motif (FRRGT), WD40 repeat domains and ATG8-family interacting motifs (AIM) (Navale et al., 2014).

PbATG18 gene is 1247 bps in size with a single intron of 104 bps (Figure 2.4). The gene structure is as Exon 1- 130 bp, Intron 1- 104 bp and Exon 2-1013 bp. The UTR's of ATG18 gene has not been annotated, so their exact sizes are not known (Source- PlasmoDB).

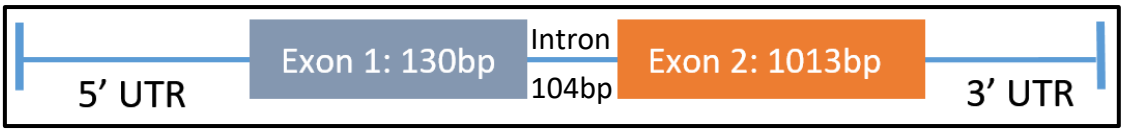

Figure 2. 4 Diagrammatic representation of *P. berghei* ATG18 gene locus, showing 5' UTR, exon1 of 130bp and exon2 of 1013 bp with 104bp single intron in between the exons and 3' UTR region. The size of UTRs of *ATG18* has not still been annotated in PlasmoDB.

Although the reviewed PDB entry for *Plasmodium* ATG18 is not present and crystal structure of ATG18 is not yet available, its yeast homologue has been studied. In yeast, ATG18 is 500 aa long and UniProt annotates the first 377 aa to be involved in forming beta-propeller domain with specific binding to phosphatidylinositol 3,5-bisphosphate (PIP2), leading to the association of the protein to the membrane. The FRRGT-motif (284-288) is essential for the cytoplasm to vacuole transport (Cvt) pathway.

The ATG2-ATG18 complex would localize to expanding membrane through these pockets forming highly curved membranes (Figure 2.5) (Suzuki et al., 2017).

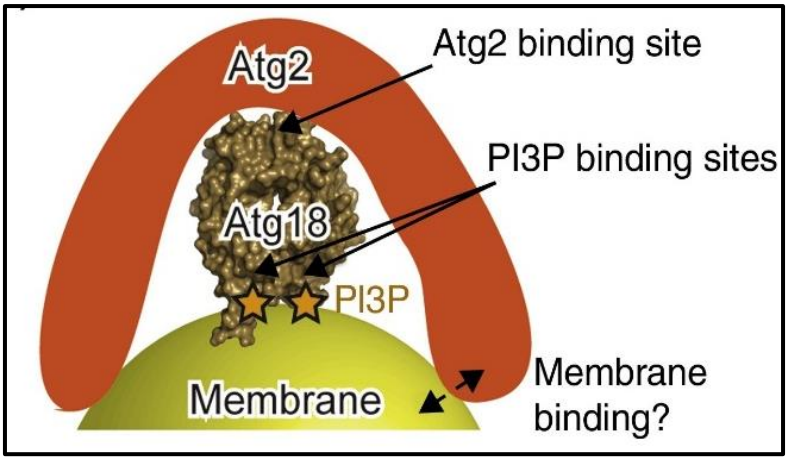

Figure 2. 5 Model of the ATG2–ATG18 complex on the curved membrane. The binding of ATG18 to vacuolar membrane through two PI3P (phosphatidylinositol-3-phosphate) binding site is shown. The presence of membrane binding site in ATG2 molecule is still in research. (Suzuki et al., 2017)

The shown crystal structure of yeast ATG18 (Figure 2.6) also do suggests ATG18 to have seven bladed beta-propeller with two binding pockets for PI3P. The structure of yeast ATG18 is reviewed here as *Plasmodium* ATG18 structure has not been resolved and they are the homologous to each other.

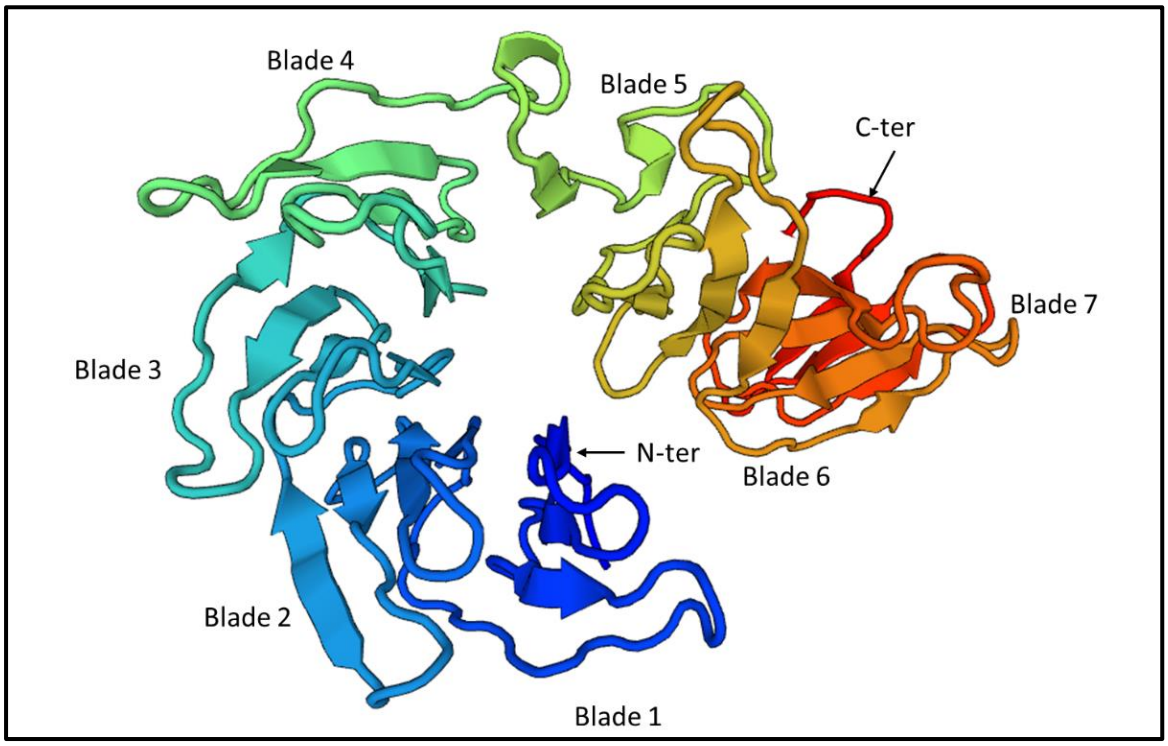

Figure 2. 6 Crystal structure of yeast ATG18 protein (PDB P43601). The coloured cartoon is viewed with JavaScript Protein Viewer (PV) in rainbow spectrum from N-terminus (blue) to C-terminus (red). The seven-bladed beta propeller structure is seen in colour. Source- Swiss-Model Repository (SMR) for PDB P43601.

CHAPTER 3
MATERIALS AND METHODS

3.1 Materials

All the biochemicals were from Sigma, Serva or SRL Biosciences unless mentioned otherwise. The bacterial culture media Lauria Bertani (broth and agar) were from ThermoScientific. PCR reagents and restriction endonucleases were from New England Biolabs (NEB), ThermoScientific, Jonaki and Takara. PCR primers were purchased from Bioserve or Euofins. The Gel extraction, PCR clean-up and Plasmid purification kits were from Machery-Nagel, Qiagen and Agilent.

Plasmodium berghei ANKA strain was obtained from the Malaria Research and Reference Reagent Resource Center (MR4), Virginia, USA. Balb/c mice were obtained and maintained at the Animal House Research Facility of CCMB. Cell culture media, supplements and Nucleofector Transfection kit were from Lonza or Gibco. Primary antibodies (anti-GFP, anti-HA), secondary antibodies (Alexa fluor 488/594 conjugated anti-rabbit), DAPI and ProLong Gold anti-fade were from Invitrogen and ThermoScientific. PVDF membrane was from Millipore. SuperSignal West Femto and Pico Chemiluminescent kits were from ThermoScientific.

3.2 Bioinformatics study of AMA1 and ATG18

First, the reviewed protein sequence for PfAMA1 (P50489) was retrieved from UniProt database (*P. berghei* AMA1 sequence is not reviewed) and the protein sequence was viewed in Pfam database (http://pfam.xfam.org). AMA1 being unique to Apicomplexa phylum, the *Plasmodium* species affecting human (*P. falciparum* and *P. vivax*), rodent (*P. berghei*), primates (*P. knowlesi*) and birds (*P. relictum*), and other apicomplexans like *Toxoplasma gondi*, *Eimeria tenella* were selected, and used as query in BLAST searches of the genomes of other malaria parasites at PlasmoDB (http://plasmodb.org), and ToxoDB (http://toxodb.org) databases.

The hits with maximum scores were selected, their protein sequences were retrieved and were used as queries in reverse BLAST searches using the Conserved Domain Architecture Retrieval Tool (CDART) at NCBI (https://www.ncbi.nlm.nih.gov/Structure/lexington/lexington.cgi?cmd=rps) to identify conserved domains and substantiate their authenticity as AMA1 proteins. Further confirmation of the similarity in domains was done by identifying the type of hits using Batch Web CD-Search Tool at NCBI (https://www.ncbi. nlm.nih.gov/Structure/bwrpsb/bwrpsb.cgi).

The sequences were aligned using the Clustal Omega (https://www.ebi.ac.uk/Tools/msa/clustalo) and edited manually, and the identified proteins were annotated as homologs of the best matching *Plasmodium* apical membrane antigen proteins.

For ATG18 homolog study, no reviewed sequence of *Plasmodium* is available, so the starting sequence was of yeast ScATG18 (P43601) from UniProt database. The same procedure and tools were used for sequence analysis as for AMA1. The protein sequence was viewed in Pfam database. ATG18 being present in all eukaryotes, its homolog in human WIPI1 (UniProt: Q5MNZ9) was retrieved. The putative ATG18 protein sequence of *Plasmodium berghei, P. falciparum, P. vivax*, *P. knowlesi*, *P. relictum* and another apicomplexan *T. gondi* was selected, and used as query in BLAST searches of the genomes of malaria parasites at PlasmoDB and ToxoDB databases. The identified protein sequences were reverse blasted in CDART at NCBI to identify the conserved domains. Multiple sequence alignment with ClustalOmega was done to identify the percentage identity between the putative sequences.

3.3 Preparation of bacterial culture media

3.3.1 Luria Bertani broth:

It contains 1% bacto-tryptone, 1% NaCl and 0.5% bacto-yeast extract. Required amounts of these components were added to Milli Q water, pH was adjusted to 7.2, volume was adjusted to desired level, and the media was autoclaved at 121°C, 15 lbs pressure for 15-20 minutes. The media was stored at room temperature until further use.

3.3.2 Luria Bertani agar

LB agar contains 1.5 % agar in LB broth. To prepare LB agar, required amount of agar was added to LB broth (prepared as described above), volume was adjusted to required level, and the suspension was autoclaved at 121°C, 15 lbs pressure for 15-20 minutes. The media was stored at room temperature until further use.

3.3.3 Ampicillin stock solution (100 mg/ml)

A 1000 X stock solution of ampicillin (100 mg/ml) was made in sterile milliQ™ water. Required amount of ampicillin powder was added to milliQ™ water, the suspension was vortexed to dissolve the powder, volume was adjusted, and the solution was sterilized by filtering through a 0.22 µm sterile filter membrane in the laminar hood. The solution was aliquoted (1 ml) in 1.5 ml microcentrifuge tubes, and stored at -20°C until further use.

3.3.4 LB Ampicillin plates

Whenever required, LB Agar was melted by heating, allowed to cool to 45-50°C, and required volume of the ampicillin stock (1000X) was added such that the final concentration is 100 µg/ml. This was poured into Petri plates (~25 ml per plate) inside the laminar hood and the media was allowed to solidify inside airflow of laminar hood. The plates were used immediately or stored at 4°C until further use (for maximum 2 weeks).

3.3.5 Super Optimal Broth (SOB) and SOB with Catabolite repression (SOC)

SOB media contains 2% tryptone, 0.5% yeast extract, 10 mM NaCl, 2.5 mM KCl. Required amounts of these components were added in milli-Q water, pH was adjusted to 7.2, and volume was adjusted to the desired level. The medium was autoclaved. $MgCl_2$ and $MgSO_4$ solutions were prepared separately and autoclaved as described above, and added to the media at a final concentration of 10 mM. SOB was used for growing competent cells.

For SOC, sterile glucose stock was added to SOB at a final concentration of 10 mM.

3.4 General laboratory protocols

3.4.1 Polymerase chain reaction (PCR)

PCR was done for amplification of target sequences, verifying the presence of the insert and orientation of insert using appropriate template and primers. High fidelity DNA polymerase was used to amplify target sequences for cloning and Taq DNA polymerase for routine PCR. Initial 2-5 cycles were at 95°C for 5 minutes /94°C for 30 seconds/55°C for 30 seconds/72°C for 2 minutes (step 4), the next 30 cycles were at 94°C for 30 seconds/58°C for 30 seconds/72°C for 2 minutes, followed by final extension at 72°C for 10 minutes. Annealing temperature and extension duration were varied if required.

3.4.2 Gel extraction and PCR clean-up of DNA

The desired DNA band from the agarose gel was excised and transferred to a 2ml microcentrifuge tube. 20 µl/mg of the gel slice of N1 solution was added and incubated at 55°C for 5 minutes to dissolve the gel. The solution was transferred to a column (Machery-Nagel™) and centrifuged at 12000 rpm for 1 minute. The column was washed with 0.6 ml of N3 wash buffer, centrifuged at 12000 rpm for 1 minute, and dried. The bound DNA was eluted with pre-warmed nuclease free water. The same protocol was followed for PCR clean up except that the volume of NT1 was 2 µl/µl of the PCR sample.

3.4.3 Ligation of DNA fragments

Restriction enzyme digested PCR products were ligated with similarly digested vectors in 1:5 molar ratio (optimized for large vector size). The ligation reaction was carried out in a 10 µl containing 1X T4 DNA ligase buffer (50 mM Tris HCl pH 7.5, 10 mM MgCl2, 10 mM DTT, 1 mM ATP and 25 mg/ml BSA) and 5 units of T4 DNA ligase. The reaction was incubated at 16°C for 16 hrs, and the ligation reaction was directly used for transformation of *E. coli* or stored at -20°C.

3.4.4 Preparation of ultracompetent cells

Ultracompetent cells were prepared according to the method of Inoue et al. A single colony of *E. coli* DH5α from a freshly streaked LB agar plate was inoculated into 5 ml LB in a 50ml tube. The culture was incubated at 37°C, 200 rpm for 16 hr. One ml of this overnight culture was inoculated into 100 ml of SOB medium and then incubated at 18°C, 200 rpm till the OD_{600} reached to 0.6. The culture was chilled on ice for 10 minutes, centrifuged at 3,000 g for 5 minutes at 4°C to pellet the cells, the pellet was gently resuspended in 32 ml of ice cold buffer I (10 mM PIPES pH 6.7, 15 mM $CaCl_2$, 250 mM KCl, 55 mM $MnCl_2$). The suspension was incubated on ice for 10 minutes, centrifuged as described above, the supernatant was discarded, and the cells were resuspended in 8 ml of ice cold buffer I with DMSO (7%). The suspension was distributed into 100 µl aliquots, flash frozen in liquid nitrogen and stored at -70°C until further use. The ultra-competent cells prepared by this method yielded a transformation efficiency of 1 x 10^8 colonies/µg of pUC18 DNA and were stable for 6 months at -70°C.

3.4.5 Bacterial Transformation

An aliquot (100 µl) of ultracompetent cells was thawed on ice. Ligation mixture (10 µl) was added to the cell suspension, mixed gently by tapping at bottom, incubated on ice for 45 minutes. The mixture was subjected to heat shock at 42°C for 90 seconds, and then the tube was placed back on ice for 2 minutes. 900 µl of prewarmed SOC media was added to the mixture and the tube was incubated at 37°C for 1 hour, 200 rpm. The cells were centrifuged for 2 minutes at 5000 rpm, 800 µl of the supernatant was discarded and the pellet was suspended in the remaining media. This suspension was plated on a LB-ampicillin plates inside the laminar hood, and allowed to dry. The plates were incubated at 37^{o}C for overnight.

3.4.6 Colony PCR

For every five colonies, 100 µl of PCR cocktail was prepared with 10 µl of 10X Taq DNA polymerase buffer, 1 µl of forward and reverse primers (100 pmol/µl), 2 µl of dNTPs (10 mM), 2 µl of $MgCl_2$ (50 mM), 1 µl of Taq DNA polymerase (5 units) and 83 µl of water.

The mixture was aliquoted into 5 PCR tubes, 20 µl each. A single bacterial colony was picked up by a 200 µl tip randomly from the agar plate, patched onto a fresh agar plate, and the tip was rinsed with the PCR cocktail. The samples were run according to the earlier PCR program and PCR products were analyzed on a 0.8 % agarose gel with ethidium bromide, and visualized on UV gel documentation system.

3.4.7 Purification of plasmid DNA

Mini scale preparation of plasmid DNA was done by the alkaline lysis method using plasmid DNA purification kits. Bacterial pellet from 5 ml overnight culture was resuspended in 0.25 ml of solution A1 (50mM glucose, 25mM Tris-HCl, pH 8.0, 100 µg/ml DNase-free pancreatic RNase), 0.25 ml of solution A2 (0.2M NaOH, 1% SDS) was added and the suspension was mixed gently till the lysate became clear. 0.3 ml of solution A3 (3M potassium acetate, 40% Guanidine hydrochloride) was added to the lysate and the contents were mixed gently, the solution was centrifuged at 12000 g for 5 minutes, the supernatant containing the plasmid DNA was transferred to a mini column. The column was centrifuged as above, washed with 0.5ml of AW solution (40% Guanidine hydrochloride and 35% isopropanol), washed again with 0.6ml of A4 wash buffer (70% ethanol). The bound plasmid DNA was eluted with 50µl of preheated nuclease free water, checked on a 0.8% agarose gel and stored at -20°C until further use. The typical yield from 5ml of culture was about 20µg.

3.4.8 Quantification of nucleic acids

The concentration of nucleic acids was estimated by measuring the OD at 260 nm (Sambrook et al., 1989) using Nanodrop Thermo 2000. The following empirical relationships was used to estimate the concentration of DNA. OD = 1 corresponds to approximately 50 µg/ml of double-stranded DNA, 40 µg/ml of RNA and 33 µg/ml of single-stranded DNA (oligodeoxynucleotides). Pure DNA and RNA preparations have OD_{260}/OD_{280} between 1.8 and 2.0. However, the DNA sample was analyzed by running in agarose for integrity.

3.4.9 Digestion of DNA with restriction endonuclease

For digestion of plasmid DNA, 500 ng - 2 µg of DNA in 20 to 40µl reaction volume was used with 2 units of desired restriction endonuclease per µg of DNA. The reaction was carried out for 4-6 hours using suitable buffers and assay conditions (temperature) specified by the manufacturers. The digested DNA fragments were analyzed by agarose gel electrophoresis.

3.4.10 Agarose gel electrophoresis of nucleic acids

DNA was resolved, depending on size, on 0.8 – 2.0% agarose gels prepared in 1X TBE buffer. Ethidium bromide (0.5µg/ml) was added to the gel before it was solidified. Appropriate amounts of 6X loading dye (0.25% bromophenol, 0.25% xylene cyanol and 30% glycerol) was added to the samples, the sample was loaded into well in the gel, and the gel was run at 100 V/cm. The nucleic acids were visualized in UV gel documentation system.

3.4.11 Plasmid DNA Sequencing

Purified plasmid DNA samples were sequenced at CCMB (Bioserve). The insert sequences were checked for authenticity by comparing with the PlasmoDB reference sequences using SnapGene® Viewer software and Clustal Omega.

3.5 Construction of HB plasmid

The transfection plasmid, HB, was constructed from two plasmids pSTCII-NGT and pTC-NGT (Singhal et al., 2014). pSTCII-NGT, as described in (Sijwali & Rosenthal, 2010), has pGEM backbone for replication in *E. coli* and two cassettes for expression in *P. berghei*. The first cassette expresses NGT [N-terminus-GFP-Transmembrane region of PfEMP1 (*P. falciparum* Erythrocyte Membrane Protein 1)] under the control of *Plasmodium yoelii* chloroquine-resistance transporter 5' UTR (PyCRT 5'UTR) and *Plasmodium vivax* actin 3' UTR (PvAc 3' UTR). The second cassette consists of *Toxoplasma gondii* dihydrofolate reductase–thymidylate synthase (TgDHFR-TS) gene under the control of *P. yoelii* α-tubulin 5'UTR (PyαTb 5'UTR) and the *P. vivax* α-tubulin 3'UTR (PvαTb 3'UTR) for selection with drug pyrimethamine. The pTC-NGT plasmid, as described in (Singhal et al., 2014), contains hDHFR (human DHFR) in place of TgDHFR-TS under the control of the same elements. Both plasmids were digested with AvrII/XhoI, the NGT/PyCRT 5'UTR/PyαTb 5'UTR/TgDHFR-TS/PvαTb 3'UTR fragment from pSTCII-NGT and the pGEM/PvAc 3'UTR from pTC-NGT were gel-extracted and ligated to construct a third plasmid named pTCIII-NGT. The pTCIII-NGT plasmid was digested with NotI/AgeI to remove the PvAc 3'UTR/NGT/PyCRT 5'UTR, and the plasmid backbone was ligated with the similarly digested GFP/PvAc 3'UTR to obtain pTDG plasmid. pTDG was digested with BamHI/KasI to remove TgDHFR/PvαTb 3'UTR, and the backbone was ligated with hDHFR/PfHrpII 3'UTR fragment to construct the HB plasmid (Figure 3.1A).

The name HB is derived such that **H** denotes the **h**uman DHFR selection marker for recombinants and **B** denotes its implication in *P. **b**erghei* transfection. This HB plasmid with construct NotI|KpnI/GFP/PvAc3'UTR/PyαTb5'UTR/hDHFR/PfHrpII3'UTR/AvrII|KasI can be used for knockin of genes such as GFP or knockout of targeted gene depending upon sequence cloned at flanks. The construct has human DHFR gene, which is resistant

to an anti-malarial drug Pyrimethamine, but the wild type parasites would be killed by drug allowing the selection of only recombinant parasites. In addition, the GFP fused to cloned flank 1 is followed by the *P. vivax* actin 3'UTR and hDHFR gene is under the *P. yoelii* alpha tubulin and *P. falciparum* Hystidine rich protein (HRP) 3'UTR. As these are the UTRs of housekeeping genes in *Plasmodium*, they were used to ensure efficient expression.

3.5.1 Construction of HB knockdown (HB KD) plasmid

In the HB plasmid, cDD (*E. coli* destabilizing domain) gene coding sequence was cloned at BamHI/XhoI site downstream of GFP to make HB KD plasmid (Figure 3.1B). The construct NotI|KpnI/GFP/**cDD**/PvAc3'UTR/PyαTb5'UTR/hDHFR/PfHrpII3'UTR/AvrII|KasI will be used for knockdown of targeted gene. The cDD gene is HA (Hemagglutinin) tagged which can be used for detection of protein expression in western blotting.

During expression, cDD upon fusion with targeted protein would destabilize the protein. However, by using a cDD inhibitor drug, Trimethoprim, targeted protein would remain intact which allows to control expression of protein of interest.

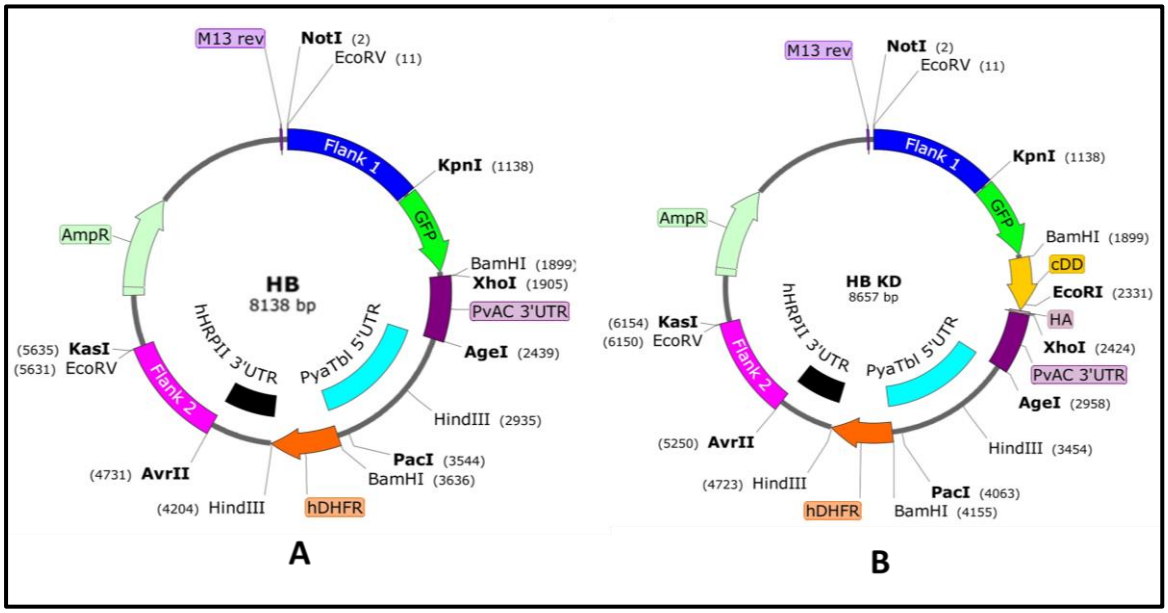

Figure 3. 1 A- HB plasmid to make knockin and knockout construct B- HB KD plasmid to make knockdown construct. The vector map was designed in Snapgene viewer. The color code represents different fragments, viz. royal blue- Flank 1, green- GFP, purple- PvAc3'UTR, cyan- PyaTbl5'UTR, orange- hDHFR, black- PfHRPII3'UTR, pink- Flank 2 and the light colored beta-lactamase gene. The restriction sites flanking every fragment in the constructs are shown. The only difference in between the HB and HB KD plasmid is the cDD fragment (yellow).

3.6 Design of primers

As the *Plasmodium* gDNA is highly (above 80%) A/T rich, the primers were designed including maximum possible G/C content.

The AMA1 gene sequence of *Plasmodium berghei* ANKA strain (PBANKA_0915000) was retrieved from PlasmoDB. For construction of both AMA1 KI and AMA1 KD plasmid, the cloning sequences are same. The primer sequences were selected from AMA1 locus as shown diagrammatically in Figure 4.36 such that AMA1 fl1 was amplified from AMA1 coding sequence (CDS) while AMA1 fl2 was amplified from the AMA1 3'UTR. In addition, restriction sites for endonucleases were added in primers such that AMA1 fl1 amplicon would carry NotI-EcoRV and KpnI enzyme site and the AMA1 fl2 would carry AvrII and EcoRV-KasI enzyme sites. The selected forward and reverse primers for the target sequence were analyzed on AmplifX 1.7.0 software for checking self-complementarity, dimerization, end stability and GC content. The primer sequences used are as follows in Table 1.

Table 1 Primer sequences to amplify the cloning sequences of AMA1 gene from gDNA. The primer binding sites on AMA1 locus is shown in Figure 4.36.

Amplicon	Size	Primer	Primer sequence
AMA1 fl1	1498 bp	P1: PbAMA-fl1F	AAAGgcggccgcgatatcATGCATGGTTCTGGTATAAGAGTT
		P2: PbAMA-fl1R	TCTAggtaccATAATATGGTTTTTGCATCAAAACGGGTGT
AMA1 fl2	957 bp	P3: PbAMA-fl2F	TAATcctaggGAAGCGTTTAAATAGTAAATAGTTAGTTAC
		P4: PbAMA-fl2R	CATAggcgccgatatCCCGATTAAGAGAAATGCTTACCAAC

The ATG18 gene sequence of *Plasmodium berghei* ANKA strain (PBANKA_1211300) was retrieved from PlasmoDB. For construction of both ATG18 KI and ATG18 KD plasmid, the ATG18 fl2 is same but the ATG18 fl1 is different among them. The primer sequences were selected from ATG18 locus as shown diagrammatically in Figure 4.37 such that ATG18 KO/KD fl2 (common for making both KO and KD) was amplified from ATG18 3'UTR, ATG18 KO fl1 was amplified from ATG18 5'UTR and ATG18 KD fl1 was amplified from ATG18 5'UTR+ CDS (coding sequence). In addition, restriction sites for endonucleases were added in primers such that ATG18 KO fl1 and ATG18 KD fl1 amplicon would carry NotI-EcoRV and KpnI enzyme site and the ATG18 fl2 would carry AvrII and EcoRV-KasI enzyme sites. The selected forward and reverse primers for the target sequences were analyzed on AmplifX 1.7.0 software for checking self-complementarity, dimerization, end stability and GC content. The primer sequences used are as follows in Table 2.

Table 2 Primer sequences to amplify the cloning sequence (flanks) of ATG18 from gDNA. The primer binding sites on AMA1 locus is shown in Figure 4.37.

Amplicon	Size	Primer	Primer sequence
ATG18 KO fl1	997 bp	P1: PbA18Kfl1-F1	GTTAgcggccgcgatatcGCTTTAGGACGAGTTTAATTTCTACG
		P2: PbA18Kfl1-R1	CCATggtaccACAGCCATAATCTTGATTAAAAGC
ATG18 KD fl1	2181 bp	P1: PbA18Kfl1-F1	GTTAgcggccgcgatatcGCTTTAGGACGAGTTTAATTTCTACG
		P2': PbA18Rep-R	TTTAggtaccATCAAAGCTATGGGAAGATATTTTAAGCAT
ATG18 KO/ KD fl2	764 bp	P3: PbA18Kfl2-F	TTTAcctaggCACGTTTTGTCACAACACATATATC
		P3: PbA18Kfl2-R1	TTTTggcgccgatatcATCGATACACTTTGTATATGCATAC

3.7 Construction of AMA1 KI and AMA1 KD plasmids

3.7.1 Cloning of AMA1 fl2 in HB and HB KD plasmids

3.7.1.1 Making AMA1 fl2 insert

The genomic DNA of *P. berghei* ANKA strain was taken from the laboratory stock. Using it as the template, AMA1 fl2 (957bp) was PCR amplified with high fidelity Phusion polymerase using primers P3 and P4 (Table 1) from AMA1 3'UTR. The PCR product was digested with flanking enzymes AvrII/KasI and gel purified to obtain AMA1 fl2 insert.

3.7.1.2 Making AMA1 fl2 KI plasmid

HB plasmid (Figure 3.1A) was used to construct AMA1 fl2 KI plasmid. For this, HB plasmid was digested with AvrII/KasI to remove the previously cloned Flank 2 and vector backbone was gel purified. The similarly digested AMA1 fl2 insert and HB vector were ligated to construct AMA1 fl2 KI plasmid. The ligated product was transformed to obtain the transformant colonies from which AMA1 fl2 KI plasmids were purified. The purified plasmids were screened for the presence of cloned AMA1 fl2 insert by digesting with AvrII/KasI.

3.7.1.3 Making AMA1 fl2 KD plasmid

Similarly, HB KD plasmid (Figure 3.1B) was used to construct AMA1 fl2 KD plasmid. For this, HB KD plasmid was digested with AvrII/KasI to remove the previously cloned Flank 2 and vector backbone was gel purified. The similarly digested AMA1 fl2 insert and HB KD vector were ligated to construct AMA1 fl2 KD plasmid. The ligated product was

transformed to obtain the transformant colonies from which AMA1 fl2 KD plasmids were purified. The purified plasmids were screened for the presence of cloned AMA1 fl2 insert by digesting with AvrII/KasI.

3.7.2 Cloning of AMA1 fl1 in AMA1 fl2 KI and AMA1 fl2 KD plasmids

3.7.2.1 Making AMA1 fl1 insert

Using the same stock of *P. berghei* ANKA strain gDNA as template, AMA1 fl1 (1498bp) was PCR amplified with high fidelity Phusion polymerase using primers P1 and P2 (Table 1). The PCR product was digested with flanking enzymes NotI/KpnI and gel purified to obtain AMA1 fl1 insert.

3.7.2.2 Making AMA1 KI plasmid

One of the positive AMA1 fl2 KI plasmid from method 3.7.1.2 was digested with NotI/KpnI to remove the previously cloned Flank 1 and vector backbone was gel purified. The similarly digested AMA1 fl1 insert and AMA1 fl2 KI vector were ligated to construct AMA1 KI plasmid (Figure 4.17A). The ligated product was transformed to obtain the transformant colonies from which AMA1 KI plasmids were purified. The purified plasmids were screened for the presence of cloned AMA1 fl1 insert by digesting with NotI/KpnI.

3.7.2.3 Making AMA1 KD plasmid

Similarly, one of the positive AMA1 fl2 KD plasmid from method 3.7.1.3 was digested with NotI/KpnI to remove the previously cloned Flank 1 and vector backbone was gel purified. The similarly digested AMA1 fl1 insert and AMA1 fl2 KD vector were ligated to construct AMA1 KD plasmid (Figure 4.17B). The ligated product was transformed to obtain the transformant colonies from which AMA1 KD plasmids were purified. The purified plasmids were screened for the presence of cloned AMA1 fl1 insert by digesting with NotI/KpnI.

Two plasmids each of AMA1 KI and AMA1 KD were proceeded for the confirmation and making transfection constructs.

3.7.3 Confirmation of AMA1 KI and AMA1 KD clones

After cloning the AMA1 fl2 and AMA1 fl1 to HB plasmid and HB KD plasmid, AMA1 KI and AMA1 KD plasmids were constructed respectively. The isolated plasmid of two positeve clones were checked for integrity of vector backbone. The construct flank1/GFP/(cDD)/PvAc3'UTR/PyαTb 5'UTR/hDHFR/PfHRPII3'UTR/flank2 were analyzed by digestion with restriction enzymes specific for the fragments as shown in vector map (Figure 4.17). Also, the cloned fragments were confirmed by DNA sequencing. The

plasmids were sent for sequencing to Bioserve, India. The primers used for the sequencing of the cloned fragments is listed in Appendix 2.

3.7.4 Generation of transfection construct

The confirmed AMA1 KI plasmid was digested with EcoRV to obtain the construct AMA1 fl1/GFP/PvAc3'UTR/PyαTb 5'UTR/hDHFR/PfHRPII3'UTR/AMA1 fl2 of size 6013bp. This was gel purified and about 5µg of construct will be used to transfect wild type parasites.

The confirmed AMA1 KD plasmid was digested with EcoRV to obtain the construct AMA1 fl1/GFP/**cDD**/PvAc3'UTR/PyαTb 5'UTR/hDHFR/PfHRPII3'UTR/AMA1 fl2 of size 6529bp. This was gel purified and about 5µg of construct will be used to transfect wild type parasites.

3.8 Construction of ATG18 KO and ATG18 KD plasmids

3.8.1 Cloning of ATG18 KO/KD fl2 in HB and HB KD plasmid

3.8.1.1 Making ATG18 KO/KD fl2 insert

The genomic DNA of *P. berghei* ANKA strain was taken from the laboratory stock. Using it as the template, ATG18 KO/KD fl2 (764bp) was PCR amplified using high fidelity Phusion polymerase using primers P3 and P4 (Table 2). The PCR product was digested with flanking enzymes AvrII/KasI and gel purified to obtain ATG18 KO/KD fl2 insert.

3.8.1.2 Making ATG18 fl2 KO plasmid

HB plasmid (Figure 3.1A) was used to construct ATG18 fl2 KO plasmid. For this, HB plasmid was digested with AvrII/KasI to remove the previously cloned Flank 2 and vector backbone was gel purified. The similarly digested ATG18 KO/KD fl2 insert and HB vector were ligated to construct ATG18 fl2 KO plasmid. The ligated product was transformed to obtain the transformant colonies from which ATG18 fl2 KO plasmids were purified. The purified plasmids were screened for the presence of cloned ATG18 fl2 KO/KD insert by digesting with AvrII/KasI.

3.8.1.3 Making ATG18 fl2 KD plasmid

Similarly, HB KD plasmid (Figure 3.1B) was used to construct AMA1 fl2 KD plasmid. For this, HB KD plasmid was digested with AvrII/KasI to remove the previously cloned Flank 2 and vector backbone was gel purified. The similarly digested ATG18 KO/KD fl2 insert and HB KD vector were ligated to construct ATG18 fl2 KD plasmid. The ligated product was transformed to obtain the transformant colonies from which ATG18 fl2 KD plasmids were purified. The purified plasmids were screened for the presence of cloned ATG18 KO/KD fl2 insert by digesting with AvrII/KasI.

3.8.2 Cloning of ATG18 KO fl1 in ATG18 fl2 KO plasmid

3.8.2.1 Making ATG18 KO fl1 insert

Using the same stock of *P. berghei* ANKA strain gDNA as template, ATG18 KO fl1 (997bp) was PCR amplified with high fidelity Phusion polymerase using primers P1 and P2 (Table 2). The PCR product was digested with flanking enzymes NotI/KpnI and gel purified to obtain ATG18 KO fl1 insert.

3.8.2.2 Making ATG18 KO plasmid

One of the positive ATG18 fl2 KO plasmid from method 3.8.1.2 was digested with NotI/KpnI to remove the previously cloned Flank 1 and vector backbone was gel purified. Then, similarly digested ATG18 KO fl1 insert and ATG18 fl2 KO vector were ligated to construct ATG18 KO plasmid (Figure 4.29). The ligated product was transformed to obtain the transformant colonies from which ATG18 KO plasmids were purified. The purified plasmids were screened for the presence of cloned ATG18 KO fl1 insert by digesting with NotI/KpnI.

3.8.3 Cloning of ATG18 KD fl1 in ATG18 fl2 KD plasmids

3.8.3.1 Making ATG18 KD fl1 insert

Using the same stock of *P. berghei* ANKA strain gDNA as template, ATG18 KD fl1 (2181bp) was PCR amplified with high fidelity Phusion polymerase using primers P1 and P2' (Table 2). The PCR product was digested with flanking enzymes NotI/KpnI and gel purified to obtain ATG18 KO fl1 insert.

3.8.3.2 Making ATG18 KD plasmid

One of the positive ATG18 fl2 KD plasmid from method 3.8.1.3 was digested with NotI/KpnI to remove the previously cloned Flank 1 and vector backbone was gel purified. Then, similarly digested ATG18 KD fl1 insert and ATG18 fl2 KD vector were ligated to construct ATG18 KD plasmid (Figure 4.30). The ligated product was transformed to obtain the transformant colonies from which ATG18 KD plasmids were purified. The purified plasmids were screened for the presence of cloned ATG18 KD fl1 insert by digesting with NotI/KpnI.

3.8.4 Confirmation of ATG18 KO and ATG18 KD clones

After cloning the ATG18 KO/KD fl2 and ATG18 KO fl1 to HB plasmid, ATG18KO plasmid was constructed. The isolated plasmid of three positive clones were checked for integrity of vector backbone. The fragments in the construct, ATG18 KO fl1/GFP/PvAc3'UTR/PyαTb 5'UTR/hDHFR/ PfHRPII3'UTR/ATG18 KO/KD fl2, were analyzed by digestion with restriction enzymes specific for the fragments as shown in

vector map (Figure 4.29). Also, the cloned fragments were confirmed by DNA sequencing. The plasmids were sent for sequencing to Bioserve, India. The primers used for the sequencing of the cloned fragments is listed in Appendix 2.

Similarly, after cloning the ATG18 KO/KD fl2 and ATG18 KD fl1 to HB KD plasmid, ATG18 KD plasmid was constructed. The isolated plasmid of three positeve clones were checked for integrity of vector backbone. The fragments in the construct ATG18 KD fl1/GFP/**cDD**/PvAc3'UTR/PyαTb 5'UTR/hDHFR/ PfHRPII3'UTR/ATG18 KO/KD fl2 were analyzed by digestion with restriction enzymes specific for the fragments as shown in vector map (Figure 4.30). Also, the cloned fragments were confirmed by DNA sequencing. The plasmids were sent for sequencing to Bioserve, India. The primers used for the sequencing of the cloned fragments is listed in Appendix 2.

3.8.5 Generation of transfection construct

The confirmed ATG18 KO plasmid was digested with EcoRV to obtain the construct ATG18 KO fl1/GFP/PvAc3'UTR/PyαTb 5'UTR/hDHFR/PfHRPII3'UTR/ATG18 KO/KD fl2 of size 5319bp. This was gel purified and about 5µg of construct will be used to transfect wild type parasites.

The confirmed ATG18 KD plasmid was digested with EcoRV to obtain the construct ATG18 KD fl1/GFP/**cDD**/PvAc3'UTR/PyαTb 5'UTR/hDHFR/PfHRPII3'UTR/ATG18 KO/KD fl2 of size 7019bp. This was gel purified and about 5µg of construct will be used to transfect wild type parasites.

3.9 Routine parasite *Plasmodium berghei* culture

3.9.1 Generation of *P. berghei* parasites

All animal experiments were performed according to the approved procedures of the Institutional Animal Ethics Committee of the Center for Cellular and Molecular Biology (CCMB). Animals were maintained at 22-25^{o}C under 12hours light and dark cycle in animal house approved by Committee for the Purpose of Control and Supervision of Experiment on Animals (CPCSEA).

Female balb/c mice were infected with wild type *Plasmodium berghei* ANKA strain by intra-peritoneal route. In addition, passage of parasites was done from infected Balb/c mice by collecting few microliters of blood from the tail snip in Alsevier's solution (2.05% dextrose, 0.8% sodium citrate, 0.055% citric acid, 0.42% sodium chloride) and injecting intra-peritoneally. Parasitemia was monitored daily from Day 4 onwards by making Giemsa stained blood smears.

A drop of blood was collected by cutting tail snip in a clean glass slide and smear was made by the end of another slide before drying. After the smear gets air-dried, it was methanol fixed and allowed to dry. The smear was stained by Giemsa (1:4 dilution in phosphate buffer) for 5 minutes, washed and dried. The slide was observed under 100x objective of a light microscope. When the parasitemia was high enough (about 10%-15%), mice were euthanized in CO_2 gas chamber and the blood was collected in Alsevier's solution by cardiac puncture. The collected blood sample was further processed either for making glycerol stock or for isolation of parasites by saponin lysis or in-vitro culture for transfection.

3.9.2 Isolation of parasites by saponin lysis

Blood was collected in 10ml Alsevier's solution from the infected mice by cardiac puncture, centrifuged at 2500 rpm for 10 minutes at 4^{o}C and the supernatant was aspirated out. The cell pellet was suspended in 10 ml of ice-cold saponin solution (0.05% w/v in 1X PBS) and incubated on ice for 5 minutes. After centrifuging at 2500 rpm for 10 minutes at 4^{o}C, the pellet was resuspended in saponin solution, centrifuged again and the supernatant was discarded. The parasite pellet was washed twice with ice cold 1X PBS to remove traces of saponin. Finally, the pellet was resuspended in 1 ml PBS, transferred to a microcentrifuge tube and centrifuged at 10000 rpm for 5 minutes at 4^{o}C. The supernatant was completely aspirated out and parasite pellet was stored at -80^{o}C until further use or used immediately for isolation of genomic DNA of parasite or preparation of parasite lysate for western blotting.

3.9.3 Cryopreservation of parasites

Blood (in 10ml Alsevier's solution) was collected from infected mice, centrifuged at 2500 rpm for 10 min at 4^{o}C and the supernatant was aspirated. The pellet was suspended in twice of its volume of freezing medium (57% glycerol, 1.6% sodium lactate, 0.3 g/liter KCl, 25mM sodium phosphate, pH 6.8). First, 0.33 times the pellet volume of freezing solution was added with gentle mixing, the suspension was incubated for 5 minutes at room temperature. Finally, 1.66 times of the pellet volume of freezing solution was added. The parasite stock was aliquoted into multiple tubes (200µl aliquots) and stored at -80°C for two days, followed by cryopreservation in liquid nitrogen.

3.9.4 Genomic DNA isolation

The parasite genomic DNA (gDNA) was isolated using Qiagen Puregene Blood core kit B. The parasite pellet was suspended in cell lysis solution (600µl per 100µl of parasite pellet). Gentle mixing was done by pipetting up and down, the suspension was incubated at 37^{o}C, 2µl of RNase was added, and the lysate was incubated at 37^{o}C for 10 minutes. 200µl of protein precipitation solution was added to the lysate, mixed gently,

and centrifuged at 16000 rpm for 10 minutes. 600µl isopropanol added to the supernatant, suspension was mixed gently, and centrifuged at 16000 rpm for one minute. The supernatant was discarded, and the DNA pellet was washed with 300µl of 70% ethanol, air dried, and resuspended in 150µl of DNA hydration at room temperature for one hour. The DNA was stored in aliquots at -30^{o}C until further use.

In some cases, the DNA pellet did not dissolve and had protein contamination. Therefore, for repurification, the DNA suspension (150µl, 1X) was mixed with 750µl cell lysis solution (5x volume of the DNA solution). The solution was mixed, 5µl of proteinase-K was added, mixed gently, and incubated at 55^{o}C for 10 minutes or until the pellet completely dissolves. 2X (double) volume of protein precipitation solution was added to the above solution, mixed and centrifuged at 16000 rpm for 2 minutes. 6X volume of isopropanol was added to the supernatant, mixed and centrifuged. The pellet was washed with 6X volume of 70% ethanol, air dried, and finally dissolved in 100µl of DNA hydration solution. The gDNA was quantified using the Nanodrop and checked for integrity by agarose gel electrophoresis.

3.9.5 Preparation of parasite lysate

The parasite pellet was resuspended in known minimum volume of 10 mM Tris, pH 7.5 so that the pellet volume can be estimated as the change in volume. Then the volume of 4X SDS sample buffer to be added is calculated and the remaining Tris buffer is added followed by addition of calculated sample buffer. The suspension was incubated at 100^{o}C for 15 minutes, centrifuged at 16000 rpm for 15 minutes at room temperature, the supernatant was transferred to a fresh tube, aliquoted into multiple 50µl volume and stored at -80^{o}C till further use.

3.10 Generation of recombinant parasite lines

3.10.1 Transfection of *P. berghei*

P. berghei was obtained as mentioned in the section 3.6.1. The blood was collected at 10% parasitemia. Transfection was done as reported by Janse, Ramesar, & Waters with minor modifications. The blood was centrifuged at 2500 rpm for 5 minutes, supernatant was aspirated, and the pellet was resuspended in the same volume of complete RPMI (Rosewell Park Memorial Institute) medium. For upto 25 ml culture volume, 10 ml of 60% Nycodenz solution was carefully layered at the bottom of a 50ml centrifuge tube. The sample was centrifuged at the slow acceleration of 9m/s^{2}and speed of 360g at room temperature. The deceleration was set to zero so that the gradient would not be disturbed. Trophozoites and schizonts collect at the interphase of Nycodenz and RPMI; it was collected by aspiration slowly in a new tube. The interphase sample was diluted with RPMI medium, centrifuged at 2000 rpm for 5 minutes, and the pellet was washed

again with RPMI. Giemsa stained smear of RBC pellet and the interphase sample were observed to check purification. The purified parasite pellet was resuspended in 25ml RPMI-FBS media, transferred to a 75cc culture flask, gassed (mixture of 5% CO_2, 5% O_2, 90% N_2), air tightened and incubated at 37˚C, 55 rpm for overnight.

Media was changed after 12-14 hours and parasites maturation to schizont stage was evaluated by making smears. When most parasites developed to schizont stage, the culture was centrifuged at 2000 rpm for 5 minutes, the supernatant was discarded, and the pellet was suspended in required volume of RPMI 1640 complete medium and aliquoted such that each aliquot contains 15-20 µl packed cell volume of parasites (parasites from one mouse can be used for 2-3 transfections). 5-6 µg of linear transfection fragment was added to 100 µl Nucleofector solution (Amaxa Nucleofector Kit for Human T cells from Lonza) and mixed with purified parasites. The parasite-DNA-Nucleofector suspension was electroporated using the U33 program of Nucleofector Device I with high-voltage pulses (0.8-1.5kV) and low capacitance settings (25 µF). 150 µl of RPMI 1640 complete medium was added to the electroporated sample, and it was injected into the tail vein of a Balb/c mouse using an insulin syringe. The mouse was given pyrimethamine in drinking water (70 µg/l00 ml; pH 5.0-5.5) 24 hours post-injection and onward for selection of recombinant parasites. Parasitemia was monitored every alternate day by making Giemsa-stained blood smears of infected mice. At around 10% parasitemia, mice were euthanized, and blood was collected as described above. 150µl of the infected blood was intraperitoneally injected into a naive mouse for second round selection of recombinant parasite. The remaining blood was used for making glycerol stock as mentioned above.

3.10.2 Validation of recombinant parasite at gene level

The AMA1 recombinant (KI and KD) parasite could not multiply after infection to mice, so visible parasitemia could not be achieved when screened by making Giemsa stained blood smears. Thus, the further validation and confirmation experiment are done on the ATG18 recombinant (ATG18KO and ATG18KD) parasites.

The genomic DNA of the recombinant (knock down and knockout) and wild type (WT) parasites were isolated as described in 3.6.4. To confirm the recombination, the recombination specific primers (5'-integration: A18CON5U-F/GFPseq-R, 3'-integration HRPseq-F/A18CON3U-R shown in Table 2) were used which would amplify only from the homologous recombined loci. A wild type specific PCR that would give an amplicon of specific size only from wild type was also set up to check whether the recombinant parasites contained wild type parasites. Another control used was Merozoite Surface Protein 1 (MSP1) gene, which was not disturbed in recombinants, should give amplicon

from both recombinant and wild type parasites. All the PCR reactions were done using Taq DNA polymerase following the earlier described PCR program, except changes in the extension time (5 minutes for larger amplicon). The PCR reactions were analyzed on 0.8% agarose gel electrophoresis.

The recombination specific PCR was done to confirm homologous recombination in ATG18 locus of genome using following primers (Table 3).

Table 3: Primers for confirming homologous recombination in ATG18 locus. The primer binding sites for confirmation of 5' and 3' recombination on ATG18 locus is shown in Figure 4.37.

Confirmation of	Primers	Sequences
Wt ATG18	PbA18F2_seq	CATCAAACATTATCGGTGTGAGAT
	PbA18Kfl2-R1	TTTTggcgccgatatcATCGATACACTTTGTATATGCATAC
5' recombination	5P: A18CON-5UF	CACTTAACCCGCTAAAATTGGCT
	6P: GFPSEQ-R	CCAGCAGCTGTTACAAACTCAAGAA
3' recombination	7P: HRP2SEQ-F	CTTTTACAATATGAACATAAAGTACAAC
	8P: A18CON-3UR	CATTATTTCGGGAAAATAAAAAAGGTAACGA
MSP1	PbMSP1-fl1-F	tAcATGCGGCCGCgatatcGCAGTGGTAAGTGGAAGCAGTGTT
	PbMSP1-fl1-R	tTTAggtaccAAATATATTAAATACAATTAATGTGATAATTAATAAAATTGAC

3.10.3 Validation of recombinant parasites at protein level

Parasite lysates from WT, KD and KO parasites were run on 12% SDS-PAGE gel in triplicates. The proteins were electro-transferred to Immobilon-P Polyvinylidene difluoride (PVDF) membrane, the membrane was incubated in the blocking buffer (2% w/v milk powder in 1X TBST-1X TBS, 0.1% Tween 20) for overnight with one change of buffer. The membrane was incubated with primary antibodies (mouse anti-GFP at 1/500, mouse anti-HA at 1/1000 and mouse anti-β-actin at 1/1000; all diluted in blocking buffer) for 1 hour at room temperature with gentle shaking. The membrane was washed three times with TBST, each for 10 minutes, and then once with blocking buffer. The membranes were incubated with anti-mouse HRP conjugated secondary antibody (1/20000 in blocking buffer) for 45 minutes, and washed four times with TBST. The signal was developed using the SuperSignal West Femto/Pico Chemiluminescent kit on X-ray film.

3.10.4 Imaging of live parasites

10µl infected blood with recombinant parasite was collected from the tail snips of mice in 200µl of Alsevier's solution, centrifuged, washed twice with PBS and finally suspended in 500µl PBS. A poly-L-Lysine coated glass slide was taken, and a rectangle boundary was marked with a water-resistant hydrophobic ink marker. Nuclear stain Hoechst 33342 (final 10µg/ml) was added to the parasite suspension, and it was layered onto the slide and incubated in a humid chamber for 15 minutes. The slide was washed with PBS to remove unbound cells, covered with a cover slip and observed for eGFP under the 100X oil-immersion objective of a Zeiss AxioImagerZ2 microscope. Images were captured with a mounted AxioCam charge-coupled device (CCD) camera and processed with AxioVision LE software.

CHAPTER 4
RESULTS

4.1 Bioinformatics analysis of AMA1

The protein sequence of *Plasmodium falciparum* AMA1 was retrieved from UniProt database and was viewed in Pfam database. PfAMA1 was found to contain only one AMA1 protein family (Figure 4.1).

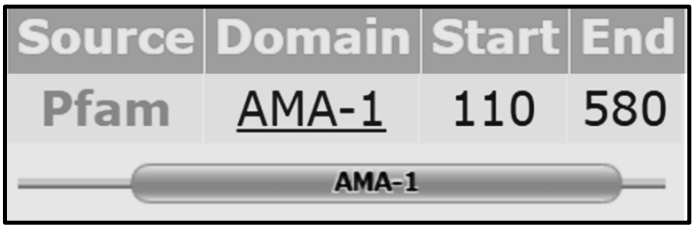

Figure 4. 1 AMA1 protein family present in PfAMA1 (UniProt P50489) viewed in Pfam database. The PfAMA1 domain was spanning from the amino acid range of 110 to 580.

The existence of this family of protein was found to be unique to species of Apicomplexa only including all the *Plasmodium* species as shown by the species distribution tree (Figure 4.2). This distribution tree shows all those organisms that contain the queried protein family.

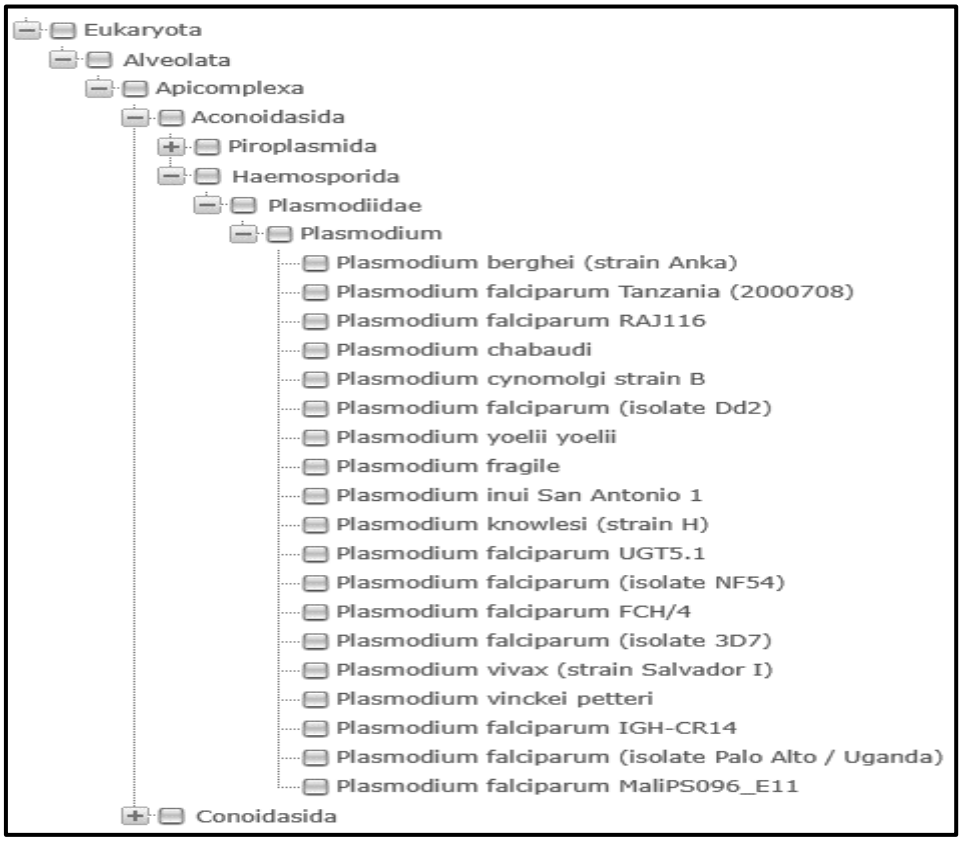

Figure 4. 2 Species distribution tree of AMA1 protein family found in Pfam database. The tree shows the existence of AMA1 protein family only in the Apicomplexans.

After knowing the presence of AMA1 protein family in reviewed query sequence, BLAST search gave the protein transcripts with same AMA1 family and the transcripts with high score are listed in Table 4.

Table 4 The AMA1 protein sequence from Apicomplexan parasites with maximum hits obtained from PlasmoDB and ToxoDB using PfAMA1 (P50489) as query

Apicomplexan species	Protein transcript name	Score
P. falciparum	PF3D7_1133400.1-p1	1226
P. vivax	PVP01_0934200.1-p1	678
P. knowlesi	PKNH_0931500.1-p1	671
P. relictum	PRELSG_0930900.1-p1	618
P. berghei	PBANKA_0915000.1-p1	560
Eimeria tenella	ETH_00004860-t26_1-p1	158
Toxoplasma gondi	TGME49_300130-t26_1-p1	146

A domain architecture is defined as the sequential order of conserved domains in a protein sequence. The conserved domains in the retrieved protein transcripts were analyzed in CDART tool of NCBI to verify that they contained AMA1 family of protein.

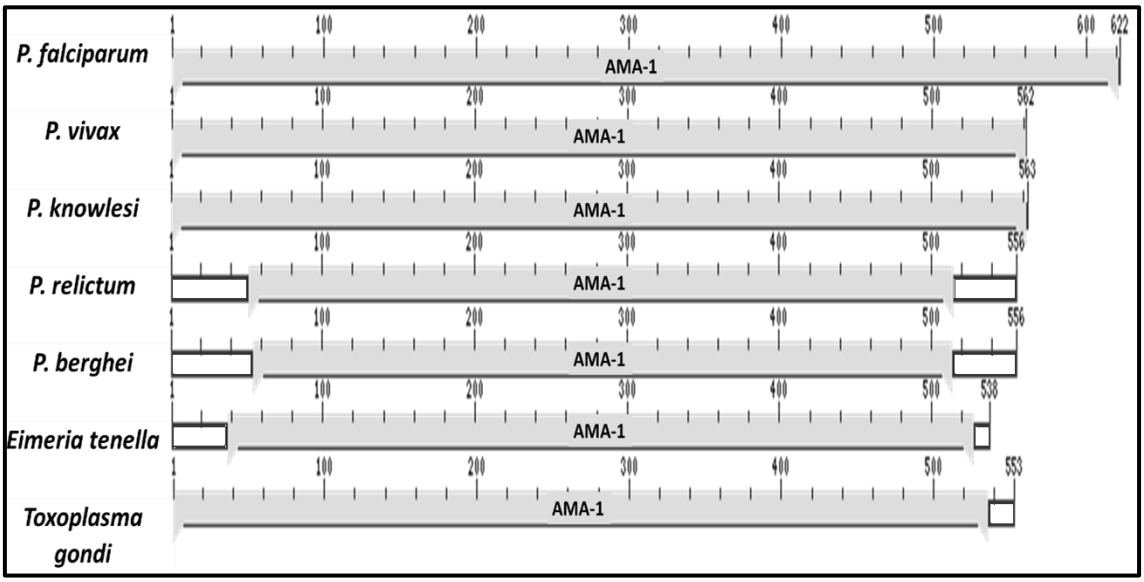

Figure 4. 3 Conserved Domain Architecture Retrieval Tool (CDART) result showing presence of AMA1 protein domain in the putative AMA1 protein sequence of selected apicomplexans. The grey region represents conserved AMA1 domain while the white portion are non-conserved regions.

All the selected apicomplexans were found to have AMA1 domain conserved, though the domain length has varied (Figure 4.3). All the queries received specific hits or the superfamily hits showing all were AMA1 superfamily protein sequences. Those putative AMA1 protein sequences of representative apicomplexans were aligned in Clustal

Omega to find the conserved regions and to identify the percentage identity between them (Table 5).

Table 5 Percentage Identity Matrix (PIM) of available AMA1 protein sequences of selected apicomplexans viz. 1: *P. falciparum, 2: P. vivax, 3: P. knowlesi, 4: P. relictum, 5: P. berghei, 6: Eimeria tenella* and *7: Toxoplasma gondi*. Clustal Omega Multiple Sequence Alignment (MSA) for the protein sequences is shown in Appendix 3.

Percent Identity Matrix - created by Clustal2.1

	1: PF	2: PV	3: PK	4: PR	5: PB	6: ET
1: PF3D7_1133400.1	100					
2: PVP01_0934200.1	56.76	100				
3: PKNH_0931500.1	56.58	85.05	100			
4: PRELSG_0930900.1	55.23	54.63	55.72	100		
5: PBANKA_0915000.1	48.92	54.76	55.13	50.46	100	
6: ETH_00004860-t26_1	28.82	30.39	28.60	28.48	28.60	100
7: TGME49_300130-t26_1	26.90	26.54	25.87	25.47	25.73	41.49

The PIM generated by Clustal Omega (Table 5) shows the high percentage identity (about 50%) between putative AMA1 sequences of *Plasmodium* species while the identity of sequence of *Plasmodium* species with other apicomplexan *Eimeria tenella* and *Toxoplasma gondi* was also greater than 26%. In the Phylum: Apicomplexa, *Plasmodium* belong to Class: Aconoidasida while other selected species *E. tenella* and *T. gondi* belong to Class: Conoidasida. So, the phylogenetic distance between the *Plasmodium* and these later ones might be the reason for less identity.

4.2 Bioinformatics analysis of ATG18

The protein sequence of *Saccharomyces cerevisiae* ATG18 (P43601) was retrieved from UniProt database and was viewed in Pfam database. ScATG18 was found to contain two WD40 protein domains (Figure 4.4).

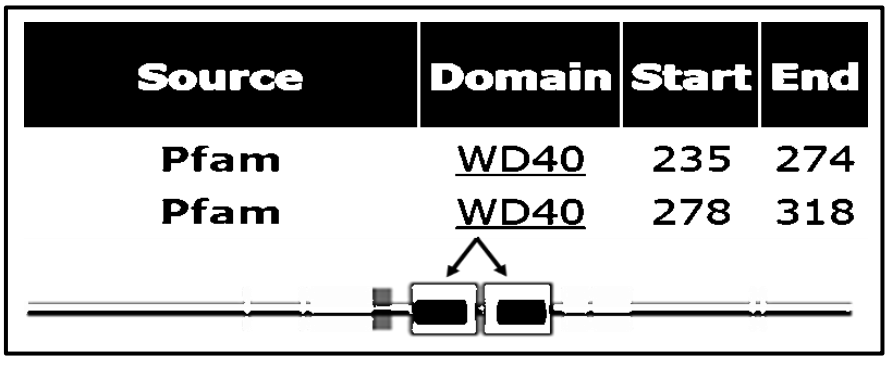

Figure 4. 4 WD40 repeat domains present in ScATG18 (UniProt P43601) protein viewed in Pfam database. Two WD40 repeat domains is present is ScATG18 protein.

This WD40 domain is involved in making beta-propeller structure through which it binds to the vacuolar membrane. WD is a short structural motif of about 40 aa ending with Try-Asp (WD). The tandem repeats would form a type of circular solenoid protein

domain. The domain is associated with multiple other proteins and involved in variety of functions such as signal transduction, autophagy and apoptosis.

This domain family was found to be distributed in all the Eukaryotes spanning from Protists to Mammalia including the Apicomplexan family and even humans as shown by Pfam database. So, the ATG18 protein sequences from human homolog WIPI1 (UniProt Q5MNZ9), putative *Plasmodium* ATG18 and *T. gondi* ATG18 sequences with maximum hits were retrieved. Reverse blasting on CDART of NCBI showed that the WD40 conserved domains were present in all of the putative sequences (Figure 4.5).

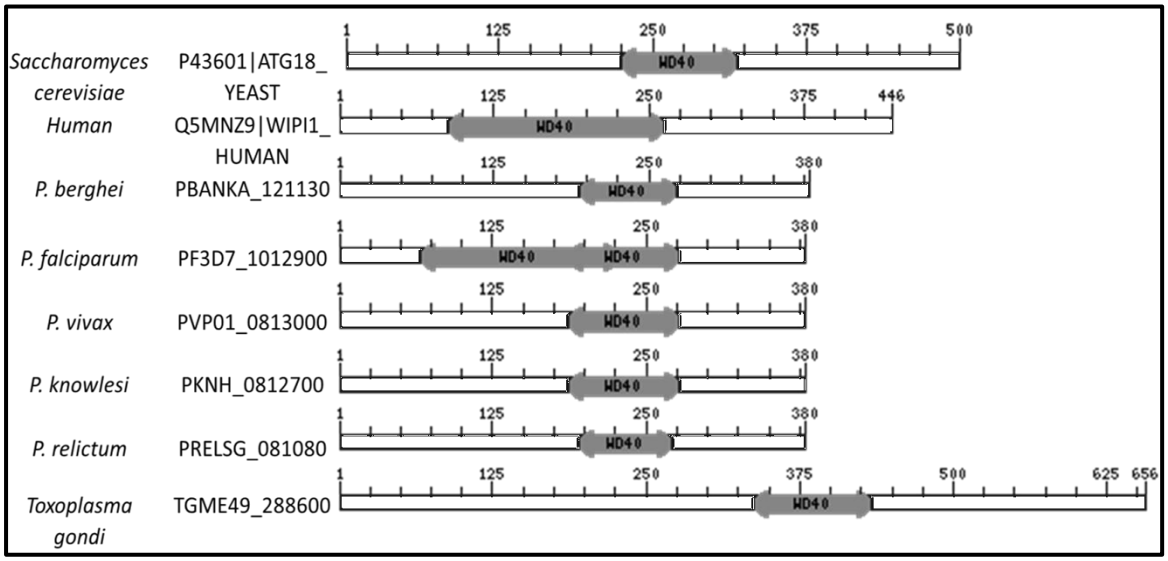

Figure 4. 5 Conserved Domain Architecture Retrieval Tool (CDART) result showing presence of WD40 repeat domain in the putative ATG18 protein sequence of yeast, human, and apicomplexans. The WD40 domain is shown in grey colour while the white colour sequence is not conserved.

All the selected putative protein sequences found superfamily hit confering homology in between. Further, multiple sequence alignment of all those sequences were done in Clustal Omega and the respective identity between the sequences was found. It was found that the putative ATG18 protein sequence is highly conserved (above 90%) among the *Plasmodium* species. Compared to putative *Plasmodium* ATG18 sequences, the yeast ATG18 is about 30% identical, human ATG18 is 27% identical while *Toxoplasma* ATG18 is only 23% identical. The yeast and human ATG18 are 34% identical (Table 6).

Table 6 Percentage Identity Matrix (PIM) of available ATG18 sequences of selected eukaryotes viz. 1: *Saccharomyces cerevisiae*, 2: human, 3: *P. berghei, 4: P. falciparum, 5: P. vivax, 6: P. knowlesi, 7: P. relictum* and *8: Toxoplasma gondi*. Clustal Omega Multiple Sequence Alignment (MSA) for the protein sequences is shown in Appendix 4.

Percent Identity Matrix - created by Clustal2.1

	1: YEAST	2: HUMAN	3: PB	4: PF	5: PV	6: PK	7: PR
1: sp|P43601|ATG18_YEAST	100						
2: sp|Q5MNZ9|WIPI1_HUMAN	34.58	100					
3: PBANKA_1211300.1	30.11	28.96	100				
4: PF3D7_1012900.1	30.11	27.76	91.58	100			
5: PVP01_0813000.1	29.57	28.06	90.53	97.63	100		
6: PKNH_0812700.1	29.57	28.66	91.05	97.11	98.42	100	
7: PRELSG_0810800.1	29.84	27.76	90.26	97.37	95.53	95.00	100
8: TGME49_288600-t26_1	28.11	26.87	23.65	23.36	23.36	23.65	23.93

4.3 Construction of AMA1 KI and AMA1 KD plasmids

4.3.1 Cloning AMA1 fl2 in HB and HB KD plasmids

From PbANKA WT gDNA, AMA1 fl2 (957bp) was PCR amplified (Figure 4.6) from AMA1 3'UTR using primers P3 and P4 (Table 1). HB plasmid, HB KD plasmid and AMA1 fl2 were digested with AvrII/KasI (Figure 4.7), and gel purified to obtain HB vector, HB KD vector and AMA1 fl2 insert.

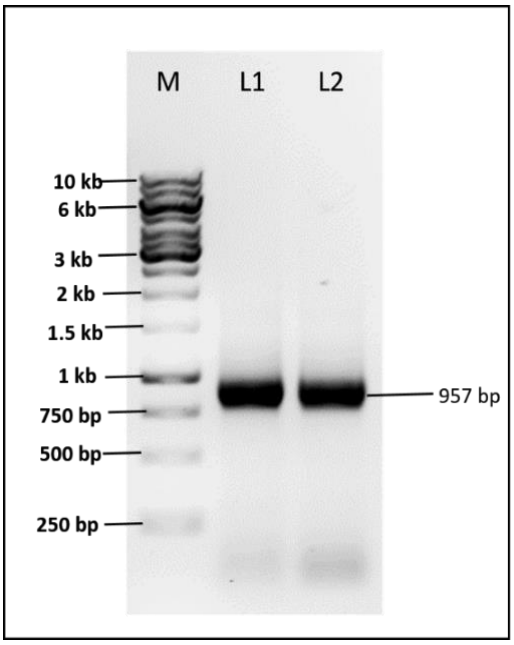

Figure 4. 6 AMA1 fl2 amplicon of size 957bp amplified from AMA1 3'UTR (L1 and L2). Lane M is 1kb ladder.

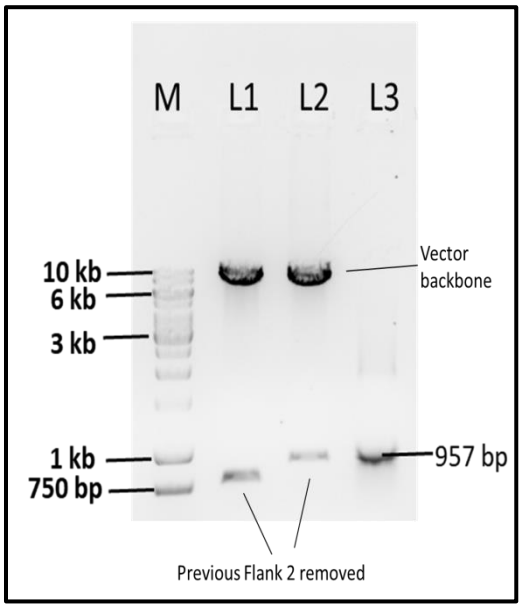

Figure 4. 7 Restriction digestion of HB plasmid (L1), HB KD plasmid (L2) and AMA1 fl2 (L3) by AvrII/KasI. Both the vectors show release of previously cloned Flank 2. Lane M is 1kb ladder.

HB vector backbone (Figure 4.7 L1) was ligated with AMA1 fl2 insert (Figure 4.7 L3) to obtain AMA1 fl2 KI plasmid. The ligated mix was transformed into *E. coli* cells to obtain several colonies. These colonies were screened for the presence of AMA1 fl2 insert by colony PCR (Figure 4.8) using primers P3 and P4 (Table 1).

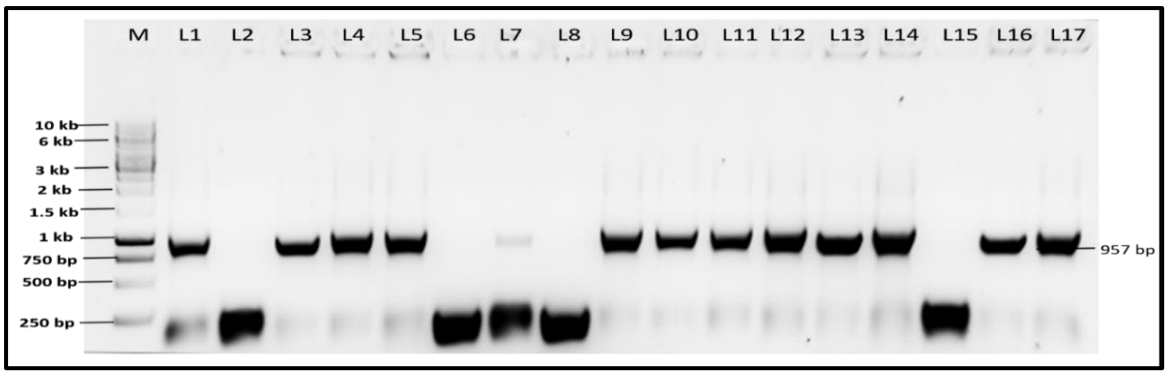

Figure 4. 8 Colony PCR of AMA1 fl2 KI transformant colonies showing the presence of AMA1 fl2 insert (957bp). Lane M is 1kb ladder, L1 is positive control with gDNA template, L2 is negative control without template and L3 to L17 are transformants.

Similarly, HB KD vector backbone (Figure 4.7 L2) was ligated with same AMA1 fl2 insert (Figure 4.7 L3) to obtain AMA1 fl2 KD plasmid. The ligated mix was transformed into *E. coli* cells to obtain several colonies. These colonies were screened for the presence of AMA1 fl2 insert by colony PCR (Figure 4.9) using primers P3 and P4 (Table 1).

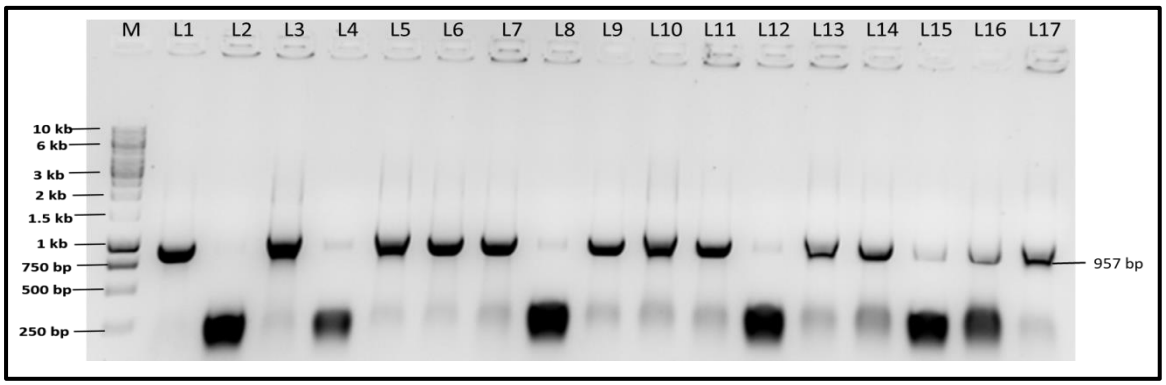

Figure 4. 9 Colony PCR of AMA1 fl2 KD transformant colonies showing the presence of AMA1 fl2 insert (957bp). Lane M is 1kb ladder, L1 is positive control with gDNA template, L2 is negative control without template and L3 to L17 are transformants.

Among several positive AMA1 fl2 KI and AMA1 fl2 KD clones, pDNA was isolated from four clones each of AMA1 fl2 KI and AMA1 fl2 KD. Isolated plasmids were evaluated for the presence of AMA1 fl2 by digestion with AvrII/KasI (Figure 4.10). This showed the release of insert just cloned, which revealed the presence of expected size of insert (957bp).

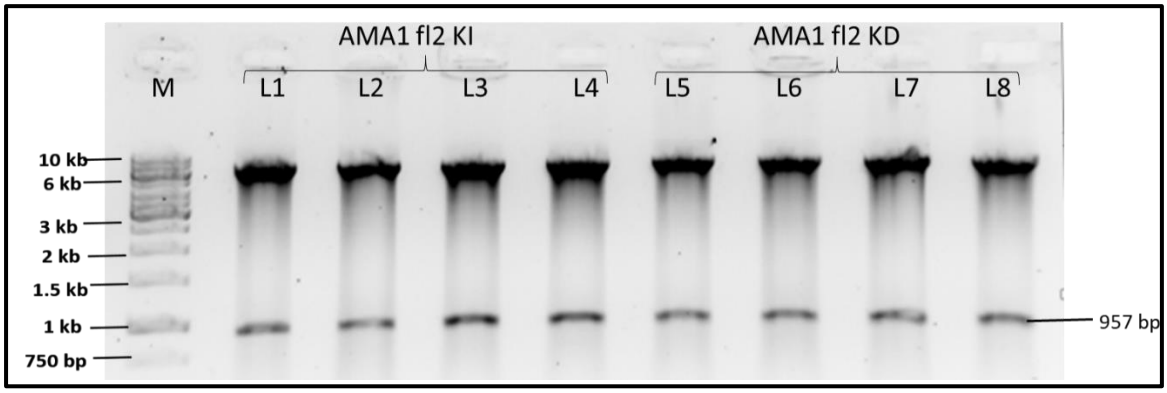

Figure 4. 10 AMA1 fl2 KI plasmids (L1-L4) and AMA1 fl2 KD plasmids (L5-L8) showing the release of cloned AMA1 fl2 insert (957 bp) by restriction digestion with AvrII/KasI. Lane M is 1 kb ladder.

4.3.2 Cloning AMA1 fl1 in AMA1 fl2 KI and AMA1 fl2 KD plasmids

Similarly, from PbANKA WT gDNA, AMA1 fl1 (1498bp) was PCR amplified (Figure 4.11) from AMA1 coding sequence (CDS) using primers P1 and P2 (Table 1) and digested with flanking NotI/KpnI enzymes to make AMA1 fl1 insert. For cloning flank1, the AMA1 fl2 cloned plasmids (AMA1 fl2 KI and AMA1 fl2 KD) were digested with NotI/KpnI (Figure 4.12). The digested AMA1 fl1 insert, AMA1 fl2 KI vector and AMA1 fl2 KD vector were gel purified.

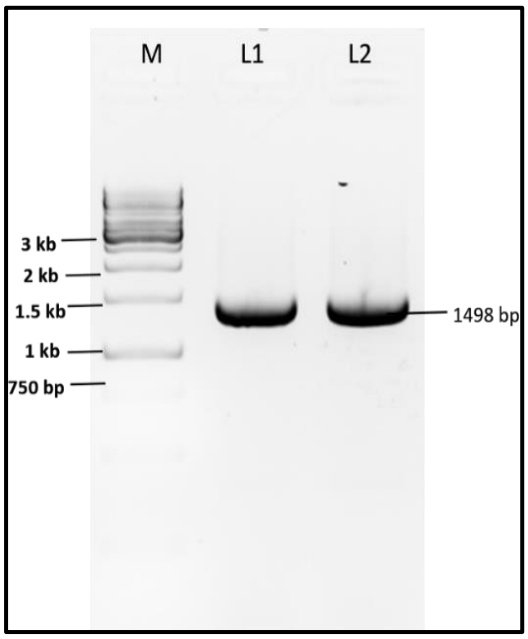

Figure 4. 11 AMA1 fl1 amplicon (1498bp) amplified from AMA1 coding sequence (L1 and L2). Lane M is 1kb ladder.

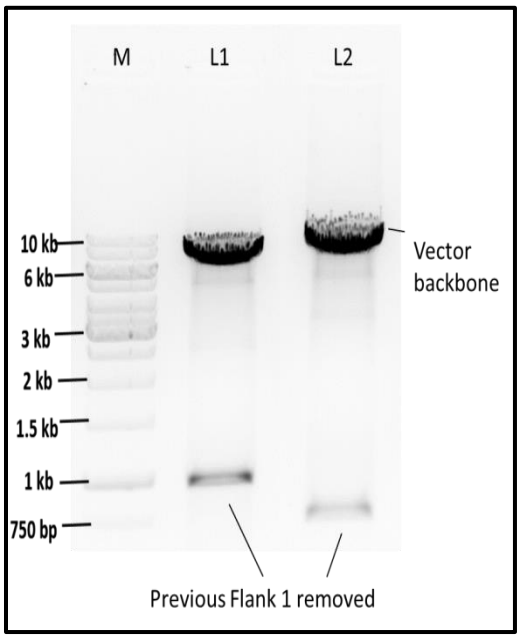

Figure 4. 12 Restriction digestion of AMA1 fl2 KI plasmid (L1) and AMA1 fl2 KD plasmid (L2) by NotI/KpnI to make vector. Both the vectors show release of previously cloned Flank 1 insert. Lane M is 1kb ladder.

AMA1 fl2 KI vector backbone (Figure 4.12 L1) was ligated with AMA1 fl1 insert to obtain AMA1 KI plasmid. The ligated mix was transformed into *E. coli* cells to obtain transformant colonies. As very few colonies were obtained after transformation, the confirmation of cloning was not done by colony PCR. The obtained clones were directly processed for plasmid isolation and restriction digestion. The presence of cloned AMA1 fl1 was confirmed by restriction enzyme digestion of pDNA isolated from transformant colonies of AMA1 KI (Figure 4.13) and AMA1 KD (Figure 4.14) by flanking enzymes NotI/ KpnI.

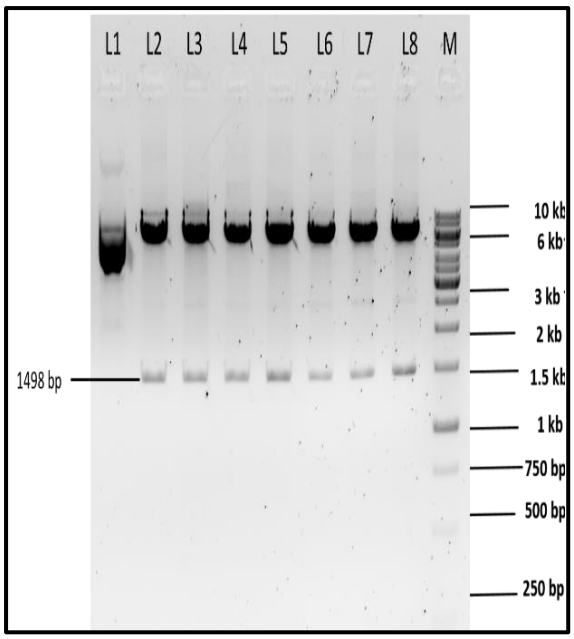

Figure 4. 13 AMA1 KI clones showing release of AMA1 fl1 insert (1498bp) after restriction digestion by NotI/KpnI (L1 to L8). Lane M is 1kb ladder

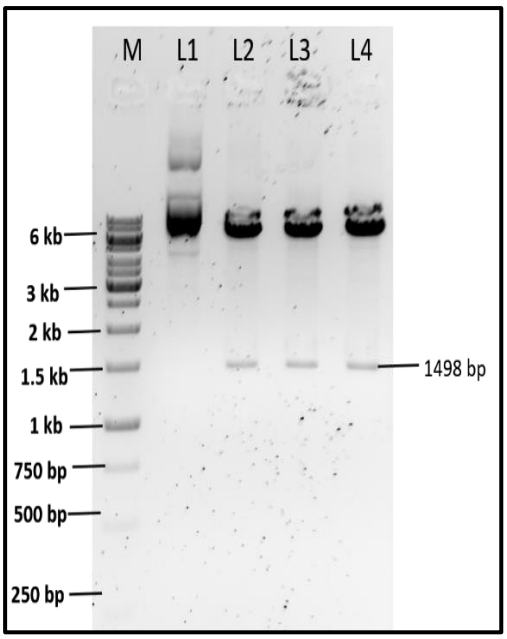

Figure 4. 14 AMA1 KD clones showing release of AMA1 fl1 insert (1498bp) after restriction digestion by NotI/KpnI (L1 to L4). Lane M is 1kb ladder.

Out of eight AMA1 KI clones, seven clones were positive while out of four AMA1 KD clones, three clones were positive. These positive clones are processed further to check the integrity of other fragments in the plasmid and sequence confirmation of cloned fragments.

4.3.3 Fragment analysis of AMA1 KI and AMA1 KD plasmids

Any two confirmed clones of AMA1 KI were analyzed by restriction enzyme digestion to check the integrity of other regions in the plasmid (Figure 4.17) which showed that they contained all the expected regions of appropriate sizes. The presence of other fragments in the construct AMA1 fl1/GFP/PvAc3'UTR/PyαTb5'UTR/hDHFR/ PfHRPII3'UTR/AMA1 fl2 of AMA1 KI plasmids were analyzed by digestion with restriction enzymes specific for the fragments (Figure 4.15).

Similarly, any two confirmed clones of AMA1 KD were analyzed by restriction enzyme digestion to check the integrity of other regions The presence of other fragments in the construct AMA1 fl1/GFP/**cDD**/PvAc3'UTR/PyαTb 5'UTR/hDHFR/PfHRPII3'UTR/AMA1 fl2 of AMA1 KD plasmids were analyzed by digestion with restriction enzymes specific for the fragments (Figure 4.16).

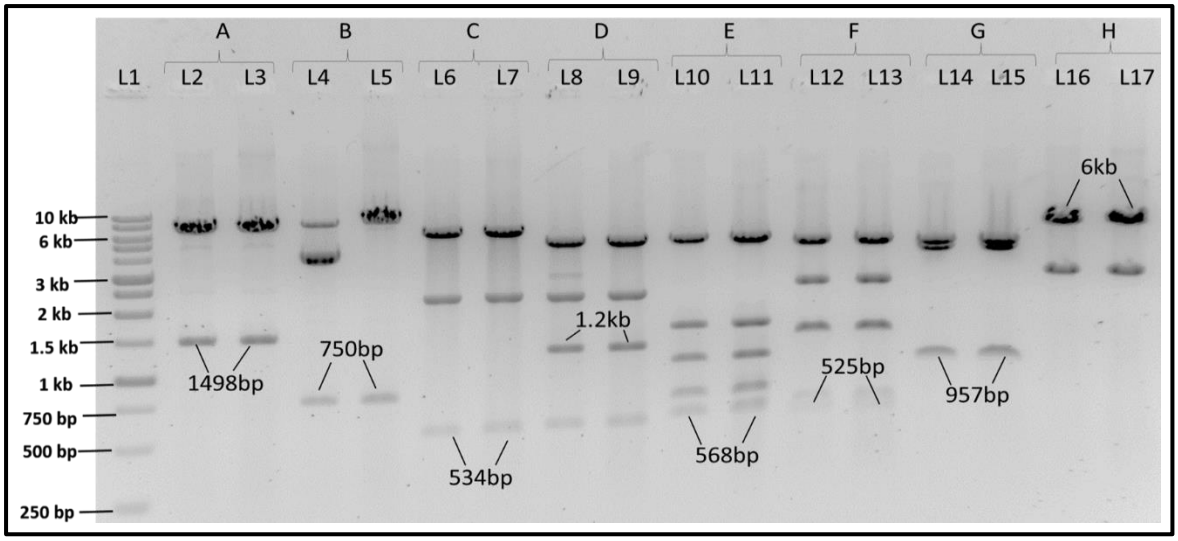

Figure 4. 15 Fragment analysis of AMA1 KI plasmids by restriction digestion, A: Flank 1 excision with NotI/KpnI (1.49 kb), B: GFP release with KpnI/XhoI (~750bp), C: PvAc3'UTR (534bp) release by XhoI/AgeI, D- PyαTbl5'UTR (1.2 kb) release with AgeI/BamHI, E- hDHFR (568bp) excision with BamHI/HindIII, F: PfHRPII3'UTR (525bp) release with HindIII/AvrII, G: Flank 2 release by AvrII/KasI and H: linear transfection cassette (6013bp) with EcorV which will be used to transfect PbANKA wt parasites. Lane L1 is 1kb DNA ladder. The unlabelled bands are due to the digestion at internal restriction sites of the enzymes used. Refer to plasmid map Figure 4.17 for clear overview of digestion.

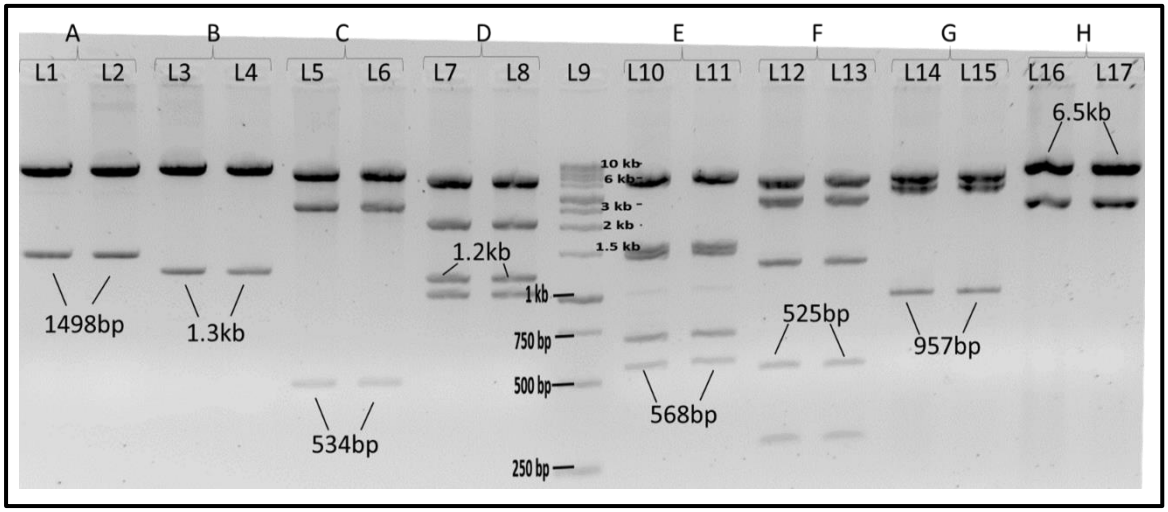

Figure 4. 16 Fragment analysis of AMA1 KD plasmids by restriction digestion. A: Flank 1 (1.49 kb, NotI/KpnI, B: eGFP+CDD (~1.3kb, KpnI/XhoI), C: PvAc3'UTR (534bp, XhoI/AgeI), D: PyαTbl5'UTR (1.2 kb, AgeI/BamHI), E: hDHFR (568bp, BamHI/HindIII), F: PfHRPII3'UTR (525bp, HindIII/AvrII), G: Flank 2 (957bp, AvrII/KasI) and H: linear transfection cassette (6529bp, EcorV) which will be used to transfect PbANKA wt parasites. Lane L9 is 1kb DNA ladder. The unlabelled bands are due to digestion at the internal restriction sites of the enzymes used. Refer to plasmid map Figure 4.17 for clear overview of digestion.

After cloning the AMA1 fl1 at Not1/KpnI site and AMA1 fl2 at AvrII/KasI site of HB vector, AMA1 KI plasmid was obtained (Figure 4.17A). Similarly, AMA1 KD plasmid was obtained after cloning of same flanks into HB KD vector (Figure 4.17B).

AMA1 fl1 (1498 bps) for PbAMA1 KI/KD was amplified with PbAMA1Fl1-F/PbAMA1Fl1-R primers

AAAG**gcggccgc**gatatcATGCATGGTTCTGGTATAAGAGTTGATTTAGGTGAAGATGCACGTGTGGAAAATCGTGATTATAGAATACCTTCAG
GTAAATGTCCAGTTATAGGGAAAGGTATAACTATTCAAAATTCTGAAGTATCATTTTTAACACCAGTAGCTACCGGTGATCAGTCAGTGAGA
AGTGGAGGTTTAGCACTTCCTAAAACAGATGTACACCTTTCTCCTATAACAATTGATAATCTCAAAACAATGTATAAAGAACATCCAGAAAT
AGTAAAATTAAATAATATGTCATTGTGTGCAAAACATACCTCATTTTATGTTCCCGGTAACAATGCCAATTCAGCATATAGACACCCCGCTGT
TTATGATAAATCTAATAGTACTTGCTACATGTTGTATGTAGCAGCCCAAGAAAATATGGGTCCAAGATATTGTAGTAATAATGCAAATAATG
ATAATCAACCATTTTGTTTTACACCCGAAAAAATAGAAAAATATAAAAATTTATCCTATTTAACTAAAAATTTGCGTGATGATTGGGAAACCA
GTTGTCCTAATAAAAGTATAAAAAATGCTAAATTTGGAATTTGGGTTGATGGTTATTGTAAAGATTATCAAAAGCATACAGTTCATGATAGT
GATTCATTATTAAAATGTAATCAAATTATTTTTAACGAAAGTGCTTCTGATCAACCTAAACAATATGAAAAACACCTAGAAGATACTACCAAA
TTTCGACAAGGAGTTGCAGAGAGGAATGGTAAACTTATAGGTGAAGCTTTATTACCAATAGGATCTTATAAATCAGATCAAATTAAAAGCC
ATGGAAGGGGATATAACTGGGGAAATTATGATAGTCAAAACAAAAAATGTTACATTTTCGAAACAAAACCAACATGTTTAATTAATGATAG
GAATTTCATTGCAACAACTGCTTTATCTAGTACAGAAGAGTTCGAAGAACAATTTCCTTGTGATATATATAAAAATAAAATAAACGAAGAAA
TTAAAGTCTTGAACAAAAACATCTCTAATGGAAATAATTCCATTGAATTTCCTAGGATATTTATTTCAACTGACAAAAATAGTTTAAATTGCC
CATGTGAACCTACGCAACTGACTGAGAGCAGTTGTAATTTTTATGTGTGTAATTGTGTAGAGAAAAGACAATATATAGCTGAGAATAATGA
TGTTGAAATAAAAGAAGAGTTTAGAAGTGAATATGAAAGCCCATCAAACCAGAGAGTAATAGTTATTATAATTTTTATTTGTGTTGGAATTA
TATTAGTTATTCTATTAGTGGGTTATTTCTTTAAAAGTAATAAAAAAGGTGAAAATTATGATAGAATGGGTCAAGCAGATATTTATGGTAAA
GCTAATTCCAGAAAAGATGAAATGTTAGACCCAGAAGTGTCATTTTGGGGTGAAGATAAAAGGGCATCACACACAACACCCGTTTTGATGC
AAAAACCATATTAT**ggtacc**TAga

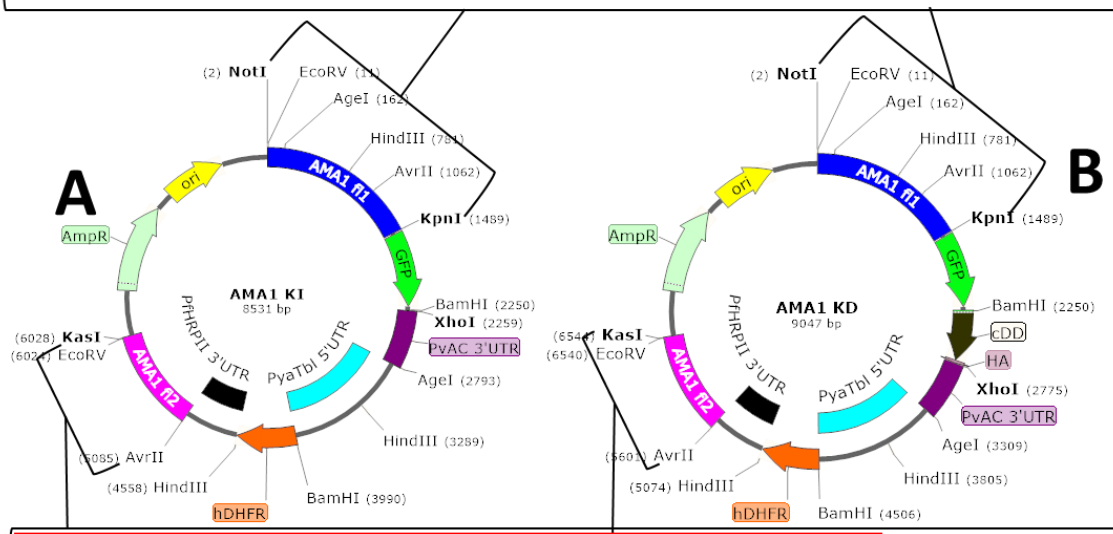

AMA1 fl2 (957 bp) for PbAMA1 KI/KD was amplified with PbAMA1Fl2-F/PbAMA1Fl2-R primers

TAAT**cctagg**GAAGCGTTTAAATAGTAAATAGTTAGTTACTAATAATTTAGTAGTCAAGAAAATATAATTAAATAATGAAGCGTTTAAATAGT
AAATAGTTAGTTACTAATAATTTAGTAGTCAAGAAAATATAATTAAATAATGAAGCGTTTAAATAGTTAAATAATTAATTATTAATAATTAA
GTAAAATATTAACTAGCCAATCAATATTGAATATATATATATTAACAGACAGAATATTTTTTCATTTATACGTATTAATTAACATTTTTGAAG
ATCCAAAAATTCAAATAAATTATACAAATATATATTGACAATAATGTCAAAATAATTAAAATAAGAATTAAAAAATATTAATTTAGATATGT
AATAACATTGTTATATTGACATGAATTATTACTATATATACTAAAACGACTTATCAACTTGTATTGTTTTTACCTGTGCTTAAAGAATATTCAT
AATATTTTAGCTACAAAATATTATATATCATTATTATTGTTTTTTTTGTTTATGTCTTATTATATAATATATTTTAATAATTATAGTGTGTTATA
TTTTGCTCTATTAATAAGCAATATACACATAAACATTTTTTTTTTTTTTTTTTGAAGTGATATTCTATATCTCTTATTTGATGATTGTTATAATT
AGAAGATAAGATATTTCATTTGCATGTATATATTTTTTAAGAATGTTTTTGTGATGTTTTATTATCATTATATGCATATAAAGAGAAAGAAAT
TCATATTTAAAAAAAAAAAAAAAAAAACTTTAACACTTTTTTTAAATTATAATAGTAATATTTTTTTTATATAATTACCTATGCTGCTTTGGGC
ATTCTTTCAATAATATTTTTTTAAATTTTGCGCATTATTTAAAATGCCTTGTTTGTTATTCACAATTTTTTAAAAGTTGGTAAGCATTTCTCTTA
ATCGGgatatc**ggcgcc**TATG

Figure 4. 17 (A) AMA1 KI plasmid map to target knockin and (B) AMA1 KD plasmid map to target knockdown of *Plasmodium berghei* AMA1; AMA1 fl1 is cloned at Not1/KpnI and AMA1 fl2 is cloned at AvrII/KasI. The cloned fragments are same for both knockin and knockdown. The difference lies in the vector with additional cDD segment downstream of GFP at BamHI/XhoI site whose presence is verified by restriction digestion in the agarose gel Figure 4.16. The sequences of flanks are shown with primers underlined. The highlighted sequence is the recognition site for restriction enzyme digestion before cloning. Plasmid map is designed in SnapGene Viewer.

4.3.4 Sequence confirmation of cloned fragments

The cloned flanks were confirmed by DNA sequencing at BioServe, India. The sequence analysis result showed that cloned AMA1 fl1 sequence ended with KpnI site and followed by GFP CDS (Coding Sequence) in both AMA1 KI plasmid (Figure 4.18) and AMA1 KD plasmid (Figure 4.20). In addition, cloned AMA1 fl2 sequence started with AvrII

site after PfHRPII 3'UTR of construct in both AMA1 KI plasmid (Figure 4.19) and AMA1 KD (Figure 4.21) plasmid. This confirmed that the flanks were cloned into targeted site in the plasmid.

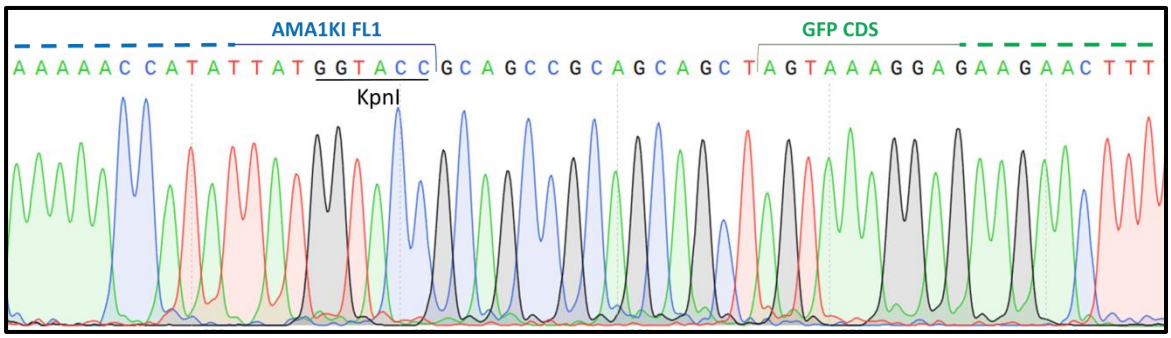

Figure 4. 18 Chromatogram showing the cloned AMA1 fl1 sequence in AMA1 KI plasmid ending with KpnI site. AMA1 fl1 is linked to GFP coding sequence (CDS) via poly-Alanine linker.

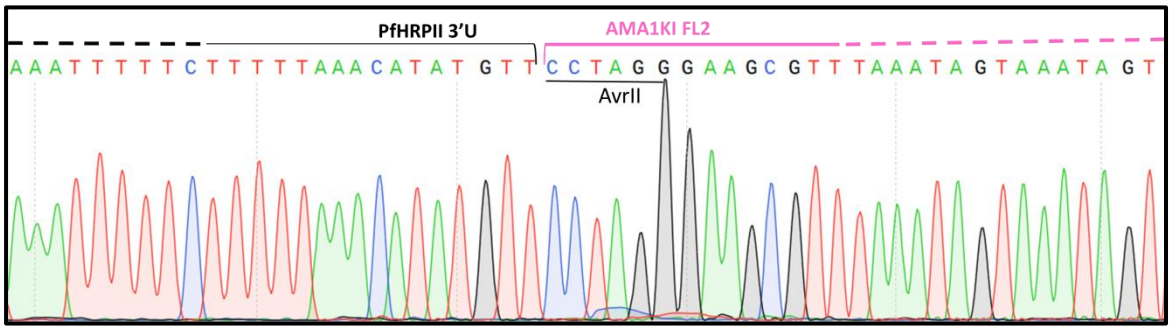

Figure 4. 19 Chromatogram showing the cloned AMA1 fl2 sequence in AMA1 KI plasmid starting with AvrII site. PfHRPII 3'UTR is present upstream of cloned AMA1 fl2 in the plasmid.

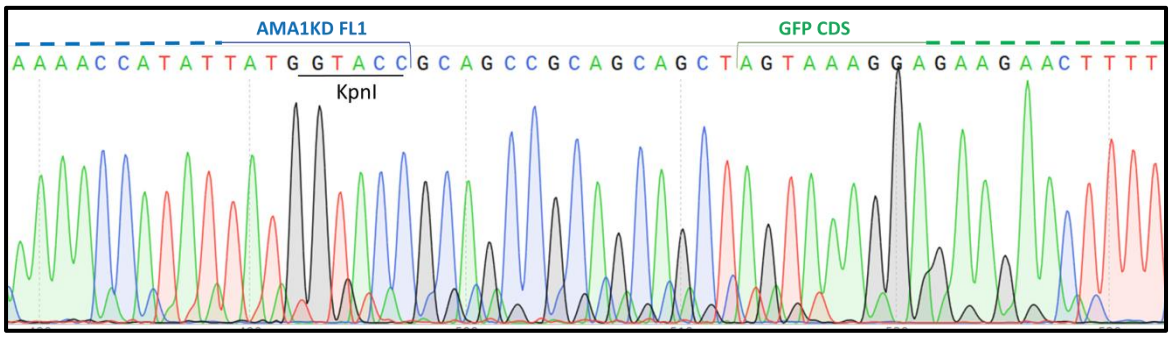

Figure 4. 20 Chromatogram showing the cloned AMA1 fl1 sequence in AMA1 KD plasmid ending with KpnI site. AMA1 fl1 is linked to GFP coding sequence (CDS) via poly-Alanine linker.

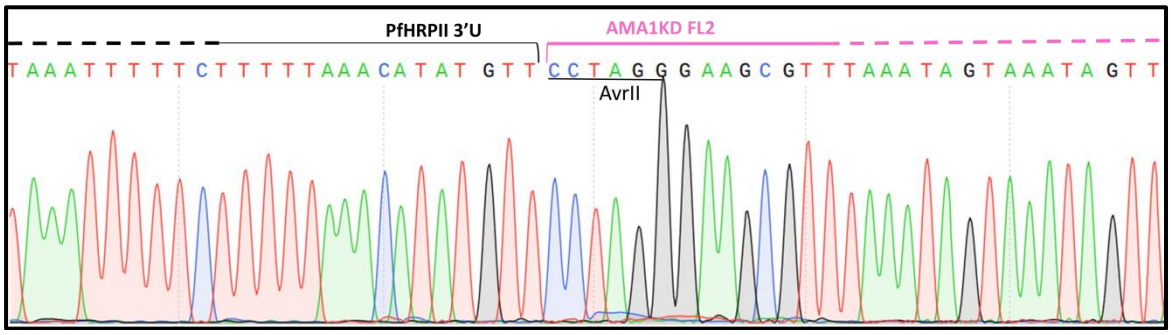

Figure 4. 21 Chromatogram showing the cloned AMA1 fl2 sequence in AMA1 KD plasmid starting with AvrII site. PfHRPII 3'UTR is present upstream of cloned AMA1 fl2 in the plasmid.

4.4 Construction of ATG18 KO and ATG18 KD plasmids

4.4.1 Preparation of ATG18 inserts

Using PbANKA WT gDNA, ATG18 KO fl1 (997bp) was PCR amplified from ATG18 5'UTR region using primers P1 and P2, ATG18 KO/KD fl2 (764bp) was PCR amplified from ATG18 3'UTR region using primers P3 and P4, and ATG18 KD fl1 (2181bp) was PCR amplified from ATG18 5'UTR+ CDS using primers P1 and P2' (Figure 4.22). All the primers are listed in Table 2.

The ATG18 KO/KD fl2 was digested with AvrII/KasI while ATG18 KO fl1 and ATG18 KD fl1 were digested with NotI/KpnI. Digested PCR amplicons were gel purified to obtain the respective inserts.

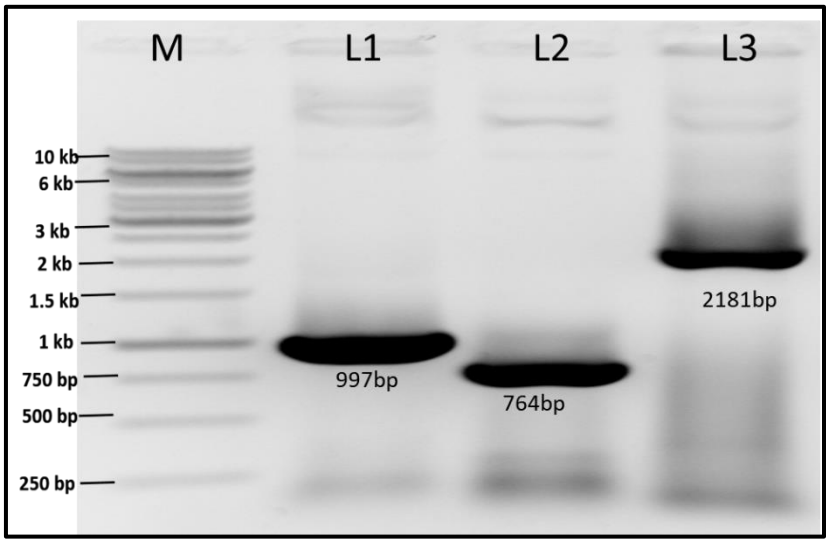

Figure 4. 22 PCR amplicon of ATG18 KO fl1 (L1) from ATG18 5'UTR (primers P1 and P2), ATG18 KO/KD fl2 (L2) from ATG18 3'UTR (primers P3 and P4) and ATG18 KD fl1 (L3) from ATG18 5'UTR+CDS (primers P1 and P2'). The given primers are listed in Table 2. Expected size of the amplicon is given underneath the respective bands. Lane M is the 1kb DNA ladder.

4.4.2 Cloning ATG18 KO/KD fl2 in HB and HB KD plasmids

HB plasmid and HB KD plasmids were digested with AvrII/KasI (Figure 4.7), and gel purified to obtain HB vector and HB KD vector.

HB vector backbone (Figure 4.7 L1) was ligated with ATG18 KO/KD fl2 insert to obtain ATG18 fl2 KO plasmid. The ligated mix was transformed into *E. coli* cells to obtain several colonies. These colonies were screened for the presence of ATG18 KO/KD fl2 insert by colony PCR (Figure 4.23) using primers P3 and P4 (Table 2).

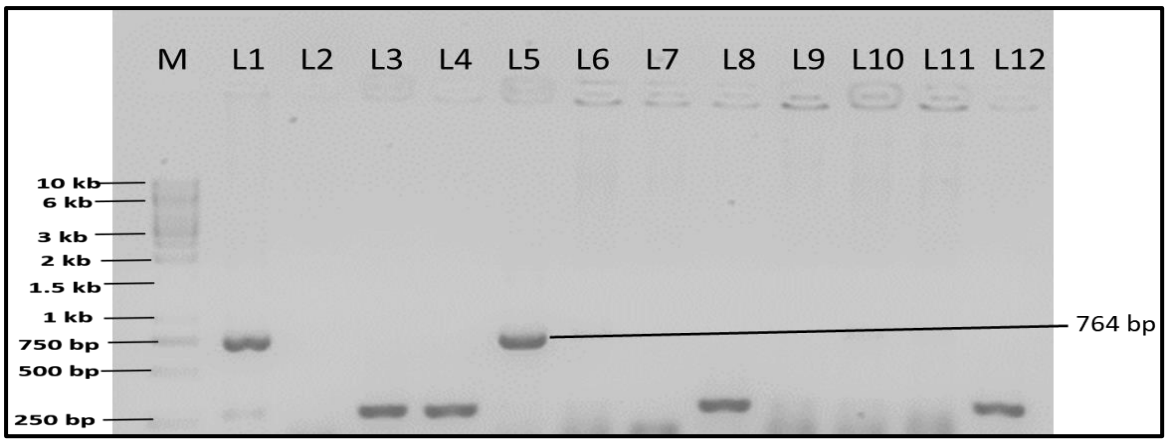

Figure 4. 23 Amplification of ATG18 KO/KD fl2 (764bp) by colony PCR of ATG18 fl2 KO clones using primers P3 and P4. Lane M is 1kb DNA ladder, L1 is positive control with gDNA template and other lanes contain PCR products (L2-L12).

HB KD vector backbone (Figure 4.7 L2) was ligated with ATG18 KO/KD fl2 insert to obtain ATG18 fl2 KD plasmid. The ligated mix was transformed into *E. coli* cells to obtain several colonies. These colonies were screened for the presence of ATG18 KO/KD fl2 insert by colony PCR (Figure 4.24) using primers P3 and P4 (Table 2).

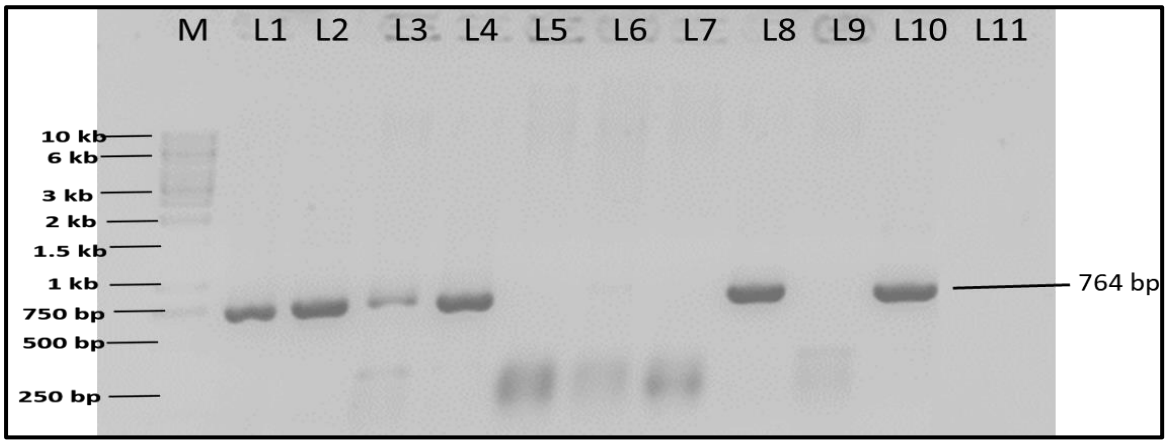

Figure 4. 24 Amplification of ATG18 KO/KD fl2 (764bp) by colony PCR of ATG18 fl2 KD clones using primers P3 and P4 (Table 2). Lane M is 1kb DNA ladder, L1 is positive control with gDNA template and other lanes contain PCR products (L2-L12).

Among several positive ATG18 fl2 KO and ATG18 fl2 KD clones, pDNA was isolated from four clones each of ATG18 fl2 KO and ATG18 fl2 KD. Isolated plasmids were evaluated for the presence of ATG18 KO/KD fl2 by digestion with AvrII/KasI (Figure 4.25). This showed the release of insert just cloned, which revealed the presence of expected size of insert (764bp).

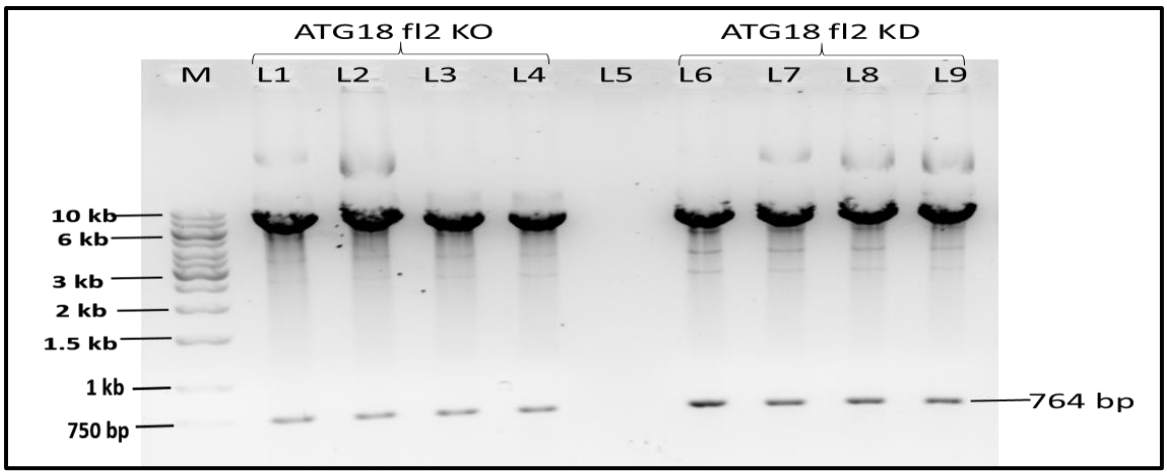

Figure 4. 25 Release of ATG18 KO/KD fl2 (764bp) upon restriction digestion of ATG18 fl2 KO and ATG18 fl2 KD by AvrII/KasI. Lane M is the 1 kb DNA ladder. L1, L2, L3, L4 are ATG18KO fl2 plasmids and L6, L7, L8, L9 are ATG18KD fl2 plasmids.

All the selected clones released the expected size of cloned ATG18 KO/KD fl2 insert upon digestion by flanking enzymes AvrII/KasI.

4.4.3 Construction of ATG18 KO and ATG18 KD plasmids

Any one of ATG18 KO/KD fl2 cloned plasmid, i.e. ATG18 fl2 KO was digested with NotI/KpnI and was ligated with similarly digested ATG18 KO fl1 to obtain ATG18 KO plasmid (Figure 4.29). The ligated mix was transformed into *E. coli* cells to obtain several colonies. These colonies were screened for the presence of ATG18 KO fl1 insert of size 997bp by plasmid isolation and restriction digestion with flanking enzymes NotI/KpnI (Figure 4.26).

Similarly, any one of ATG18 KO/KD fl2 cloned plasmid, i.e. ATG18 fl2 KD was digested with NotI/KpnI and was ligated with similarly digested ATG18 KD fl1 insert to obtain ATG18 KD plasmid (Figure 4.30). The ligated mix was transformed into *E. coli* cells to obtain several colonies. These colonies were screened for the presence of ATG18 KD fl1 insert of size 2181bp by plasmid isolation and restriction digestion with flanking enzymes NotI/KpnI (Figure 4.26).

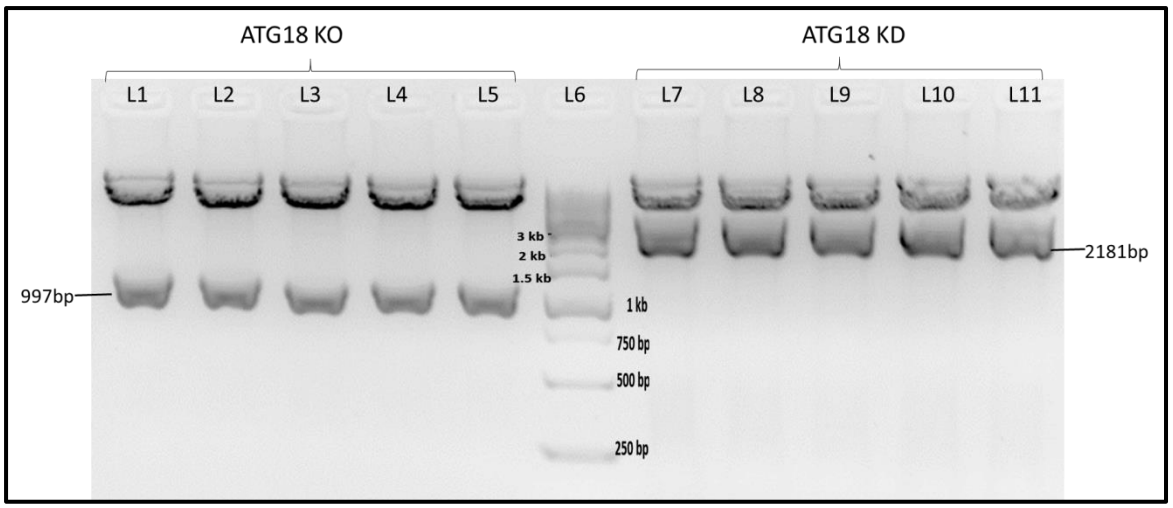

Figure 4. 26 Release of ATG18 KO fl1 (997bp) from ATG18 KO plasmids (L1 to L5) and release ATG18 KD fl1 (2181bp) from ATG18 KD plasmids (L7 to L11) upon restriction digestion by NotI/KpnI. Lane L6 is 1kb DNA ladder.

4.4.4 Fragment analysis of ATG18 KO and ATG18 KD plasmids

Any three confirmed clones of ATG18 KO showing the presence of both ATG18 KO fl1 and ATG18 KO/KD fl2 were analyzed by restriction enzyme digestion to release all the fragments (Figure 4.27). Clearer overview of digestion can be obtained from the vector map (Figure 4.29).

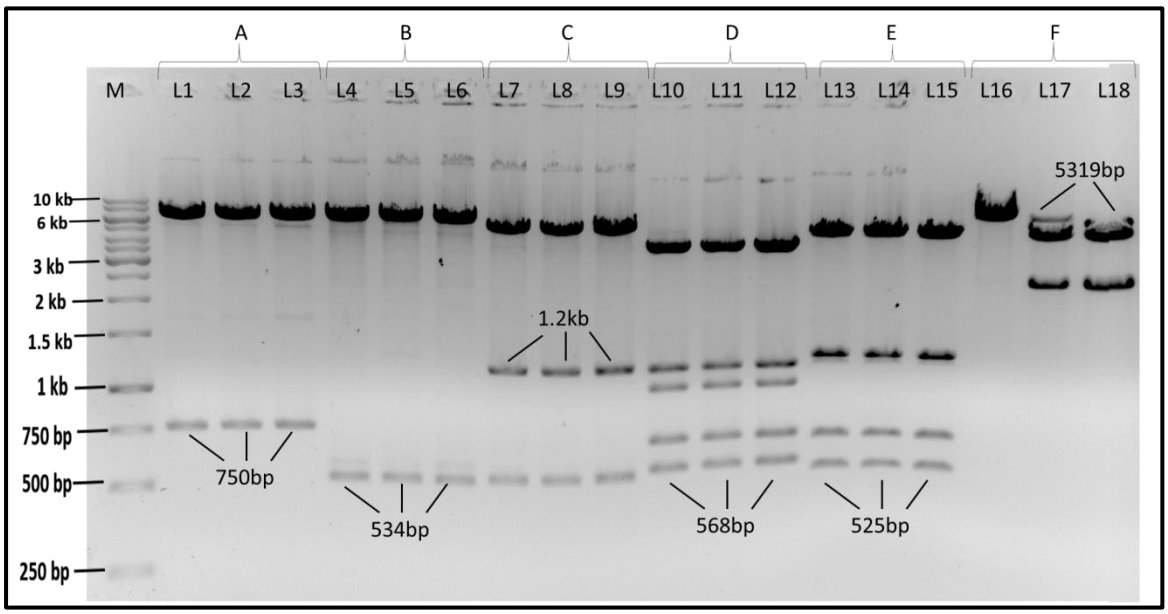

Figure 4. 27 Fragment analysis of ATG18 KD plasmids by restriction digestion; A-KpnI/XhoI eGFP (~750bp), B-XhoI/AgeI PvAc3'UTR (534bp), C-AgeI/BamHI PyαTbl5'UTR (1.2 kb), D-BamHI/HindIII hDHFR (568bp), E-HindIII/AvrII PfHRPII3'UTR (525bp), F- EcorV for linear transfection construct (5319bp) which will be used to transfect PbANKA wt parasites. M is the 1kb DNA ladder. The clone L16 did not release an expeted size of fragment upon digestion by EcoRV, so it was not used for transfection. The unlabelled bands are due to the internal restriction sites of the enzymes used. Refer to vector map Figure 4.29 for clear overview of digestion.

Any three confirmed clones of ATG18 KD showing the presence of both ATG18 KD fl1 and ATG18 KO/KD fl2 were analyzed by restriction enzyme digestion to release all the fragments (Figure 4.28). The difference in size of KpnI/XhoI digest in the ATG18 KO and ATG18 KD can be observed clearly. From ATG18 KO clones, only GFP is released (750bp) while from ATG18 KD clones, GFP+cDD is released (1.3kb). Clearer overview of digestion can be obtained from the vector map (Figure 4.30).

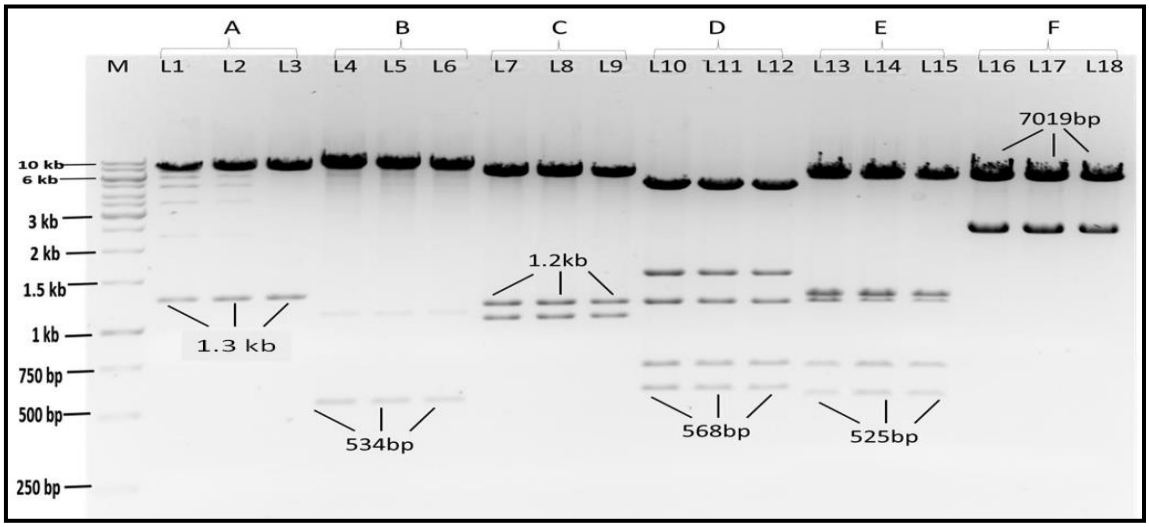

Figure 4. 28 Fragment analysis of ATG18 KD plasmids by restriction digestion. A-KpnI/XhoI eGFP+cDD (~1.3kb), B-XhoI/AgeI PvAc3'UTR (534bp), C-AgeI/BamHI PyαTbl5'UTR (1.2 kb), D-BamHI/HindIII hDHFR (568bp), E-HindIII/AvrII PfHRPII3'UTR (525bp), F- EcorV for linear transfection construct (7019bp) which will be used to transfect PbANKA wt parasites. Lane M is the 1kb DNA ladder. The unlabelled bands are due to the internal restriction sites of the enzymes used. Refer to vector map Figure 4.30 for clear overview of digestion.

Out of three PbATG18 KO clones checked by fragment analysis, EcoRV did not linearize one clone upon digestion (Figure 4.29 Lane F). Therefore, that clone was discarded and other two clones were used for transfection. Similarly, when PbATG18 KD clones were checked by fragment analysis, all of them showed respective size of bands. After cloning the ATG18 KO fl1 in Not1/KpnI site and ATG KO fl2 in AvrII/KasI site of HB vector, ATG18 KO plasmid was obtained (Figure 4.29). Similarly, AMA1 KD plasmid was obtained after cloning of same flanks into HB KD vector (Figure 4.30).

ATG18KO fl1 (997 bps) was amplified with PbA18Kfl1-F1 /PbA18Kfl1-R1 primers

GTTAgcggccgcgatatcGCTTTAGGACGAGTTTAATTTCTACGTTTTAAAATGCTTATATAATAAAATATAGGAAATGTAATAATAAAA
AAATAAAATAAATAGTAATTAAAATAAATAAATATTTATATAATAATTTATAGCATTTCATTATTATGTCATTTTATATTTTTTAATTA
ATGATATATATAACTTTTTCCATTTATAATAATTTATATATTTTACTGTTAGTTTCTTTCATTATTTTATGGTATTAATGTCAATATATA
TTATAATATATTTTACATGGAAATTTCTTCATTTTTTTTCTTATTCTTACAAGTCCAGTAAATATATATATATATATATTATAGTATT
TTTTTTATCATAATAAAATACATTAATATGAATAAGGATATATTTATTATAATTAATGTTTATAAGTATATGATTTTTTAAGTATATGA
TTATTTTTCATGTAATATATGTAGTTATATTTGTACTACAATATTAACTGTTCTAAGAAATTATTTTACTAGAACTCCCATTTTAAACT
TTTAAATAAATATATACATATGCACATGCATACTGTAAATATATATAATTAGTTTTTGTTTCATCATTTAACTTAGTAATTGAAATAT
ATTCTTTTAATTCTTTGTGAGGTGATTAATTTTTTTATTTTTTAGATGGGCATAAAATAATAATGACAGTATATATTTTATATTAAAAA
AAGGGAATATATGAGCATGTGTATATATGCTTACATATACGTCTACATAATATATATATACGTATGCAGCTGATACGCATATATGTA
TTTATATACACGTGTAGGCACCATTCAGCAACCTTGTTCTATAATAACAGAAATATTGTGTCAATCCCCTTATTTATTTTTGCTTTTTT
GTAATTGTTCCCAATTTATATACAAAGAAAAAATAAAATGGTATCATTAAGATTAGATAATAATAGATATATAGCTTTTAATCAAGA
TTATGGCTGTggtaccATGG

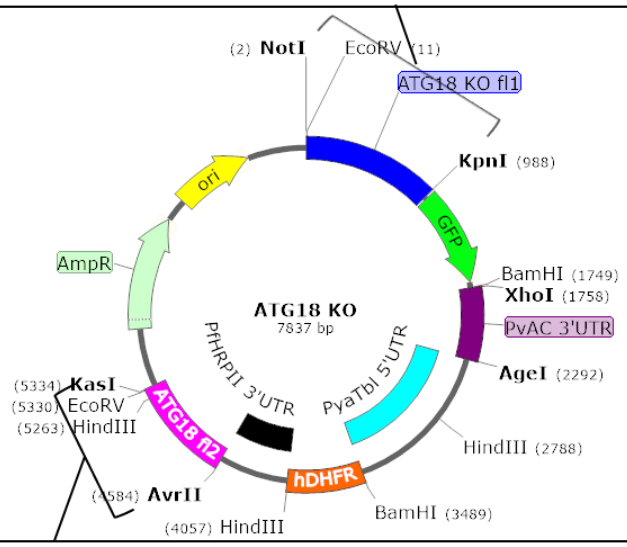

ATG18KO/KD fl2 (764bps) was amplified using PbA18Kfl2-F / PbA18Kfl2-R1 primers

TTTA**cctagg**CACGTTTTGTCACAACACATATATCTATACTTGATAGGCATATTATATTTTCGATTACATATTTATTTGAGTTTGCTGT
TTCGGCGCGCACATTCACAATATATATTTGTATTTGTTGTGAAAGATAACATAATTAATTAGTTTATTAATGACGTGGATATATGTG
ATATTTTATGAATAATATAAATATCTTTTTTACATATGGAATACATAGGTATGTATATACACACATGTATGGTTTCTTATATATATAA
TAATTTTTTTGTTTCACTATTTTTAAAGTACATATTATATTTATAAAGATACTGCATGGAATGTGATTCGTTTTATTGCTTCCAATGT
ACGAAAAAAAAAATTAATCATACAAGCATGTATATATGCATAATACATATCTACCTTAATCACATTATATTAAGGACCTTTTTTTCTT
ATCTATATTTTTTGCATAATTTATTTGTGCATTTTATATATTCATTAGTTGAAATTTTAAAATATATGTTGTAACGTGTCTTTGATGA
ATTTATATGTTGTATTTTCATTTTTTTTTTCCTTTGGATTTTTAATGTTTATTATTATATTTTTTTTTATGCCCACTATTAAATATTTTAT
TCATAAGTGGAAGTTTTAAACAGTTATATTAACACTTTTGTTAAAAAAGTAATTTTAAAGTTACAAAGCTTATGTAATAGTTGTATG
CATATTTTAGTCATATATGTATGCATATACAAAGTGTATCGATgatatc**ggcgcc**AAAA

Figure 4. 29 ATG18 KO plasmid map to target knockout of *Plasmodium berghei* ATG18 ; ATG18 KO fl1 is cloned at Not1/KpnI and ATG18 KO/KD fl2 is cloned at AvrII/KasI. The 5' UTR and 3' UTR of PbATG18 is taken as flank to completely remove coding region after recombination. The sequences of flanks are shown with primers underlined. The highlighted sequence is the recognition site for restriction enzyme digestion before cloning. Plasmid map is designed in SnapGene Viewer.

ATG18KD fl1 (2181 bps) was amplified using PbA18Kfl1-F1/ PbA18Rep-R primers

GTTA**gcggccgc**gatatcGCTTTAGGACGAGTTTAATTTCTACGTTTTAAAATGCTTATATAATAAAATATAGGAAATGTAATAATAAAA
AAATAAAATAAATAGTAATTAAAATAAATAAATATTTATATAATAATTTATAGCATTTCATTATTATGTCATTTTATATTTTTTAATTA
ATGATATATATAACTTTTTCCATTTATAATAATTTATATATTTTACTGTTAGTTTCTTTCATTATTTTATGGTATTAATGTCAATATATA
TTATAATATATTTTACATGGAAATTTCTTCATTTTTTTTCTTATTCTTACAAGTCCAGTAAATATATATATATATATATTATAGTATT
TTTTTTATCATAATAAAATACATTAATATGAATAAGGATATATTTATTATAATTAATGTTTATAAGTATATGATTTTTTAAGTATATGA
TTATTTTTCATGTAATATATGTAGTTATATTTGTACTACAATATTAACTGTTCTAAGAAATTATTTTACTAGAACTCCCATTTTAAACT
TTTAAATAAATATATACATATGCACATGCATACTGTAAATATATATAATTAGTTTTTGTTTCATCATTTAACTTAGTAATTGAAATAT
ATTCTTTTAATTCTTTGTGAGGTGATTAATTTTTTTATTTTTTAGATGGGCATAAAATAATAATGACAGTATATATTTTATATTAAAAA
AAGGGAATATATGAGCATGTGTATATATGCTTACATATACGTCTACATAATATATATATACGTATGCAGCTGATACGCATATATGTA
TTTATATACACGTGTAGGCACCATTCAGCAACCTTGTTCTATAATAACAGAAATATTGTGTCAATCCCCTTATTTATTTTTGCTTTTTT

GTAATTGTTCCCAATTTATATACAAAGAAAAAATAAAATGGTATCATTAAGATTAGATAATAATAGATATATAGCTTTTAATCAAGA
TTATGGCTGTTTGTGTATGGCCAACGAAAAGGGATTTAAGATTTACAATACAAATCCTTTCACTCAAACGTATAGTAGAGGTAATA
GCATTACATGTGTAAATATTGGTTTGAATATTTATATGATATATGACGACGCCACACTCAAACATTGTTATTTTATTTTATTTTATTTT
ATATTTTAGATTTAACTGATCGGAATAAAAATGGGTTATACATAGCAGAAATGCTTTATCGTTGCAATATTTTAGCAATAACTGGAA
ACAAAAATGATAGAAAAGGAAAGTGGGCAAAAAATGTTTTAATAATATGGGATGATAGACAAATGAGAGAAATAGCAAAATTGA
CATTTTCATCAAACATTATCGGTGTGAGATTATTAAGAGAAATAATTGTGGTCATTTTAGAATATAAATTATGTATATACAGGTTAA
AAGATATAATATTATTAGAAACCCTGAATACAACAAAAAATCCATCAGGATTATGTTGCTTATCAAATATTGATAAAAATATTATTA
TTGCATATTTGTCACCTATAAAAGGTCGAGTTAATATTCATATATTTGAAAAAAATGCTAGTGAAAATGTTCATGAAGAACTCCCTT
ATATAAATTTTAAAACCGATTTAAGTATATATGCTCATGATAATCCAATTGGATGTATAAATTTAAGTAATGATGGAAAACTATTAG
TAACCGCTTCTACAAAGGGAACAATTATAAGATTATTTAATACTTTCGATGGAAGTTTATTAAACGAATTTAGAAGAGGTACTAAA
AATGCAAAAATATTATCCTTAAATATCAGTAATGATAATAATTGGCTGTGTTTAACTTCAAATAGAAATACTGTACATGTATTTTCTA
TATATAAAAGAAATCGACCCCCAAGAAAAGTAGATATAATATCTAAAGGAAAAAATATATCTTCACATGTTATGCTAAATTATGAA
AAAGAATCAAAAAATAAAAAATCATCTATTAAATGTTTATTACCTTGTCATCCGTACTTAAATAGCGATTGGAGTTTTTCATCATAT
AAAATCCCTGGGAAAAAAATATCATCAATTTGTGCATTTGTAAGTGACCAAAATTGTATTATTGTTATATGTTCAAATGGACTTATT
TATAAATTGAGATTTAATGAGCATGTAGGAGGAGAAATGCTTAAAATATCTTCCCATAGCTTTGATggtaccTAAA

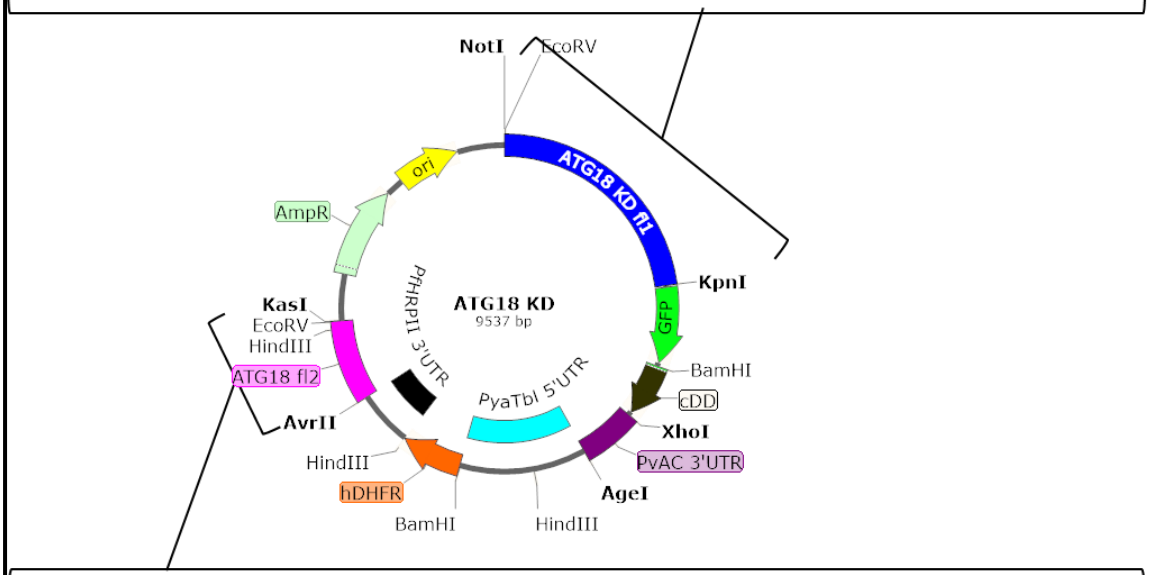

ATG18KO/KD fl2 (764bps) was amplified using PbA18Kfl2-F / PbA18Kfl2-R1 primers

TTTAcctaggCACGTTTTGTCACAACACATATATCTATACTTGATAGGCATATTATATTTTCGATTACATATTTATTTGAGTTTGCTGTT
TCGGCGCGCACATTCACAATATATATTTGTATTTGTTGTGAAAGATAACATAATTAATTAGTTTATTAATGACGTGGATATATGTGA
TATTTTATGAATAATATAAATATCTTTTTTACATATGGAATACATAGGTATGTATATACACACATGTATGGTTTCTTATATATATAAT
AATTTTTTTGTTTCACTATTTTTAAAGTACATATTATATTTATAAAGATACTGCATGGAATGTGATTCGTTTTATTGCTTCCAATGTAC
GAAAAAAAAATTAATCATACAAGCATGTATATATGCATAATACATATCTACCTTAATCACATTATATTAAGGACCTTTTTTTCTTATC
TATATTTTTTGCATAATTTATTTGTGCATTTTATATATTCATTAGTTGAAATTTTAAAATATATGTTGTAACGTGTCTTTGATGAATTT
ATATGTTGTATTTTCATTTTTTTTTTCCTTTGGATTTTTAATGTTTATTATTATATTTTTTTTTATGCCCACTATTAAATATTTTATTCATA
AGTGGAAGTTTTAAACAGTTATATTAACACTTTTGTTAAAAAAGTAATTTTAAAGTTACAAAGCTTATGTAATAGTTGTATGCATAT
TTTAGTCATATATGTATGCATATACAAAGTGTATCGATgatatcggcgccAAAA

Figure 4. 30 ATG18 KD plasmid map to target knockdown of *P. berghei* ATG18; ATG18 KO fl1 is cloned at Not1/KpnI and ATG18 KO/KD fl2 is cloned at AvrII/KasI. The 5' UTR+coding region and 3' UTR of PbATG18 is taken as flank not to remove coding region of gene after recombination. The difference lies in the vector with additional cDD segment downstream of GFP at BamHI/XhoI site which will regulate the expression of ATG18 after recombination. The sequences of flanks are shown with primers underlined. The highlighted sequence is the recognition site for restriction enzyme digestion before cloning. Plasmid map is designed in SnapGene Viewer

4.4.4 Sequence confirmation of cloned fragments

The sequencing result of ATG18 KO and ATG18 KD plasmids showed that cloned ATG18 fl1 sequence ended with KpnI site and followed by GFP CDS in both ATG18 KO and ATG18 KD plasmids (Figure 4.31- Figure 4.33). In addition, cloned ATG18 KO/KD fl2 sequence started with AvrII site after PfHRPII 3'UTR of construct in both ATG18 KO and ATG18 KD plasmids (Figure 4.32- Figure 4.34).

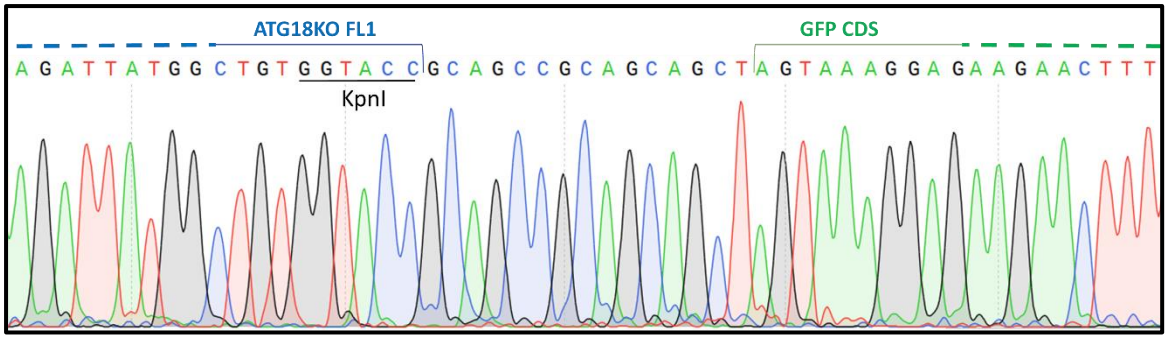

Figure 4. 31 Chromatogram showing the cloned ATG18 KO fl1 sequence in ATG18 KO plasmid ending with KpnI site. Fl1 is linked to GFP coding sequence (CDS) via poly-Alanine linker.

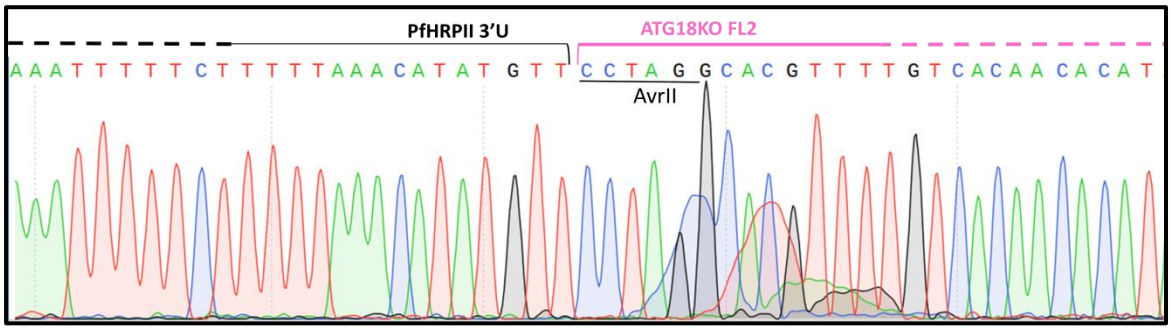

Figure 4. 32 Chromatogram showing the cloned ATG18 KO/KD fl2 sequence in ATG18 KO plasmid starting with AvrII site. PfHRPII 3'UTR is present upstream of cloned Fl2 in the plasmid.

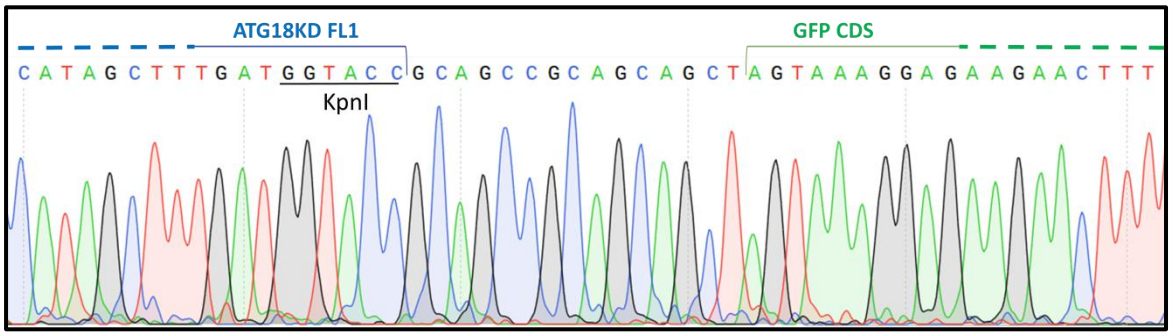

Figure 4. 33 Chromatogram showing the cloned ATG18 KD fl1 sequence in ATG18 KD plasmid ending with KpnI site. Fl1 is linked to GFP coding sequence (CDS) via poly-Alanine linker.

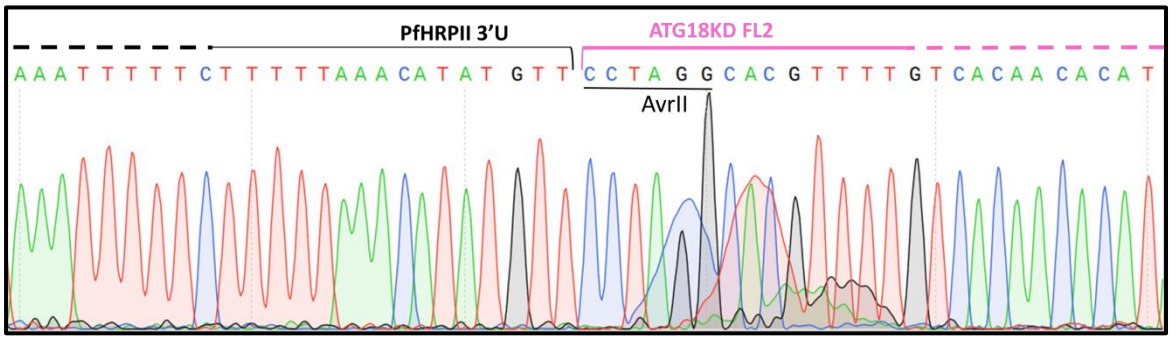

Figure 4. 34 Chromatogram showing the cloned ATG18 KO/KD fl2 sequence in ATG18 KD plasmid starting with AvrII site. PfHRPII 3'UTR is present upstream of cloned Fl2 in the plasmid.

After fragment analysis and sequencing confirmation only, the clones with all the correct digestion and presence of all fragments were subjected for linearization of vector to make ATG18 transfection constructs.

4.5 Preparation of parasites for transfection

The purified wild type parasitesby Nycodenz gradient (Figure 4.35A), as mentioned in method 3.7.1, were cultured in-vitro without RBCs which allowed them to be matured to schizont stage (Figure 4.35B). As the culture is not supplemented with RBCs, the parasites sense the absence of host cells for infection. Due to lack of RBCs required for another erythrocytic schizogony, parasites halt their growth in schizont stage. In addition, the schizont stage is multinucleated and electroporation of foreign DNA would have maximum probability for entry into the parasite. This would allow homologous recombination in the targeted gene locus, so transfection is efficient in schizont stage of parasites.

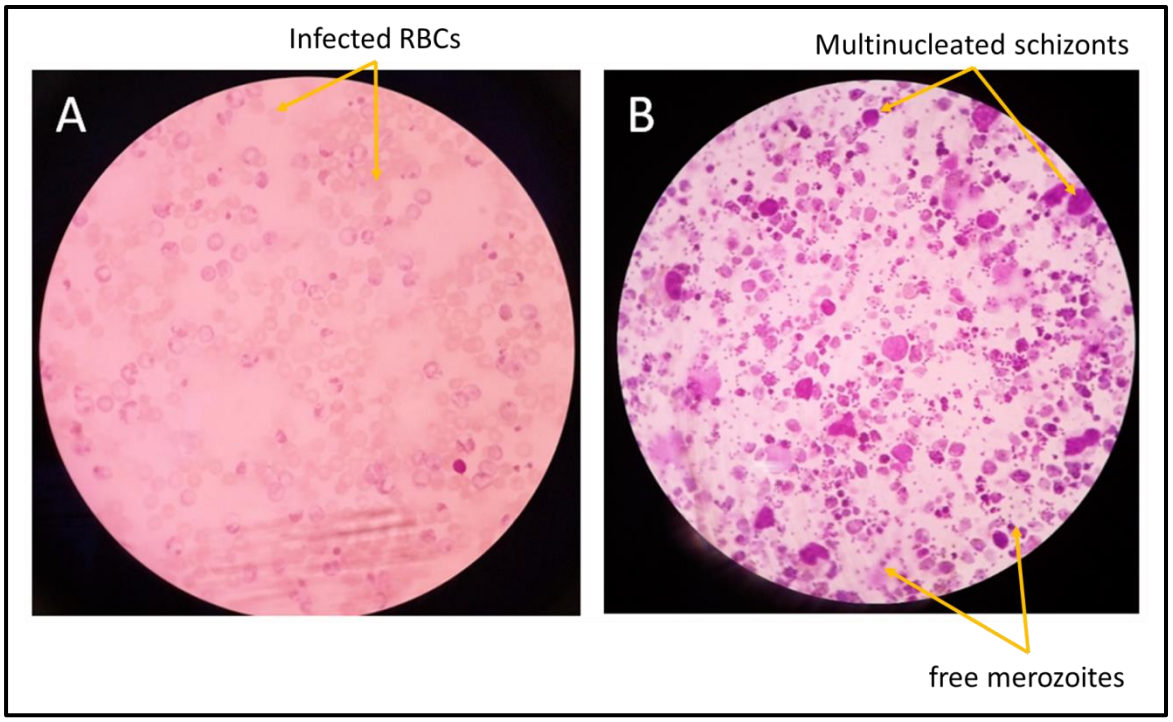

Figure 4. 35 Giemsa stained smears of PbANKA wild type parasites (A) after Nycodenz separation before culturing in-vitro to schizont stage and (B) after culturing to schizont stage in-vitro. Small clusters of dots are of merozoites released upon rupture of schizonts. This is done to obtain most of the parasite in schizont stage as electroporation of construct DNA is done to this stage.

4.6 Homologous recombination in parasites

Here, in this study, we targeted *Plasmodium berghei* AMA1 locus by AMA1 KI construct (Figure 4.36A) and AMA1 KD construct (Figure 4.36B) using homologous recombination approach through double crossover in the homologous flanking sequences. The

linearized transfection construct, which shares homology with the targeted gene loci, in part, is electroporated to *Plasmodium berghei* wild type in high quantity (5 µg). This makes the parasite realize the loss of its genomic DNA fragment and would try to incorporate by homologous recombination.

The wt AMA1 locus would be followed by the GFP/hDHFR cassette in AMA1 KI recombinants (Figure 4.36A) and followed by GFP/cDD/hDHFR cassette in AMA1 KD recombinants (Figure 4.36B) via double crossover.

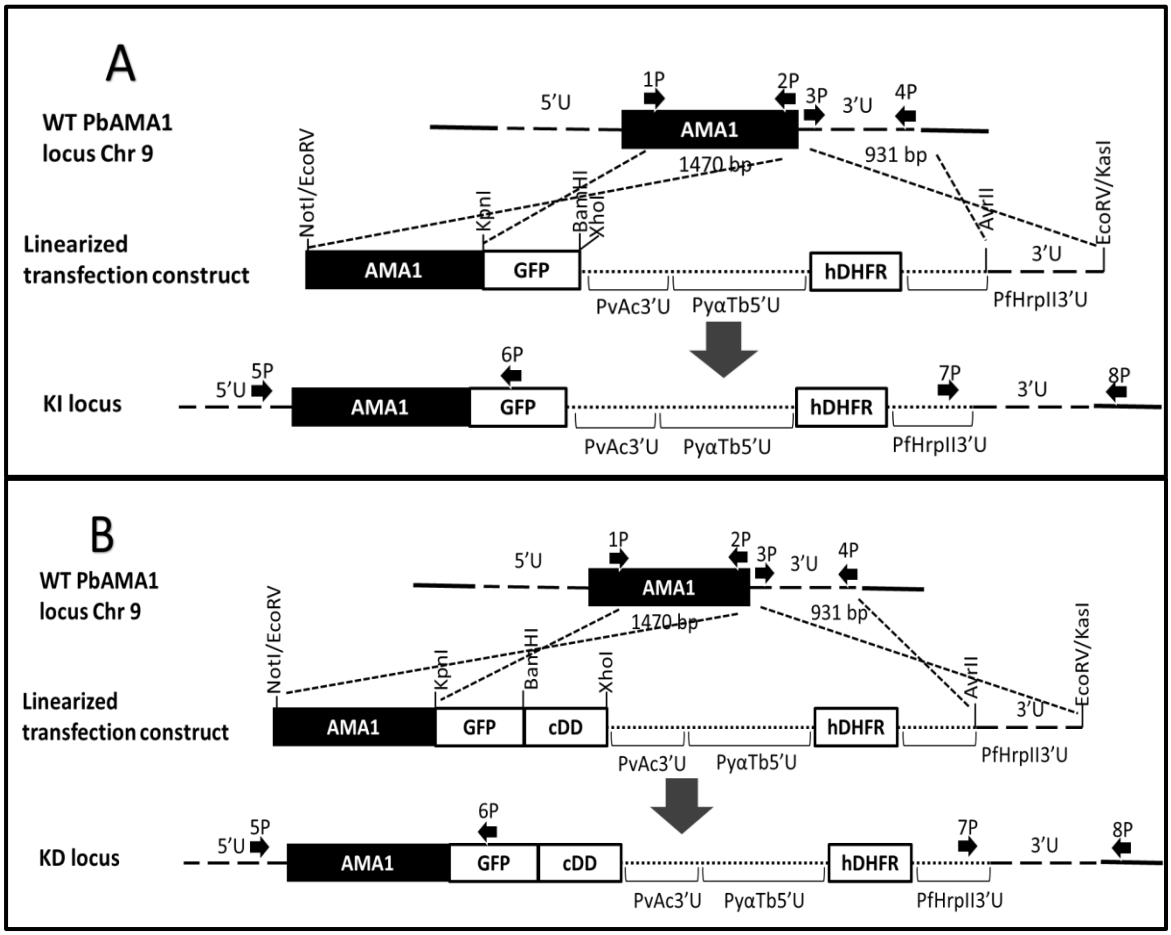

Figure 4. 36 Schematic representation of integration of the linearized transfection construct to target KI (A) and KD (B) into the chromosomal wild-type (WT) AMA1 locus. The AMA1 gene, the flanking untranslated regions (5'U and 3'U), the location and orientation of PCR primers (horizontal arrows), GFP- and hDHFR-coding regions, the regulatory regions in the linearized transfection construct (PvAC3'U, PyαTb5'U and PfHrpII3'U), and restriction endonuclease sites are labelled. The solid lines represent chromosomal DNA regions. The wt AMA1 locus would be followed by the GFP/hDHFR cassette in KI (A) and GFP/cDD/hDHFR cassette in KD (B) via double crossover (shown with X). Here, 1P- PbAMA-fl1F, 2P- PbAMA-fl1R, 3P- PbAMA-fl2F and 4P- PbAMA-fl2R are the primers to amplify the flanks as listed in Table 1. 5P, 6P, 7P and 8P are the primers to confirm recombination in AMA1 locus by PCR.

Though upto three transfection experiments were repeated to target AMA1 KI and AMA1 KD, parasitemia was not observed in the mice model after injection of transfected parasites.

Similarly, ATG18 locus was also targeted by ATG18 KO construct (Figure 4.37A) and ATG18 KD construct (Figure 4.37B) using homologous recombination approach through double crossover in the homologous flanking sequences. The wt ATG18 locus would be replaced by the GFP/hDHFR cassette in ATG18 KO recombinants (Figure 4.37A) and wt ATG18 locus would be followed by GFP/cDD/hDHFR cassette in ATG18 KD recombinants (Figure 4.37B) via double crossover.

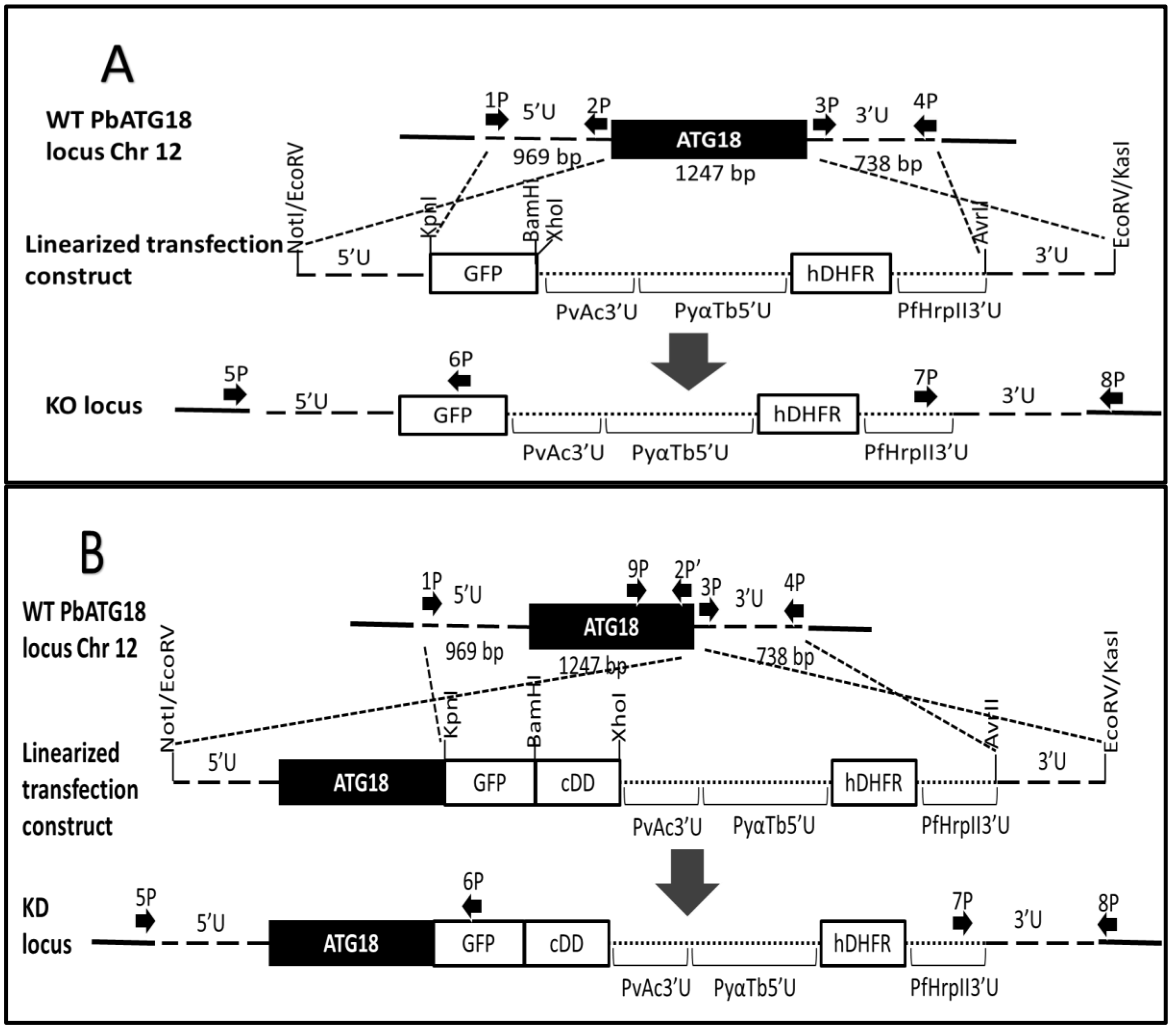

Figure 4. 37 Schematic representation of integration of the linearized transfection construct to target KO (A) and KD (B) into the chromosomal wild-type (WT) ATG18 locus. The labelling is same as in Figure 4.36. The wt ATG18 locus would be replaced by the GFP/hDHFR cassette in KO (A) and followed by GFP/cDD/hDHFR cassette in KD (B) via double crossover (shown with X). Here, 1P- PbA18Kfl1-F1, 2P- PbA18Kfl1-R1, 3P- PbA18Kfl2-F and 4P- PbA18Kfl2-R1 are the primers to amplify the flanks for KO while 1P, 2P- PbA18Rep-R, 3P and 4P were to amplify the flanks for KD as listed in Table 1. 5P- A18CON-5UF, 6P- GFPSEQ-R, 7P- HRP2SEQ-F and 8P- A18CON-3UR are the primers to confirm recombination in ATG18 locus while 1P/4P and 9P- PbA18F2_seq/4P were to confirm presence of wt ATG18 locus by PCR as listed in Table 2.

The parasites appeared 10 days post-transfection in case of ATG18 locus recombinants, i.e. KO and KD after regular microscopic observation of Giemsa stained blood smears.

The blood from infected mice were passaged to other mice to get enough recombinant parasites for confirmation at genomic and protein level.

4.7 AMA1 recombinant parasites could not be obtained

The knockout of AMA1 would not generate the parasites, if attempted, as it is one of the essential gene for pathogenicity and development of parasite. So, GFP knockin to AMA1 locus and making AMA1 knockdown recombinant parasites were attempted. In AMA1 KD, a destabilizing domain called cDD was fused in-frame at the C-terminus of wild type gene sequence along with eGFP as shown in the schematic (Figure 4.36). The transfection was done thrice following the same protocol as that of ATG18 (Janse et al., 2006) but parasites did not appear.

4.8 Expression of eGFP in ATG18 recombinant parasites

Parasites were observed after 10 days of transfection in both ATG18 KO and ATG18 KD recombinants. The KO parasites were maintained under pyrimethamine while the KD parasites were maintained under pyrimethamine and trimethoprim. Pyrimethamine would kill the wild type parasites in both while trimethoprim would stabilize the cDD domain from degradation of the fusion protein.

eGFP signal was seen during microscopy of ATG18 KO parasites (Figure 4.38). Cytosolic expression of GFP was observed in all the stages (ring, Trophozoite and schizont). Though nuclear fission seems to be occurring in schizont stage in reference to blue colored nuclear stain Hoechst, the GFP expression is seen in all of the parasite cytosol.

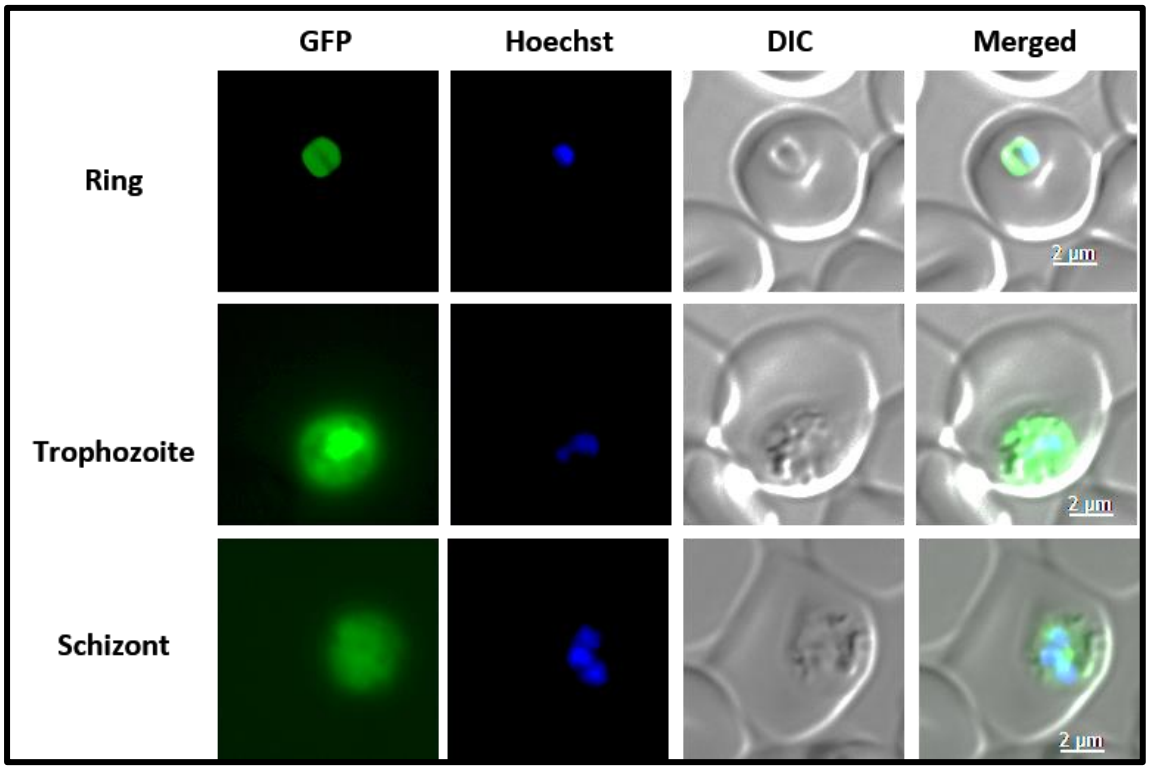

Figure 4. 38 Expression and localization of GFP in ATG18 knockout parasites. Live parasites were examined for GFP fluorescence, and the images show ring, trophozoite and schizont stages. The panels from left to right show the GFP signal (eGFP), nuclear signal (Hoechst), parasite and erythrocyte boundaries (DIC- Differential interference contrast/ Bright field), and merge of all three (Merged).

The strategy for knockdown of ATG18 was to keep the ATG18 gene intact followed by fusion of GFP/cDD, which would allow both localization and conditional knockdown of the fusion protein. The GFP signal was observed as puncta (Figure 4.39). Different levels of GFP expression and different localization could be observed in recombinant ATG18 KD parasites. In addition, the dispersed puncta of GFP fluorescence seems to merge at the center in late schizont stage of parasite.

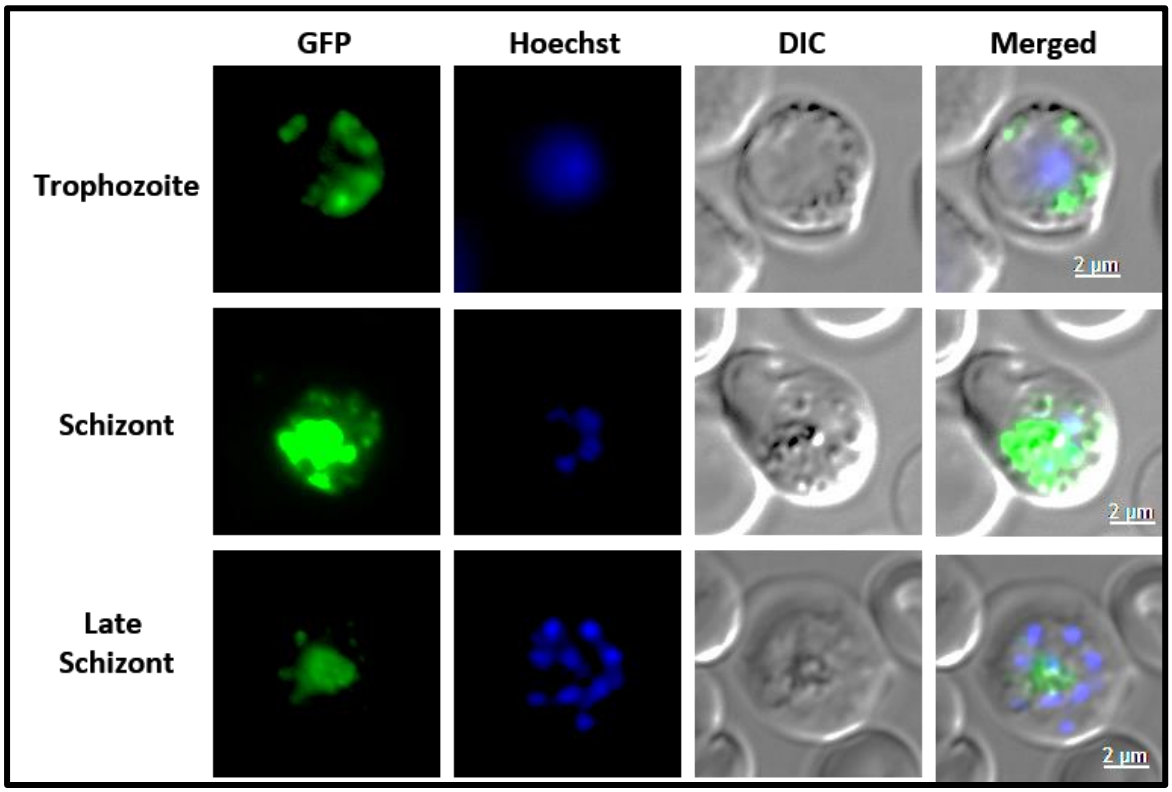

Figure 4. 39 Subcellular localization of GFP in ATG18 knockdown parasites. Live parasites were examined for GFP fluorescence; the images show trophozoite, schizont and late schizont stages. The panels from left to right show the GFP signal (eGFP), nuclear signal (Hoechst), parasite and erythrocyte boundaries (DIC- Differential interference contrast/ Bright field), and merge of all three (Merged).

4.9 PCR confirmation of recombinant GFP expressing parasites

After GFP expression was observed in the parasites, analysis of the genotype of the transgenic parasites was carried out to confirm the recombination at the targeted locus. The standard techniques applicable for this confirmation can be diagnostic PCR for the presence of gene fragment using integration specific primers or Southern analysis of genomic DNA.

Diagnostic PCR using integration specific and wild type specific primers were selected such that the one primer binds to UTR region at the target site that was not present in any of the flanks and other primer binds to the construct only. The combination of these two would give amplicon only if recombination has occurred.

The gene (here PbATG18) specific primers (one each from the 5' and 3' UTRs selected) combination would give amplicon of smaller size from WT gDNA template. In same condition, the recombinant gDNA should not give the same size amplicon unless the wild type parasite population is also present. This is because of inserting new DNA sequences as a cassette as in Figure 4.37. This helps to identify the presence of pure recombinant parasite lines, which is essential for other studies like drug resistance, immune responses and others.

4.9.1 Analysis of ATG18KO parasite at gene level

Figure 4.40 suggests that ATG18KO parasites were pure line and contained WT parasite only. The 5' and 3' recombination specific amplicon was not detected, suggesting that the homologous recombination did not occur in any two sites. This deludes the presence of WT parasite, as the similar amplicon would occur in the parasite, which has episomal expression of construct, and the presence of WT genome copy inside the nucleus is not affected. Similar questions appear for the amplicon using MSP specific primers. Hence, it is likely that GFP is expressed from an episomal copy of the plasmid, and ATG18 is likely essential.

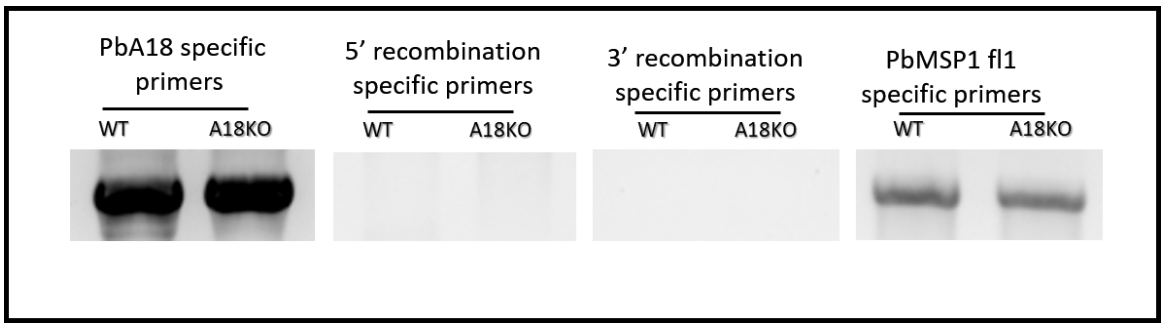

Figure 4. 40 PCR products from gDNA of WT and ATG18 KO parasites. The used primer sets are as mentioned in Table 3 and their binding region is shown in schematic Figure 4.37.

4.9.2 Analysis of ATG18 KD parasite at gene level

The PCR results of ATG18 KD parasite (Figure 4.41) showed that WT parasite were also present along with recombinant parasites. However, the result is appropriate as the recombination specific primers amplified from the gDNA of ATG18KD, indicating that homologous recombination (DCO) has occurred and supports the expression of GFP.

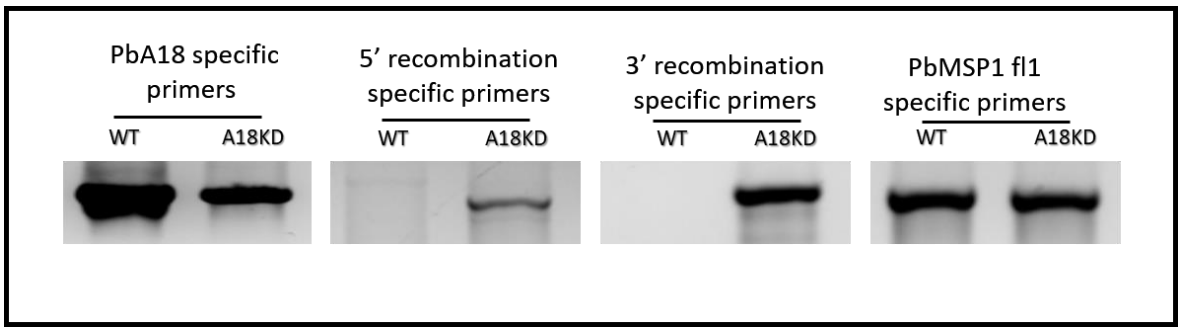

Figure 4. 41 PCR products from gDNA of WT and ATG18 KD parasites. The used primer sets are as mentioned in Table 3 and their binding region is shown in schematic Figure 4.37.

4.10 Validation of recombinant parasite at protein level

Protein expression was studied by western blotting of the parasite lysate against anti-GFP, anti-HA and anti-β-actin antibodies. In ATG18KD lysate, anti-GFP and anti-HA would detect the same size of fusion protein (84.5 kDa, ATG18+GFP+CDD+HA fused). In ATG18KO lysate, however, anti-GFP would give a 26.7 kDa protein corresponding to free GFP. Anti-β-actin would give a 46 kDa protein in the recombinant as well as the wild type lysate, serving as a loading control.

Figure 4.42 represents the western blot of parasite lysate against antibodies as mentioned. anti-β-actin is detecting protein from all lysate as it is the positive control, anti-HA is detecting from only KD lysate while anti-GFP is detecting protein with higher size in KD lysate while lower size in KO lysate.

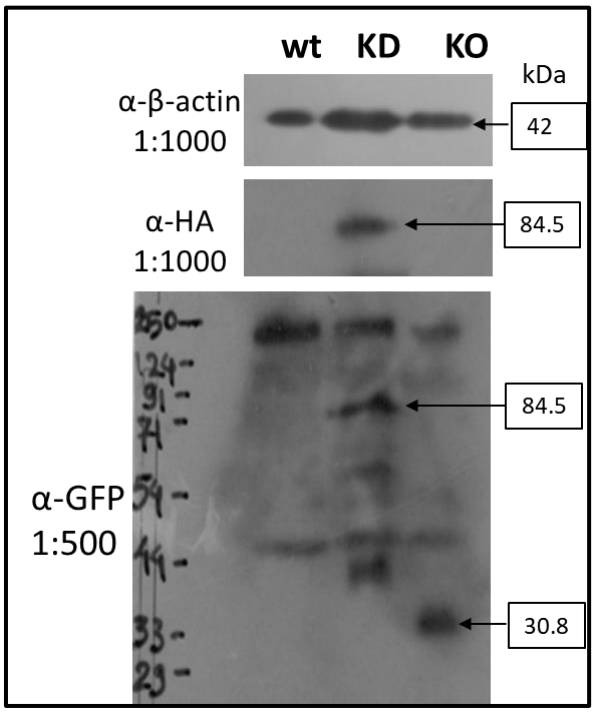

Figure 4. 42 Western blot of WT, ATG18 KD and ATG18 KO parasite lysates developed on X-ray film using anti-β-actin, anti-HA and anti-GFP antibodies.

CHAPTER 5
DISCUSSION

5.1 *Plasmodium* AMA1 is a AMA1 superfamily protein

Analysis of the PfAMA1 protein sequence against CDD (Conserved Domain Database) and Pfam revealed the presence of AMA-1 superfamily protein, which is present in all apicomplexans. This protein family found superfamily hit in the putative AMA1 sequence of *Plasmodium* species as well as in other apicomplexans. As apicomplexans are the protozoal parasites and have apical organelles, this supports the hypothesis that AMA1 protein is produced by these apical organelles and is involved in host erythrocyte invasion (Gratzer & Dluzewski, 1993).

Sequence comparison of PfAMA1 with putative AMA1 sequence of selected apicomplexans showed that it has almost twice more sequence identity with its *Plasmodium* homologues (>50%) than non-*Plasmodium* homologue (>25%). Sequence alignment of PfAMA1 and its putative homologues showed the highly conserved cysteine residues involved in disulfide bonding. This is reported to involve in forming the prosequence and three domains; DI, DII and DIII (Remarque et al., 2008).

5.2 ATG18 is a WD40 repeat domain protein

The analysis of yeast ATG18 protein sequence against CDD (Conserved Domain Database) and Pfam revealed the presence of two WD40 domains, which is present in all eukaryotes. WD40 is a short structural motif and its repeat would favor the formation of circular solenoid secondary structure. This structural conformation supports the predicted beta-propeller structure of ATG18 protein.

This protein family found superfamily hit in the putative ATG18 sequence of *Plasmodium* species, other apicomplexans an even in human. Due to its distribution in almost all living organisms, ATG18 could be one of the housekeeping genes. In addition, the WD40 domain is found to be present in many other proteins involved in cell signaling, autophagy and apoptosis (Source- Pfam WD40).

Sequence comparison of ScATG18 with putative ATG18 sequence of selected eukaryotes showed that *Plasmodium* homologues share more than 90% identity among themselves while non-*Plasmodium* homologues shared about 25% identity. Sequence alignment of ScATG18 and its putative homologues showed the short highly conserved FRRGT motif involved in binding PI3P and PIP2 and association with vacuolar membrane (Suzuki et al., 2017).

5.3 Making *P. berghei* transfection constructs

The transfection construct for *P. berghei* contained the eGFP and/or cDD fused to the targeted gene. As the homologous recombination strategy was adopted to make recombinant parasites, the region of homology was cloned into the construct. For the DCO events to occur by recombination, two regions of homology should flanking at each end of the construct. As *Plasmodium* genome is highly A/T rich and such sequences are unstable in *E. coli* (Carvalho & Ménard, 2005), this complicated the preparation of transfection construct. During cloning of the homology regions, after any one region is cloned, the cloning of other region would destabilize the whole plasmid. Therefore, the use of some other competent cells could help for cloning experiments.

5.4 Nucleofector technology for transfection

Plasmodium berghei transfection is efficiently done by using the nonviral Nucleofector technology (Janse et al., 2006). This high transfection efficiency of 10^{-3} to 10^{-4} will reduce time, number of animals and the amount of exogenous DNA to generate transformed parasites. The crucial step in this process is the collection of mature blood-stage schizonts of *P. berghei* containing fully developed merozoites. The in-vitro maturation of blood stage parasite will prevent spontaneous rupture of schizonts which can be collected by the Nycodenz density-gradient centrifugation. This protocol allows collection of about 10^8 schizonts per mice enough to carry out 2-3 transfections.

The mentioned transfection process was optimized in the laboratory to get more schizonts. The Nycodenz separation of schizonts from collected blood before the in-vitro maturation allowed more efficient purification of mature schizonts for transfection (as mentioned in Singhal et al., 2014).

5.5 Homologous recombination in genome editing

Genetic manipulation is an important tool for studying the function of a gene, which can help to understand biological function of gene. Most of the existing genome editing approaches use the host DNA-damage repair pathway. Of the different gene manipulation methods for *Plasmodium*, homologous recombination has been reviewed as a versatile system (Carvalho & Ménard, 2005). Recombination repair pathway is induced by double strand breaks in the DNA which code for specific nucleases for repair. The presence of dsDNA, which shares homology with the targeted region, favors the recombination event. The crossover will allow exchange of several kilobases long regions between the foreign DNA and the host genome (Hoshijima et al., 2016).

The linearized transfection construct, which shares homology with the targeted gene loci in part, is electroporated to *Plasmodium berghei* wild type in high quantity (5 µg).

This makes the parasite realize the loss of its genomic DNA fragment and would try to incorporate by homologous recombination. So, this genome editing mechanism utilizes the parasite's own error-prone mechanism in making recombinant parasites.

The *Plasmodium* genome is highly A/T rich, which always holds the possibility of integration of vector by homologous recombination elsewhere than at expected locus. However, this transfection technique holds great essence in research purposes like identification of gene function, transgene expression of fluorescent tagged proteins to study host-parasite interaction, study of immune responses against recombinant parasite and much more.

5.6 AMA1 gene locus could not be edited

Disrupting AMA1 in *Plasmodium* was not successful, which is consistent with earlier reports (Triglia et al., 2000), and substantiates essential role of AMA1 in parasite development. The molecular mechanisms of AMA1 functions have also been postulated in the invasion of host erythrocytes by merozoites (Srinivasan et al., 2011).

The possible explanation for no AMA1 recombinant parasite could be that addition of GFP/CDD fusion in the C-terminus of AMA1 interfered with the structure and function of AMA1. In this regard, fusion of AMA1 with a shorter tag like Hys tag, myc tag might have no or less severe effect on parasite growth. The AMA1 knockdown recombinants can also be made with only cDD but without GFP fusion. As cDD has a haemagglutinin (HA) tag, the KD parasites can be assessed by western blotting using anti-HA antibody.

5.7 Analysis of ATG18 KO parasite lines

Live imaging of ATG18 KO parasites showed eGFP fluorescence all over the parasite irrespective of stage of erythrocytic life cycle (Figure 4.38). According to the expression pattern, one of the following two possibilities remain:

1) homologous recombination in target locus

If double crossover would have occurred, the generated parasites would be ATG18 knockout. These parasites would express GFP under ATG18 promoter in the locus. But this possibility is ruled out by the recombination specific PCR as it confirmed that homologous recombination did not occur at the ATG18 locus.

2) no recombination and episomal expression of eGFP

The transfected linear construct might have re-circularized, as both the ends are blunt and compatible for ligation, thereby, GFP would be expressed under ATG18 promotor present in ATG18 KO fl1 (5'UTR) of ATG18 KO construct.

5.8 Analysis of ATG18 KD parasite lines

As the parasite develops into trophozoite stage, it feeds on host RBC cytoplasm including haemoglobin and the free heme is polymerized into hemozoin pigment . As food vacuole is the organelle for hemoglobin degradation in *Plasmodium*; this event requires more number of food vacuole explaining the puncta of GFP signal (Kapishnikov et al., 2012) (Figure 4.39). This suggests that PbATG18 might be associated with the vacuolar membrane as that of other vacuolar membrane marker proteins (Dluzewski et al., 2008).

In addition, it was observed that puncta of GFP fluorescence converge towards a single spot in the late schizont stage. The possible hypothesis can be the merging of small food vacuoles into a single large food vacuole in agreement .with the localization of other vacuolar proteins of *Plasmodium* like Merozoite Surface Protein 1 fragment – $MSP1_{19}$ and Chloroquine resistance gene (CRT) (Dluzewski et al., 2008)

5.9 Essentiality of PbATG18 gene

ATG18, in the eukaryotic model *Saccharomyces cerevisiae,* is studied to be one of the key components of autophagy pathway. Similar to localization of ATG18 in yeast, the *Plasmodium* ATG18 is also expected to be localized on the vacuolar membrane, endosomes and might have potential role in cytoplasm to vacuolar targeting of cargos in addition to autophagy (“SGD Saccharomyces Genome Database").

A new speculation could be derived reasoning the failure of knocking out ATG18 gene in three attempts that ATG18 could be an essential gene. This can be further supported by the fact that ATG18 knockdown parasites were generated under permissive conditions (in the presence of TMP). If any gene is essential for the growth and development of an organism, the check and balance mechanism would not let loose that particular gene (Joyce & Grindley, 1984). The failure of generation of ATG18 KO parasites would also support the essentiality of ATG18 gene. This holds the great future perspectives in studying the autophagy pathway, and ATG18 might be a novel drug target for developing new antimalarial to treating malaria.

5.10 Fused GFP expression in ATG18 KD parasites

The western blotting experiment more clarifies the GFP expression in ATG18 KD recombinant parasites observed during live imaging. The size of GFP protein at 84.5 kDa depicts that the GFP fluorescence seen in live imaging was actually the fused GFP, not free GFP which would be of size 30.8 kDa in the latter. This also verifies that the homologous recombination occurred and knockdown parasites were generated. At ATG18 locus of recombinant ATG18 KD parasite, ATG18 coding sequence is followed by GFP sequence, along with fused cDD sequence.

5.11 Obtaining pure line parasites

To infer any result from recombinant parasites, it should be ensured that they are the pure genetic lines as the presence of wild type parasite may contradict any result and even affect the phenotype. Parasite's sensitivity to antimalarial drugs and further immunological study also require pure line recombinant parasites.

The easy and effective way to obtain the pure line recombinant parasite is their selection under drug pressure immediately followed by transfection . However, the delay in drug selection will ease even the non-recombinants to grow giving mixed population of parasites. A single parasitized RBC needs to be isolated from it which upon culture give homogeneous parasite population. Traditionally, this is attained by limiting dilution in which the parasitemia is calculated by microscopy and diluted to desired parasitemia such that one infected RBC is present in single culture volume. This is a simple method but requires more animal models and need to be confirmed at genetic and protein level. It can also be done by micromanipulation system observing under inverted microscope. Recently, more advanced flow-sorting protocol (FACS) are also being used to isolate genetically transformed blood stages of *P. berghei* (Miao & Cui, 2011). In addition, drug-selectable marker-free recombinant malaria parasites can also be generated by GOMO- Gene Out Marker Out strategy (Manzoni et al., 2015).

CHAPTER 6

SUMMARY

Apical membrane antigen 1 (AMA1) protein of *Plasmodium* is one of the proteins involved in host-pathogen interactions leading to invasion of erythrocytes by merozoites. As this is found to be essential in other apicomplexan *T. gondi*, the specific objective of this research was to manipulate AMA1 gene locus of *Plasmodium berghei* and produce recombinant parasites. Another aspect of this research focusses on a homeostatic autophagy pathway protein, Autophagy related 18 (ATG18) which has not been studied in *Plasmodium* in detail. Considering the functional homology to yeast ATG18, PlasmoATG18 is also expected to be involved in binding to Phagophore assembly site (PAS) and aiding to phagophore membrane expansion. This research also attempted to generate ATG18 knockout and knockdown parasite to study its localization and functional analysis in parasite life cycle.

Two transfection plasmids were constructed to modify AMA1 gene locus, first AMA1 KI to knockin GFP and second AMA1 KD to knockdown AMA1 using cDD as regulatory switch. On the other hand, two transfection plasmids were constructed to modify ATG18 gene locus, first ATG18 KO to knockout ATG18 and second ATG18 KD to knockdown ATG18 using same cDD as regulatory switch. cDD would degrade the fused AMA1 or ATG18 protein in KD recombinants, however application of drug, trimethoprim, would inactivate cDD protein and targeted protein is expressed allowing the regulation of expression.

The transfection of parasites was done by electroporation of constructs, the AMA1 recombinant parasites (i.e. AMA1 knockin and AMA1 knockdown both) could not multiply and produce parasitemia. The case was same even upto three repeated transfections. This suggested that AMA1 protein being involved in pathogenesis of *Plasmodium*, the fusion of any protein such as GFP (here in AMA1 KI) and GFP-cDD (here in AMA1 KD) might have affected AMA1 function. So, the recombinant parasite might have lost their capacity to invade new host RBCs and could not develop parasitemia.

Similarly, the ATG18 recombinant parasites (ATG18 KO and ATG18 KD) developed parasitemia. The functional analysis of ATG18 was done in in-vivo system, i.e. in recombinant parasites growing inside mice infected by ourselves. Thus, by monitoring the GFP fluorescence of parasites and PCR analysis of recombinant locus in genome, it was confirmed that homologous recombination occurred in both 5’ and 3’ region by double crossover in ATG18KD parasites. However, ATG18 could not be knocked out as no recombination occurred as verified by recombination specific PCR. This led us to hypothesize that ATG18 might be essential to the parasite development.

We were able to localize the expression of ATG18 in different stages of parasites development via green fluorescence in ATG18 KD parasites. Even the expressed GFP was analyzed by immunoblotting and found that GFP is expressed by fusion with ATG18 protein. ATG18 was observed as puncta during the trophozoite stage which later got merged during the late schizont stage. Food vacuole is active in all the dividing new merozoites but later stops feeding and get merged to form single central vacuole, this illuminates that ATG18 might be localized in food vacuole. This suggests the role of ATG18 in the biogenesis of food vacuole and/or food vacuole-associated activities.

CHAPTER 7
CONCLUSION

This dissertation project was taken up to generate Apical Membrane Antigen 1 (AMA1) knockin and knock down parasites and generate Autophagy related 18 (ATG18) knockout and knockdown parasites. This would subsequently allow us to study the localization and function of AMA1 and ATG18 during parasite development. Transfection experiments with AMA1 knockin and AMA1 knockdown constructs did not produce recombinant parasites. However, we were able to generate ATG18 recombinant parasites by transfecting ATG18 knockout and ATG18 knockdown constructs. The ATG18 knockout parasite lines did not show homologous recombination at the target locus, but expressed GFP, most likely from episomal copy of the plasmid in the parasite cytosol. The ATG18 knockdown parasite line showed expected homologous recombination at the target site, expressed predicted fusion protein (ATG18-GFP-cDD), indicating that ATG18 is essential for parasite development. ATG18 was associated with the food vacuole, suggesting its role in food vacuole-associated activities and/or food vacuole biogenesis. However, more work needs to be done to identify specific functions of ATG18. ATG18 knock-down parasites generated in this project would be invaluable for studying its functions, and their characterization is underway.

Recommendations/ Future perspectives:

1. AMA1 is a potential vaccine candidate for generating attenuated whole organism malaria vaccine, thus AMA1 targeting transfections could be reattempted using the existing constructs.
2. Instead of GFP, short fusion protein like hys, myc tag in the 3' end of AMA1 coding sequence could be used. Different combinations of reporter genes like GFP, luciferase, hys tag, myc tag and regulatory genes could be attempted.
3. Different strategies could be developed in designig the transfection constructs to target AMA1 locus.
    a. Functional analysis of AMA1-GFP construct in recombinant parasite
    b. Design of AMA1 KI, KO and KD constructs such that AMA1 fused with GFP is under constitutive promotor (eg beta- actin or histone)
    c. Episomal transfection strategy could be adopted targeting AMA1
4. For immunological study and to study the potency as whole parasite vaccine, a pure line of ATG18 knock-down parasites need to be established.
5. Dilution cloning and other techniques like Fluorescent activated cell sorting (FACS) could be used to pool out only the recombinant parasites. However, the parasites should be in nutrient-rich condition to ensure their survival before infection in mice model.
6. As ATG18 appears to be essential, its small molecule inhibitors should be explored which could have potential as therapeutic drugs.

CHAPTER 8

REFERENCES

Ager, A. L. (1984). Rodent Malaria Models (pp. 225–264). Springer, Berlin, Heidelberg. https://doi.org/10.1007/978-3-662-35326-4_8

Aly, A. S. I., Downie, M. J., Mamoun, C. Ben, & Kappe, S. H. I. (2010). Subpatent infection with nucleoside transporter 1-deficient *Plasmodium* blood stage parasites confers sterile protection against lethal malaria in mice. *Cellular Microbiology*, *12*(7), 930–938. https://doi.org/10.1111/j.1462-5822.2010.01441.x

Bannister, L. H., Hopkins, J. M., Dluzewski, A. R., Margos, G., Williams, I. T., Blackman, M. J., Mitchell, G. H. (2003). *Plasmodium falciparum* apical membrane antigen 1 (PfAMA-1) is translocated within micronemes along subpellicular microtubules during merozoite development. *Journal of Cell Science*, *116*(18), 3825–3834. https://doi.org/10.1242/jcs.00665

Bargieri, D. Y., Andenmatten, N., Lagal, V., Thiberge, S., Whitelaw, J. A., Tardieux, I., … Ménard, R. (2013). Apical membrane antigen 1 mediates apicomplexan parasite attachment but is dispensable for host cell invasion. *Nature Communications*, *4*, 2552. https://doi.org/10.1038/ncomms3552

Brito, T., Barone, A. A., & Faria, R. M. (1969). Human liver biopsy in *P. falciparum* and *P. vivax* malaria. *Virchows Archiv Abteilung A Pathologische Anatomie*, *348*(3), 220–229. https://doi.org/10.1007/BF00555648

Carvalho, T. G., & Ménard, R. (2005). Manipulating the *Plasmodium* genome. *Current Issues in Molecular Biology*, *7*(1), 39–56.

CDC - Malaria. (n.d.). Retrieved September 5, 2017, from https://www.cdc.gov/malaria/index.html

Chen, P. Q., Yuan, J., Du, Q. Y., Chen, L., Li, G. Q., Huang, Z. Y., Wu, L. N. (2000). Effects of dihydroartemisinin on fine structure of erythrocytic stages of *Plasmodium berghei* ANKA strain. *Acta Pharmacologica Sinica*, *21*(3), 234–8.

Chesne-Seck, M.-L., Pizarro, J. C., Normand, B. V.-L., Collins, C. R., Blackman, M. J., Faber, B. W., Bentley, G. A. (2005). Structural comparison of apical membrane antigen 1 orthologues and paralogues in apicomplexan parasites. *Molecular and Biochemical Parasitology*, *144*(1), 55–67. https://doi.org/10.1016/j.molbiopara.2005.07.007

Clyde, D. F., McCarthy, V. C., Miller, R. M., & Hornick, R. B. (1973). Specificity of protection of man immunized against sporozoite-induced *falciparum* malaria. *The American Journal of the Medical Sciences*, *266*(6), 398–403.

Collins, C. R., Das, S., Wong, E. H., Andenmatten, N., Stallmach, R., Hackett, F., Blackman, M. J. (2013). Robust inducible Cre recombinase activity in the human malaria parasite *Plasmodium falciparum* enables efficient gene deletion within a single asexual erythrocytic growth cycle. *Molecular Microbiology*, *88*(4), 687–701. https://doi.org/10.1111/mmi.12206

Combe, A., Giovannini, D., Carvalho, T. G., Spath, S., Boisson, B., Loussert, C., Ménard, R.

(2009). Clonal conditional mutagenesis in malaria parasites. *Cell Host & Microbe*, *5*(4), 386–96. https://doi.org/10.1016/j.chom.2009.03.008

Cox, F. E. (2010). History of the discovery of the malaria parasites and their vectors. *Parasites & Vectors*, *3*(1), 5. https://doi.org/10.1186/1756-3305-3-5

Deans, J. A., Alderson, T., Thomas, A. W., Mitchell, G. H., Lennox, E. S., & Cohen, S. (1982). Rat monoclonal antibodies which inhibit the in vitro multiplication of *Plasmodium knowlesi*. *Clinical and Experimental Immunology*, *49*(2), 297–309.

Deans, J. A., Thomas, A. W., Alderson, T., & Cohen, S. (1984). Biosynthesis of a putative protective *Plasmodium knowlesi* merozoite antigen. *Molecular and Biochemical Parasitology*, *11*, 189–204.

Devine, S. M., MacRaild, C. A., Norton, R. S., & Scammells, P. J. (2017). Antimalarial drug discovery targeting apical membrane antigen 1. *Med. Chem. Commun.*, *8*(1), 13–20. https://doi.org/10.1039/C6MD00495D

Dluzewski, A. R., Ling, I. T., Hopkins, J. M., Grainger, M., Margos, G., Mitchell, G. H., Bannister, L. H. (2008). Formation of the Food Vacuole in *Plasmodium falciparum*: A Potential Role for the 19 kDa Fragment of Merozoite Surface Protein 1 (MSP119). *PLoS ONE*, *3*(8), e3085. https://doi.org/10.1371/journal.pone.0003085

Ellis, J., Ozaki, L. S., Gwadz, R. W., Cochrane, A. H., Nussenzweig, V., Nussenzweig, R. S., & Godson, G. N. (1983). Cloning and expression in *E. coli* of the malarial sporozoite surface antigen gene from *Plasmodium knowlesi*. *Nature*, *302*(5908), 536–538. https://doi.org/10.1038/302536a0

Farré, J.-C., & Subramani, S. (2016). Mechanistic insights into selective autophagy pathways: lessons from yeast. *Nature Publishing Group*, *17*. https://doi.org/10.1038/nrm.2016.74

Gardner, M. J., Hall, N., Fung, E., White, O., Berriman, M., Hyman, R. W., Barrell, B. (2002). Genome sequence of the human malaria parasite *Plasmodium falciparum*. *Nature*, *419*(6906), 498–511. https://doi.org/10.1038/nature01097

Gerald, N. J., Majam, V., Mahajan, B., Kozakai, Y., & Kumar, S. (2011). Protection from Experimental Cerebral Malaria with a Single Dose of Radiation-Attenuated, Blood-Stage *Plasmodium berghei* Parasites. *PLoS ONE*, *6*(9), e24398. https://doi.org/10.1371/journal.pone.0024398

Ghorbal, M., Gorman, M., Macpherson, C. R., Martins, R. M., Scherf, A., & Lopez-Rubio, J.-J. (2014). Genome editing in the human malaria parasite *Plasmodium falciparum* using the CRISPR-Cas9 system. *Nature Biotechnology*, *32*(8), 819–821. https://doi.org/10.1038/nbt.2925

Glick, D., Barth, S., & Macleod, K. F. (2010). Autophagy: cellular and molecular mechanisms. *The Journal of Pathology*, *221*(1), 3–12. https://doi.org/10.1002/path.2697

Goonewardene, R., Daily, J., Kaslow, D., Sullivan, T. J., Duffy, P., Carter, R., Wirth, D. (1993). Transfection of the malaria parasite and expression of firefly luciferase. *Proceedings of the National Academy of Sciences of the United States of America*,

90(11), 5234–6.

Gratzer, W. B., & Dluzewski, A. R. (1993). The red blood cell and malaria parasite invasion. *Seminars in Hematology*, *30*(3), 232–47.

Gwadz, R. W., Cochrane, A. H., Nussenzweig, V., & Nussenzweig, R. S. (1979). Preliminary studies on vaccination of Rhesus monkeys with irradiated sporozoites of *Plasmodium knowlesi* and characterization of surface antigens of these parasites. *Bulletin of the World Health Organization*, *57 Suppl 1*, 165–73.

Hain, A. U. P., & Bosch, J. (2013). Autophagy in *Plasmodium*, a Multifunctional Pathway? *Computational and Structural Biotechnology Journal*, *8*(11), e201308002. https://doi.org/10.5936/csbj.201308002

Hehl, A. B., Lekutis, C., Grigg, M. E., Bradley, P. J., Dubremetz, J. F., Ortega-Barria, E., & Boothroyd, J. C. (2000). *Toxoplasma gondii* homologue of *Plasmodium* apical membrane antigen 1 is involved in invasion of host cells. *Infection and Immunity*, *68*(12), 7078–86.

Hodder, A. N., Crewther, P. E., Matthew, M. L., Reid, G. E., Moritz, R. L., Simpson, R. J., & Anders, R. F. (1996). The disulfide bond structure of *Plasmodium* apical membrane antigen-1. *The Journal of Biological Chemistry*, *271*(46), 29446–52.

Hoffman, S. L., Goh, L. M. L., Luke, T. C., Schneider, I., Le, T. P., Doolan, D. L., Richie, T. L. (2002). Protection of Humans against Malaria by Immunization with Radiation-Attenuated *Plasmodium falciparum* Sporozoites. *The Journal of Infectious Diseases*, *185*(8), 1155–1164. https://doi.org/10.1086/339409

Hoshijima, K., Jurynec, M. J., & Grunwald, D. J. (2016). Precise genome editing by homologous recombination. *Methods in Cell Biology*, *135*, 121–47. https://doi.org/10.1016/bs.mcb.2016.04.008

Htoo, S. E., Price, R. N., Nosten, F., Looareesuwan, S., Simpson, J. A., Mann, C., Angus, B. J. (2000). A case-control auditory evaluation of patients treated with artemisinin derivatives for multidrug-resistant *Plasmodium falciparum* malaria. *The American Journal of Tropical Medicine and Hygiene*, *62*(1), 65–69. https://doi.org/10.4269/ajtmh.2000.62.65

Janse, C. J., Ramesar, J., & Waters, A. P. (2006). High-efficiency transfection and drug selection of genetically transformed blood stages of the rodent malaria parasite *Plasmodium berghei*. *Nature Protocols*, *1*(1), 346–356. https://doi.org/10.1038/nprot.2006.53

Joyce, C. M., & Grindley, N. D. F. (1984). Method for Determining Whether a Gene of *Escherichia coli* Is Essential: Application to the polA Gene. *JOURNAL OF BACTERIOLOGY*, *158*(2), 636–643.

Kapishnikov, S., Weiner, A., Shimoni, E., Guttmann, P., Schneider, G., Dahan-Pasternak, N., Elbaum, M. (2012). Oriented nucleation of hemozoin at the digestive vacuole membrane in *Plasmodium falciparum*. *PNAS*.

Kemp, D. J., Coppel, R. L., Cowman, A. F., Saint, R. B., Brown, G. V, & Anders, R. F. (1983). Expression of *Plasmodium falciparum* blood-stage antigens in *Escherichia coli*:

Detection with antibodies from 'immune humans (malaria/recombinant DNA/bacteriophage A/j&galactosidase/fused polypeptides). *Immunology*, *80*, 3787–3791.

Kitamura, K., Kishi-Itakura, C., Tsuboi, T., Sato, S., Kita, K., Ohta, N., & Mizushima, N. (2012). Autophagy-Related Atg8 Localizes to the Apicoplast of the Human Malaria Parasite *Plasmodium falciparum*. *PLoS ONE*, *7*(8), e42977. https://doi.org/10.1371/journal.pone.0042977

Leiden Malaria Research | LUMC. (n.d.). Retrieved November 1, 2017, from https://www.lumc.nl/org/parasitologie/research/malaria/

Manzoni, G., Briquet, S., Risco-Castillo, V., Gaultier, C., Topçu, S., Ivănescu, M. L., Silvie, O. (2015). A rapid and robust selection procedure for generating drug-selectable marker-free recombinant malaria parasites. *Scientific Reports*, *4*(1), 4760. https://doi.org/10.1038/srep04760

McCarthy, J. S., & Good, M. F. (2010). Whole parasite blood stage malaria vaccines: A convergence of evidence. *Human Vaccines*, *6*(1), 114–123. https://doi.org/10.4161/hv.6.1.10394

McIntosh, H. M., & Olliaro, P. (1998). Treatment of uncomplicated malaria with artemisinin derivatives. A systematic review of randomised controlled trials. *Medecine Tropicale : Revue Du Corps de Sante Colonial*, *58*(3 Suppl), 57–8.

Miao, J., & Cui, L. (2011). Rapid isolation of single malaria parasite–infected red blood cells by cell sorting. *Nature Protocols*, *6*(2), 140–146. https://doi.org/10.1038/nprot.2010.185

Nair, M., Hinds, M. G., Coley, A. M., Hodder, A. N., Foley, M., Anders, R. F., & Norton, R. S. (2002). Structure of domain III of the blood-stage malaria vaccine candidate, *Plasmodium falciparum* apical membrane antigen 1 (AMA1). *Journal of Molecular Biology*, *322*(4), 741–53.

Nair, U., Cao, Y., Xie, Z., & Klionsky, D. J. (2010). Roles of the lipid-binding motifs of Atg18 and Atg21 in the cytoplasm to vacuole targeting pathway and autophagy. *The Journal of Biological Chemistry*, *285*(15), 11476–88. https://doi.org/10.1074/jbc.M109.080374

Narum, D. L., & Thomas, A. W. (1994). Differential localization of full-length and processed forms of PF83/AMA-1 an apical membrane antigen of *Plasmodium falciparum* merozoites. *Molecular and Biochemical Parasitology*, *67*(1), 59–68.

Navale, R., Atul, Allanki, A. D., & Sijwali, P. S. (2014). Characterization of the autophagy marker protein Atg8 reveals atypical features of autophagy in *Plasmodium falciparum*. *PLoS ONE*, *9*(11), 1–36. https://doi.org/10.1371/journal.pone.0113220

Nunes, A., Thathy, V., Bruderer, T., Sultan, A. A., Nussenzweig, R. S., & Ménard, R. (1999). Subtle mutagenesis by ends-in recombination in malaria parasites. *Molecular and Cellular Biology*, *19*(4), 2895–902.

Nussenzweig, R. S., Vanderberg, J., Most, H., & Orton, C. (1967). Protective immunity produced by the injection of x-irradiated sporozoites of *Plasmodium berghei*.

Nature, *216*(5111), 160–2.

Pace, T., Scotti, R., Janse, C. J., Waters, A. P., Birago, C., & Ponzi, M. (2000). Targeted terminal deletions as a tool for functional genomics studies in *Plasmodium*. *Genome Research*, *10*(9), 1414–20.

PETERS, W. (1970). Chemotherapy and drug resistance in malaria. *Chemotherapy and Drug Resistance in Malaria.*

Peterson, M. G., Marshall, V. M., Smythe, J. A., Crewther, P. E., Lew, A., Silva, A., … Kemp, D. J. (1989). Integral membrane protein located in the apical complex of *Plasmodium falciparum*. *Molecular and Cellular Biology*, *9*(7), 3151–4. https://doi.org/10.1128/MCB.9.7.3151

Pizarro, J. C., Vulliez-Le Normand, B., Chesne-Seck, M.-L., Collins, C. R., Withers-Martinez, C., Hackett, F., Bentley, G. A. (2005). Crystal Structure of the Malaria Vaccine Candidate Apical Membrane Antigen 1. *Science*, *308*(5720), 408–411. https://doi.org/10.1126/science.1107449

PlasmoDB : The *Plasmodium* Genomics Resource. (n.d.). Retrieved October 31, 2017, from http://plasmodb.org/plasmo/

Prevention, C.-C. for D. C. and. (n.d.). CDC - Malaria - About Malaria - History. Retrieved from https://www.cdc.gov/malaria/about/history/

Reggiori, F., & Klionsky, D. J. (2013). Autophagic processes in yeast: Mechanism, machinery and regulation. *Genetics*, *194*(2), 341–361. https://doi.org/10.1534/genetics.112.149013

Remarque, E. J., Faber, B. W., Kocken, C. H. M., & Thomas, A. W. (2008). Apical membrane antigen 1: a malaria vaccine candidate in review. *Trends in Parasitology*, *24*(2), 74–84. https://doi.org/10.1016/j.pt.2007.12.002

Richard, D., MacRaild, C. A., Riglar, D. T., Chan, J.-A., Foley, M., Baum, J., Cowman, A. F. (2010). Interaction between *Plasmodium falciparum* apical membrane antigen 1 and the rhoptry neck protein complex defines a key step in the erythrocyte invasion process of malaria parasites. *The Journal of Biological Chemistry*, *285*(19), 14815–22. https://doi.org/10.1074/jbc.M109.080770

Rieckmann, K. H., Beaudoin, R. L., Cassells, J. S., & Sell, K. W. (1979). Use of attenuated sporozoites in the immunization of human volunteers against *falciparum* malaria. *Bulletin of the World Health Organization*, *57 Suppl 1*, 261–5.

SGD Saccharomyces Genome Database. (n.d.). Retrieved September 4, 2017, from www.yeastgenome.org/locus/S000001917

Siddiqui, W. A., Taylor, D. W., Kan, S. C., Kramer, K., Richmond-Crum, S. M., Kotani, S., … Kasumoto, S. (1979). Immunization of experimental monkeys against *Plasmodium falciparum*: use of synthetic adjuvants. *Bulletin of the World Health Organization*, *57 Suppl 1*, 199–203.

Sigler, C. I., Leland, P., & Hollingdale, M. R. (1984). In vitro infectivity of irradiated *Plasmodium berghei* sporozoites to cultured hepatoma cells. *The American Journal of Tropical Medicine and Hygiene*, *33*(4), 544–7.

Sijwali, P. S., & Rosenthal, P. J. (2010). Functional evaluation of *Plasmodium* export signals in *Plasmodium berghei* suggests multiple modes of protein export. *PLoS ONE*, *5*(4). https://doi.org/10.1371/journal.pone.0010227

Singer, M., Marshall, J., Heiss, K., Mair, G. R., Grimm, D., Mueller, A.-K., & Frischknecht, F. (2015). Zinc finger nuclease-based double-strand breaks attenuate malaria parasites and reveal rare microhomology-mediated end joining. *Genome Biology*, *16*(1), 249. https://doi.org/10.1186/s13059-015-0811-1

Singhal, N., Atul, Mastan, B. S., Kumar, K. A., & Sijwali, P. S. (2014). Genetic ablation of plasmoDJ1, a multi-activity enzyme, attenuates parasite virulence and reduces oocyst production. *Biochemical Journal*, *461*(2), 189–203. https://doi.org/10.1042/BJ20140051

Sommer, H. E., Thomson, K. J., Walter, A. W., Freund, J., & Pisani, T. (1947). Immunization of Ducks against Malaria by Means of Killed Parasites with or without Adjuvants 1. *The American Journal of Tropical Medicine and Hygiene*, *s1-27*(2), 79–105. https://doi.org/10.4269/ajtmh.1947.s1-27.79

Sommer, H. E., Walter, A. W., Pisani, T. M., Freund, J., & Thomson, K. J. (1948). Immunization of Monkeys against Malaria by Means of Killed Parasites with Adjuvants 1,2. *The American Journal of Tropical Medicine and Hygiene*, *s1-28*(1), 1–22. https://doi.org/10.4269/ajtmh.1948.s1-28.1

Spaccapelo, R., Janse, C. J., Caterbi, S., Franke-Fayard, B., Bonilla, J. A., Syphard, L. M., … Crisanti, A. (2010). Plasmepsin 4-deficient *Plasmodium berghei* are virulence attenuated and induce protective immunity against experimental malaria. *The American Journal of Pathology*, *176*(1), 205–17. https://doi.org/10.2353/ajpath.2010.090504

Srinivasan, P., Beatty, W. L., Diouf, A., Herrera, R., Ambroggio, X., Moch, J. K., Miller, L. H. (2011). Binding of *Plasmodium* merozoite proteins RON2 and AMA1 triggers commitment to invasion. *Proceedings of the National Academy of Sciences of the United States of America*, *108*(32), 13275–80. https://doi.org/10.1073/pnas.1110303108

Stanisic, D. I., & Good, M. F. (2015). Whole organism blood stage vaccines against malaria. *Vaccine*, *33*(52), 7469–7475. https://doi.org/10.1016/j.vaccine.2015.09.057

Suzuki, H., Osawa, T., Fujioka, Y., & Noda, N. N. (2017). Structural biology of the core autophagy machinery. *Current Opinion in Structural Biology*, *43*, 10–17. https://doi.org/10.1016/J.SBI.2016.09.010

Taxonomy - NCBI. (n.d.). Retrieved November 1, 2017, from https://www.ncbi.nlm.nih.gov/taxonomy

Ting, L.-M., Gissot, M., Coppi, A., Sinnis, P., & Kim, K. (2008). Attenuated *Plasmodium yoelii* lacking purine nucleoside phosphorylase confer protective immunity. *Nature Medicine*, *14*(9), 954–958. https://doi.org/10.1038/nm.1867

Totino, P. R. R., Daniel-Ribeiro, C. T., Corte-Real, S., & de Fátima Ferreira-da-Cruz, M. (2008). *Plasmodium falciparum*: erythrocytic stages die by autophagic-like cell

death under drug pressure. *Experimental Parasitology*, *118*(4), 478–86. https://doi.org/10.1016/j.exppara.2007.10.017

Triglia, T., Healer, J., Caruana, S. R., Hodder, A. N., Anders, R. F., Crabb, B. S., & Cowman, A. F. (2000). Apical membrane antigen 1 plays a central role in erythrocyte invasion by *Plasmodium* species. *Molecular Microbiology*, *38*(4), 706–18.

USE OF ANTIMALARIAL DRUGS. (1954). *The Lancet*, *263*(6826), 1340–1342. https://doi.org/10.1016/S0140-6736(54)92225-4

van Dijk, M. R., Waters, A. P., & Janse, C. J. (1995). Stable transfection of malaria parasite blood stages. *Science (New York, N.Y.)*, *268*(5215), 1358–62.

Vincke, I. H., & Lips, M. (1948). Un nouveau *Plasmodium* d'un rongeur sauvage du Congo *Plasmodium berghei* n. sp. *Annales de La Societe Belge de Medecine Tropicale (1920)*, *28*(1), 97–104.

Wagner, J. C., Platt, R. J., Goldfless, S. J., Zhang, F., & Niles, J. C. (2014). Efficient CRISPR-Cas9–mediated genome editing in *Plasmodium falciparum*. *Nature Methods*, *11*(9), 915–918. https://doi.org/10.1038/nmeth.3063

Watkins, W. M., & Mosobo, M. (n.d.). Treatment of *Plasmodium falciparum* malaria with pyrimethamine-sulfadoxine: selective pressure for resistance is a function of long elimination half-life. *Transactions of the Royal Society of Tropical Medicine and Hygiene*, *87*(1), 75–8.

Wellde, B. T., Diggs, C. L., & Anderson, S. (1979). Immunization of Aotus trivirgatus against *Plasmodium falciparum* with irradiated blood forms. *Bulletin of the World Health Organization*, *57 Suppl 1*, 153–7.

White, N. J., & Olliaro, P. (1998). Artemisinin and derivatives in the treatment of uncomplicated malaria. *Medecine Tropicale : Revue Du Corps de Sante Colonial*, *58*(3 Suppl), 54–6.

World Malaria Report. (2017). World Health Orgnization.

Wu, Y., Kirkman, L. A., & Wellems, T. E. (1996). Transformation of *Plasmodium falciparum* malaria parasites by homologous integration of plasmids that confer resistance to pyrimethamine. *Proceedings of the National Academy of Sciences of the United States of America*, *93*(3), 1130–4.

Wu, Y., Sifri, C. D., Lei, H. H., Su, X. Z., & Wellems, T. E. (1995). Transfection of *Plasmodium falciparum* within human red blood cells. *Proceedings of the National Academy of Sciences of the United States of America*, *92*(4), 973–7. https://doi.org/10.1073/pnas.92.4.973

Zepp, F. (2010). Principles of vaccine design—Lessons from nature. *Vaccine*, *28*, C14–C24. https://doi.org/10.1016/j.vaccine.2010.07.020

APPENDICES

Appendix 1: Preparation of Buffers and Reagents

1.1 10X TBE

108 gm of Tris-base, 55 gm Boric acid and 7.4 gm (or 40 ml of 0.5M) of EDTA sodium salt was dissolved in 800ml of distilled water and pH 8.3 was maintained. Finally, volume was made upto 1000ml and autoclaved. Each time while using the buffer, the stock is diluted 10 times to bring the concentration to 1X.

1.2 6X agarose gel loading dye

0.25% w/v bromophenol blue, 0.25% xylene cyanol, 30% v/v glycerol in H2O

1.3 4X SDS Gel Loading Buffer

200mM Tris-Cl, 8% w/v SDS, 0.4% w/v bromophenol blue, 40% w/v glycerol and 400mM dithiothreitol (from 1M stock)

1.4 10X TGS/ SDS running buffer

30.2 gm of Tris-base and 144 gm of Glycine was dissolved in 500ml of distilled water. 10gm of SDS was dissolved in 50ml of warm distilled water. The two solutions were mixed and the volume was brought to 1 litre with distilled water.

1.5 Ammonium Persulfate (APS) -10% w/v

100 mg in 1000 µl of water, prepared fresh before use

1.6 Coomassie blue Staining solution

0.25gm Coomassie brilliant blue R-250 dissolved in 45 ml of water. 45 ml methanol and 10 ml glacial acetic acid were added to the solution. The solution was filtered afterwards.

1.7 Coomassie destaining solution

45 ml methanol, 45 ml water and 10 ml glacial acetic acid

1.8 1.5M Tris pH 8.8

181.7 gm Tris base was dissolved in 800ml water. pH was adjusted to 8.8 with conc. HCl and volume was made up to 1 litre.

1.9 1M Tris pH 6.8

121.1 gm Tris base was dissolved in 800ml water. pH was adjusted to 6.8 with conc. HCl and volume was made up to 1 litre.

1.10 Ethidium bromide (10 mg/ml)

1.11 Phosphate Buffered Saline (PBS) - 10X 1 lt

80gm NaCl, 2gm KCl, 14.4gm Na_2HPO_4, 2.4g KH_2PO_4 in 800ml of water. pH was adjusted to 7.4 and volume was made up to 1 litre.

1.12 Preparation of transfer buffer (1 litre)

14.4 gm of Glycine and 3.33 gm of Tris-base was added to 500 ml of distilled water. 200ml of methanol was added to it just before use and the volume was brought to 1litre with distilled water.

Appendix 2 Primers used for sequencing of cloned fragments (flanks)

Primer Name	Sequences
M13-R	CAGGAAACAGCTATGACC
GFPSEQ-R	CCAGCAGCTGTTACAAACTCAAGAA
HRP2SEQ-F	CTTTTACAATATGAACATAAAGTACAAC
PBAFL1-F1SEQ	TGCAAATAATGATAATCAACCA
PBAFL1-F2SEQ	TTCGAAGAACAATTTCCTTGTG
PBA18F1_SQ	CACGTGTAGGCACCATTCAGCAACC
PBA18F2_SQ	CATCAAACATTATCGGTGTGAGAT

Appendix 3 Clustal Omega MSA of putative AMA1 protein sequences

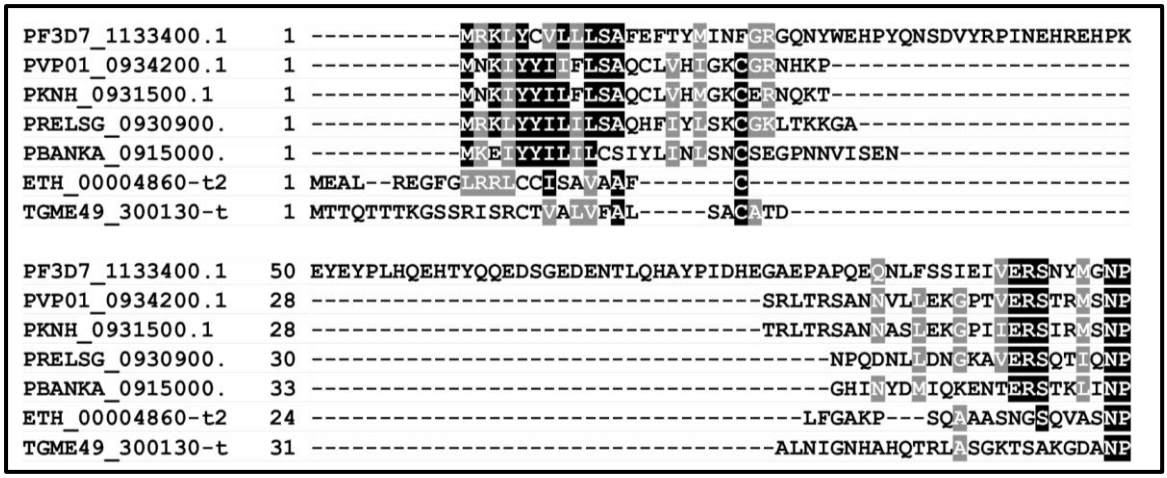

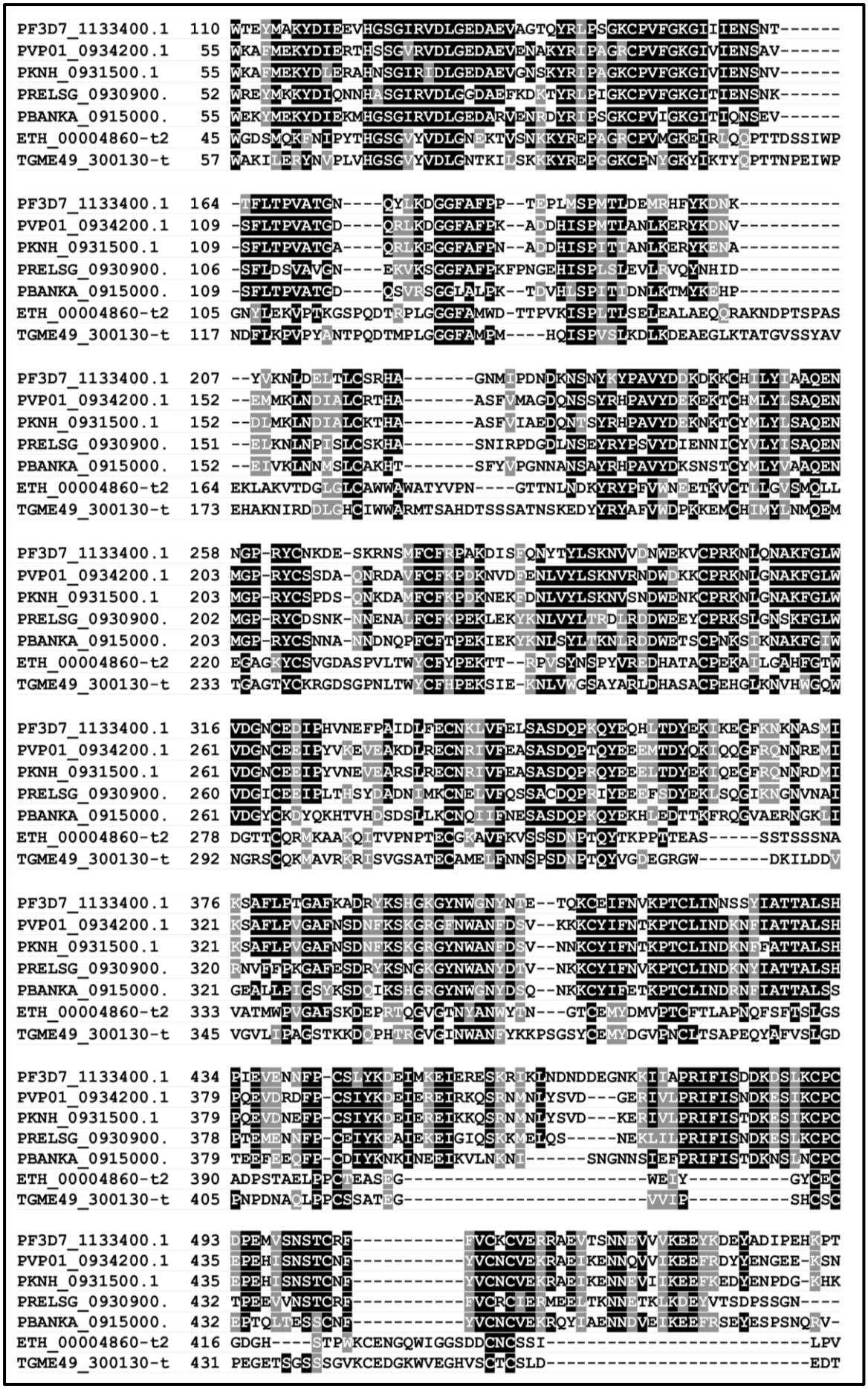
PF3D7_1133400.1 110
PVP01_0934200.1 55
PKNH_0931500.1 55
PRELSG_0930900. 52
PBANKA_0915000. 55
ETH_00004860-t2 45
TGME49_300130-t 57
PF3D7_1133400.1 164
PVP01_0934200.1 109
PKNH_0931500.1 109
PRELSG_0930900. 106
PBANKA_0915000. 109
ETH_00004860-t2 105
TGME49_300130-t 117
PF3D7_1133400.1 207
PVP01_0934200.1 152
PKNH_0931500.1 152
PRELSG_0930900. 151
PBANKA_0915000. 152
ETH_00004860-t2 164
TGME49_300130-t 173
PF3D7_1133400.1 258
PVP01_0934200.1 203
PKNH_0931500.1 203
PRELSG_0930900. 202
PBANKA_0915000. 203
ETH_00004860-t2 220
TGME49_300130-t 233
PF3D7_1133400.1 316
PVP01_0934200.1 261
PKNH_0931500.1 261
PRELSG_0930900. 260
PBANKA_0915000. 261
ETH_00004860-t2 278
TGME49_300130-t 292
PF3D7_1133400.1 376
PVP01_0934200.1 321
PKNH_0931500.1 321
PRELSG_0930900. 320
PBANKA_0915000. 321
ETH_00004860-t2 333
TGME49_300130-t 345
PF3D7_1133400.1 434
PVP01_0934200.1 379
PKNH_0931500.1 379
PRELSG_0930900. 378
PBANKA_0915000. 379
ETH_00004860-t2 390
TGME49_300130-t 405
PF3D7_1133400.1 493
PVP01_0934200.1 435
PKNH_0931500.1 435
PRELSG_0930900. 432
PBANKA_0915000. 432
ETH_00004860-t2 416
TGME49_300130-t 431

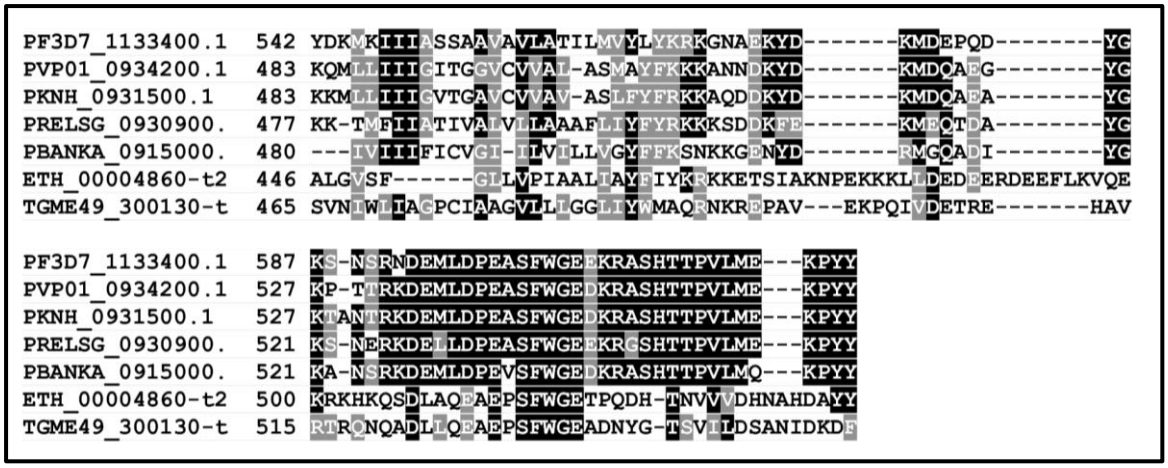

Multiple sequence alignment of putative AMA1 sequences of apicomplexans listed in Table 3 was done in ClustalOmega. The alignment is viewed in BoxShade server of ExPASy server at https://embnet.vital-it.ch/software/BOX_form.html. The black shading shows more than 80% identity in which black shading resembles the same amino acid and grey shading shows amino acid of similar properties between sequences, while no shading means no identity between the amino acids aligned. The actual percentage identity between each of sequences is shown in PIM Table 5.

Appendix 4 Clustal Omega MSA of putative ATG18 sequences

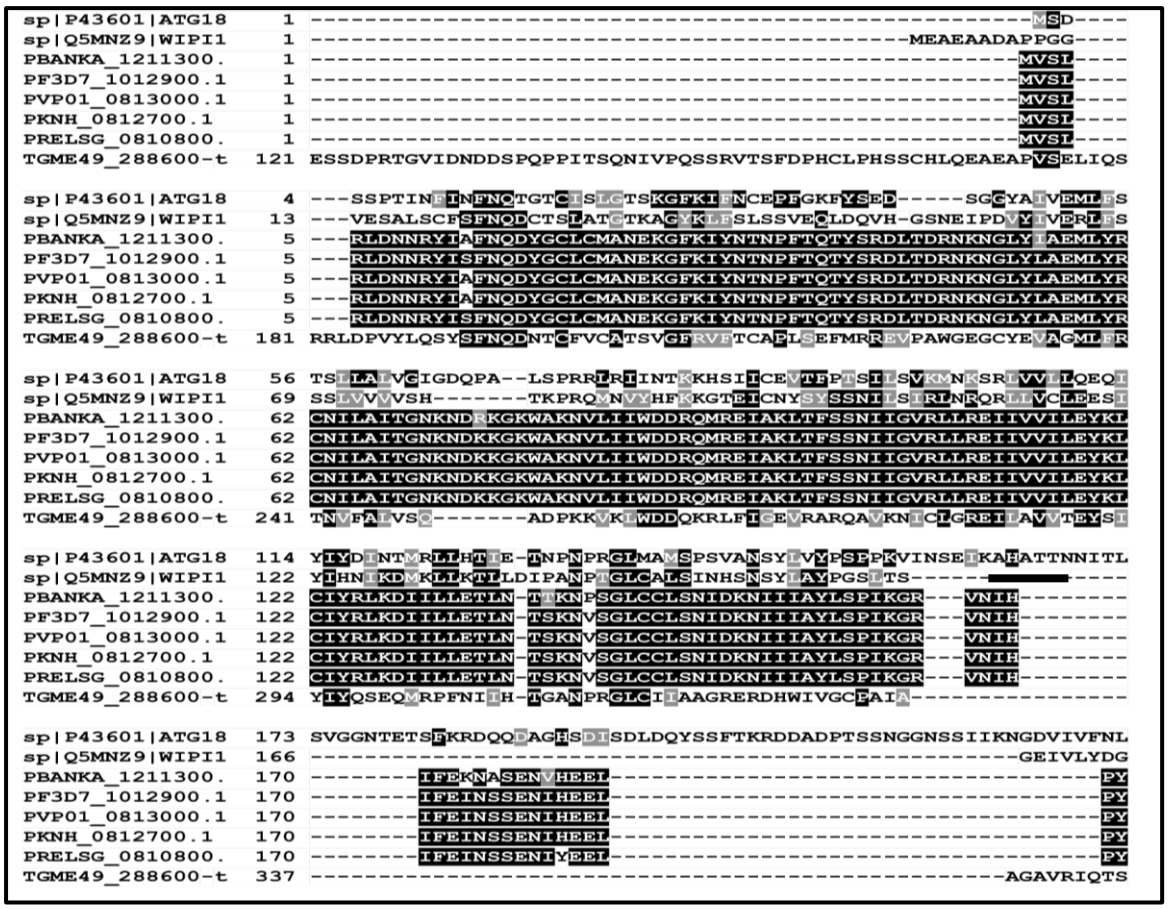

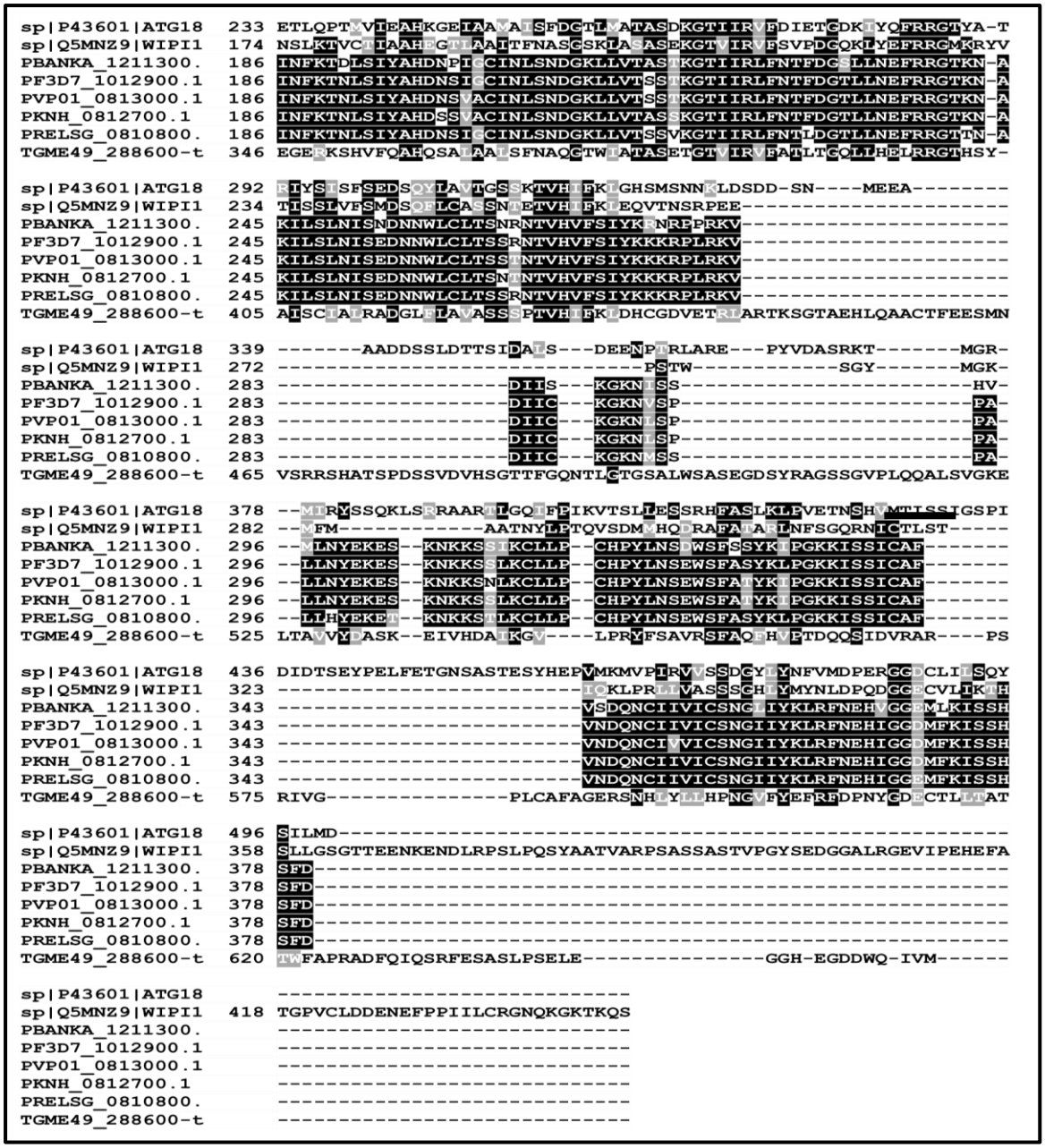

Multiple sequence alignment of putative ATG18 sequences of eukaryotes listed in Table 4 was done in Clustal Omega. The alignment was viewed in BoxShade server at ExPASy where black shading resembles the same amino acid and grey shading shows amino acid of similar properties between sequences, while no shading means no identity between the amino acids aligned. The actual percentage identity between each of sequences is shown in Percentage Identity Matrix at Table 6. The FRRGT motif involved in binding phosphatidylinositol 3-phosphate (PtdIns3P) and phosphatidylinositol 3,5-bisphosphate (PIP2) is present in all the organisms compared (underlined).